UTILIZING GENE AND PROTEIN ENGINEERING TO CREATE TOOLS IN SYNTHETIC BIOLOGY

By

Connor J Grady

A DISSERTATION

Submitted to
Michigan State University
in partial fulfillment of the requirements
for the degree of

Biomedical Engineering – Doctor of Philosophy

2023

ABSTRACT

Synthetic biology is a field of study that involves redesigning and constructing parts of a cell or organisms through engineering principles to gain new abilities. Many tools have been developed using synthetic biology techniques designed to control, sense, or manipulate cellular function. While many of these systems are controlled by a light or chemical stimulus, we looked to mechanisms in nature to expand the synthetic biology toolbox. One such mechanisms from nature is magnetoreception, or the ability to sense and detect magnetic fields. The Electromagnetic Perceptive Gene (EPG) is a protein from the glass catfish (*Kryptopterus vitreolus*) is known for its magnetoreceptive properties. Here we show the ability to use the EPG as a synthetic tool through magnetic induction. We have found the EPG protein has a conformational change that can be used as a method of reconstituting split proteins using magnetic fields. This method was used to reconstitute three separate split proteins; NanoLuc, APEX2, and Herpes Simplex Virus Type-1 Thymidine Kinase. This work serves as the starting point for design and application of magnetogenetic systems for cellular control and manipulation. This technology allows for the expansion of the synthetic biology toolbox and will allow for studying and application to more complex systems.

ACKNOWLEDGEMENTS

I would like to thank my Advisor, Dr. Assaf Gilad, for his mentorship and guidance throughout my time at Michigan State University. I would also like to acknowledge all the member of my guidance committee: Dr. Sudin Bhattacharya, Dr. Aitor Aguirre, and Dr. Jens Schmidt.

A special thanks to all the members of the Gilad, Pelled, and Kanada labs who I've worked with over the years. I would like to thank Harvey Lee who I started the program with and created a special project with as well as making the graduate experience more enjoyable. I also would like to acknowledge Drs. Sunayana Mitra, Vijay Krishnan, Shengqiang (David) Xu, and Eric Peterson who each played an instrumental role in my training, expanding my knowledge, and shaping my career. Nathan Kauffmann, Brianna Ricker, Olivia Han, and Katie Krell who all helped to contribute to this work. Thank you to Gabriela Saldana who taught me so much during my graduate career and made sure I had everything I needed to succeed.

Lastly, I would like to thank the funding sources that made this research possible from the National Institute of Health/National Institute of Biomedical Imaging and Bioengineering: R01-EB031008; R01-EB030565; R01-EB031936, National Institute of Health/National Institute of Neurological Disorders and Stroke: R01-NS098231; R01-NS104306, and the National Science Foundation: 2027113. I would also like to thank BEACON for providing me with a fellowship over the past 5 years.

TABLE OF CONTENTS

LIST OF SYMBOLS

<	Less Than
>	Greater Than
±	Plus or Minus
=	Equals
™	Trademark
Δ	Delta (Change)

LIST OF ABBREVIATIONS

5-MDHT	5-methyl dihydroxythymidine
CEST-MRI	Chemical Exchange Saturation Transfer-Magnetic Resonance Imaging
DPD	Dihydropyrimidine Dehydrogenase
GFP	Green Fluorescent Protein
kDa	Kilo Dalton
NADPH	Nicotinamide Adenine Dinucleotide Phosphate
HMBP	Heavy Metal Binding Protein
FAD	Flavin Adenine Dinucleotide
FMN	Flavin Mononucleotide
$FeSO_4$	Iron (II) Sulfate
GLamouR	Green Lanmodulin-based Reporter
GCaMP6m	GFP Calmodulin Peptide version 6-medium
REE	Rare Earth Element
PMA	Phorbol 12-Myristate 13-Acetate
EPG	Electromagnetic Perceptive Gene
IRES	Internal Ribosome Entry Site
cAMP	Cyclic AMP
CRE	Calcium or cAMP Responsive Elements
CaRE	Calcium Regulatory Element
PCR	Polymerase Chain Reaction
NFAT	Nuclear factor of activated T-cells

BRET	Bioluminescence Resonance Energy Transfer
s.e.m.	Standard Error of Mean
trEPG	Truncated EPG
APEX	Ascorbate Peroxidase
NoSS	No Signal Sequence
NoTM	No Transmembrane Sequence
dEPG	Double EPG
NoSSTM	No Signal or Transmembrane Sequence
LED	Light Emitting Diode
RT	Room Temperature
HSV1-tk	Herpes Simplex Virus Type-1 thymidine kinase
GCV	Ganciclovir
FIAU	Fialuridine
OD600	Optical Density at 600nm
PET	Positron Emission Tomography

INTRODUCTION

I.1: Synthetic biology and molecular biology

Synthetic biology is a field that allows researchers to take biological parts from different parts of nature and engineer them to create novel tools for molecular biology. The addition of gene assembly technologies such as Gibson Assembly[1] and Golden Gate Assembly[2] as well as the decreases in prices to both synthesize and sequences genes[3], synthetic biology has been able to quickly advance as a field. Because of these techniques, researchers can now take natural proteins with novel abilities and express them in new systems to harness their abilities for molecular biological approaches. Synthetic biology has created various systems designed to control[4-7], sense[8-11], or manipulate[12, 13] molecular systems. These technologies continue to expand to this day.

Chemogenetics and optogenetics are fields that emerged due to these advances in synthetic biology and allowed researcher to control of cellular function from exogenous compounds or direct light. These techniques have allowed for the exploration of cellular mechanisms. These methods have also allowed for greater control of synthetic systems. The optogenetic systems are mainly based on light sensitive channels[14, 15], pumps[16], or transcription factors[17]. Whereas chemogenetic systems are ligand-gated ion channels or G-protein-coupled receptor based[18]. Although these systems are well established and have good efficacy, there are drawbacks to both the chemical and optical approaches. Administering chemicals or drugs to induce systems could have issues crossing blood brain barrier or be unable to diffuse out of cell in a timely manner. Using drugs or chemicals also can take hours for the effect to take place[19]. The optogenetic approach needs direct light to stimulate cell in close proximity which usually

requires implants to produce the light[20]. This approach is invasive which could be challenging in deep tissue regions.

I.2: Split proteins

Split proteins are a part of a method of fragmenting a functional protein into two parts to disrupt the function to which it can be reconstituted back into a functional protein with a stimulus. This came into prominence with the protein-fragment complementation assay to study protein-protein interactions. To study these interactions, two proteins of interest would be fused to a part of the split protein, which usually exhibits a reporter functionality. If the two proteins interact, this should allow for the split protein to be reconstituted and therefore regain function, allowing for a readout to the researcher. The split proteins reporters used have expanded greatly since the origin using the Gal4 transcription factor in the yeast two hybrid system. The current split proteins allow for reporter assays of colorimetric, fluorescence[21], bioluminescence[22] and drug resistance[23].

More recently this technology has been expanded beyond the standard protein-protein interaction studies and have expanded into cellular control mechanisms[24]. A chemogenetic approach was applied to PET imaging with the split reporter HSV1-tk[25]. Methods have also been developed to modulate transcription regulation using a split Cas9[26]. Enzymes such as beta-lactamase, which is necessary for antibiotic resistance, has been split and been shown to regulate gut stability with broad spectrum antibiotic treatment in mice[27]. Split proteins also can play a key role in constructing and controlling of synthetic circuits[28]. The split protein system continues to grow as more proteins are being discovered to have the capability to be split and reconstituted. As a synthetic biology approach that allows for low background in genetically engineered

systems, researchers will continue to explore this tool for systems where constant expression of a transgene is not the optimal approach.

I.3: Magnetoreception

Magnetoreception is the sense that organisms possess to detect magnetic fields. This has been seen in organisms from bacteria to vertebrates. It is generally believed this sense is to help with orientation and migration[29-32]. This sense has also been shown in non-migratory species and could be useful in the detection of predators and prey[33, 34]. There have been several mechanisms that have been proposed to how magnetoception occurs, although it may be this sense is a case of convergent evolution.

Bacteria are the most primitive organisms that are known to have magnetoreceptive properties. These magnetotactic bacteria are able to assemble a chain of iron nanoparticles, called magnetosomes, which act as an intracellular compass to the earth's magnetic field[35, 36]. This would allow the bacteria to migrate to ideal microenvironments in aquatic systems. It has also been suggested these magnetosomes could play a role in removal of reactive oxygen species[37], iron storage, an electrochemical battery, or a gravity sensor[38].

Birds have been one of the most studied magnetoreceptive animals due to their known migratory patterns. The leading proposed mechanism in birds is the radical-pair mechanism. This mechanism relies on the spin states of two unpaired electrons and the generation of radical pairs causing singlet and triplet states which can be modulated by magnetic fields[39]. The initial radical state is initiated by absorption of photons by the bird photoreceptor. Then a series of electron transfers occur from a series of tryptophans to the FAD chromophore[40].

Fish have also been shown to exhibit magnetoreceptive properties. Several field studies

have shown several species of fish have exhibited magneto sensing abilities[41]. Though these studies have shown the ability, it is still unknown many of the mechanism of magnetoreception in fish. It has been proposed it relies on one of three mechanisms of magnetite coupled to mechanosensitive channels, electromagnetic induction, or a chemical induction similar to the mechanism in birds[42, 43]. This all shows magnetoception though a well-established sense, has limited knowledge on the mechanisms in species other than birds.

I.4: Magnetogenetics

Magnetogenetics is a new field of study that using magnetic fields to control cells through remote activation. There are advantages of using magnetogenetics over the other established methods of chemogenetics or optogenetics. The main advantages are the stimulation is non-invasive, can be distributed in a uniform manner, no issue of penetration depth, and have 'on/off' switch functionality. One current methodology is to use a magneto-thermal-genetic approach. This is to use manganese oxide nanoparticles to activate the thermoactivated TRPV1 channel[44]. In this system, magnetic fields can be used to heat nanoparticles which activates the channel causing a calcium influx. Another method was to use TRPV4 channel fused to ferritin nanoparticles. Using oscillating magnetic fields, they proposed a mechanoactivation of this channel by the magnetic field pulling on the ferritins[45]. While this method has had controversy on the proposed mechanism, it has been shown it is theoretically possible to magnetically activate channels through magnetic fields[46]. These systems provided the first examples of using magnetic fields to activate cellular systems, but there still is room for creating a non-iron based magnetogenetic system.

I.5: Electromagnetic Perceptive Gene

The glass catfish (*Kryptopterus vitreolus*) is small transparent fish found mainly found in Southeast Asia in slow moving fresh waterways[47]. This fish has also been shown to be sensitive to the earth's magnetic field[48]. It has been discovered the gene responsible for the magneto reception in the glass catfish is the Electromagnetic Perceptive Gene (EPG)[49]. When EPG is expressed in mammalian cells there is a measurable increase in the intracellular calcium levels due to magnetic stimulus. Work is currently being done to help understand the mechanism and magnetoreception of the EPG protein in mammalian cells[50]. While EPG's mechanism is not fully understood, it is still being utilized in various systems to control cellular function by activation of calcium signaling pathways[51-53]. This work has shown EPG can be effective at activation of cells and has great potential for future magnetogenetic designs.

CHAPTER 1: Utilizing Synthetic Biology approaches in Bacteria to Create Imaging Agents

1.1: Engineering novel synthetic protein for binding gadolinium

Gadolinium has been a staple of contrast enhanced magnetic resonance imaging since its emergence in 1988[54]. It has been estimated more than 30 million doses of gadolinium based contrast agents are administered per year[55]. While there are continual efforts to create more efficient gadolinium-based chemical chelates, researchers have also been implementing protein based MRI contrast agents[56-58]. We sought to expand on this and create a novel protein-based contrast agent.

As part of a collaboration with another graduate student, Harvey Lee, we explored the possibility of creating a protein based MRI contrast agent. My main part was to design, engineer, and clone the proteins. To create the base of the contrast agent we looked to nature and found there are methylotropic bacteria that have the ability to uptake lanthanides[59], to which gadolinium is a member of. The protein that is expressed in these bacteria that binds the lanthanides is lanmodulin[60, 61]. To use this protein as a contrast agent, we looked into this family of proteins and found the eukaryotic protein of calmodulin. This protein has been shown to bind calcium and can create a sensor for calcium by combining a circularly permutated fluorescent protein and an M13 peptide sequence. We used the backbone from GCaMP6m[62] and replaced the calmodulin with lanmodulin to create the first version of this construct which was named the Green Lanmodulin-based Reporter (GLamouR 1.0). A schematic of this design is show in Figure 1A.

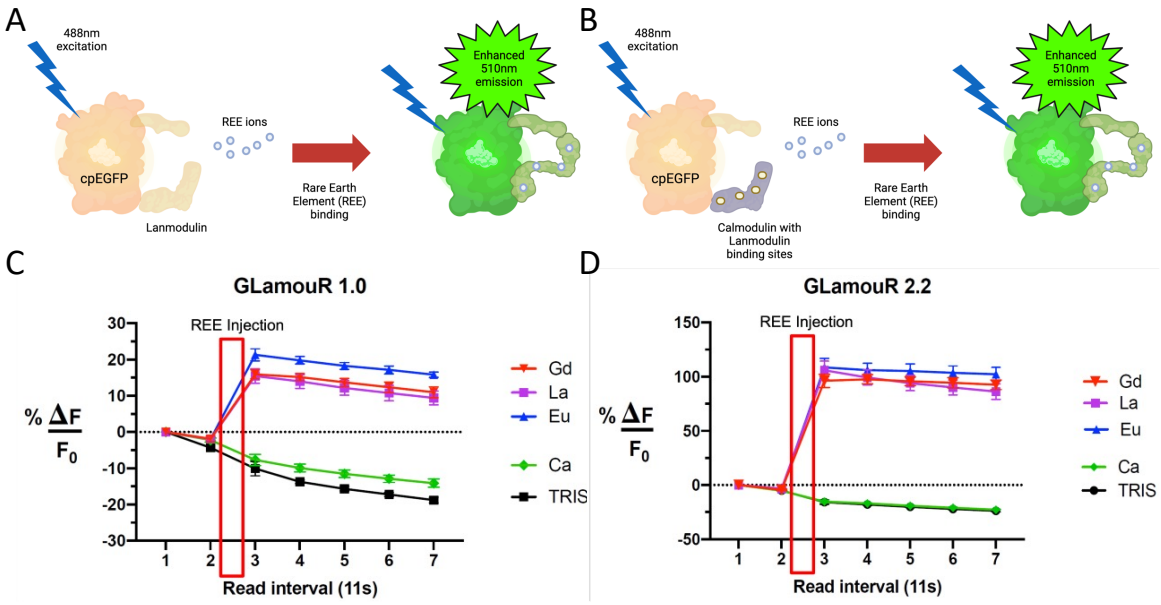

Figure 1: Development and characterization of the GLamouR protein. (A) Schematic of initial design of GLamouR. (B) Optimized design of GlamouR 2.2. Changes in fluorescent intensity due to addition gadolinium, lanthanum, europium, calcium, or TRIS buffer in GLamouR 1.0 (C) or GLamouR 2.2 (D). Results show GlamouR 2.2 has a much greater delta compared to GLamouR 1.0 in response to REEs. Experiment was performed with n=5 replicates per sample.

The GLamouR 1.0 construct was tested with three rare earth elements (REEs) of gadolinium, lanthanum, and europium. This resulted in a 15-20% increase in fluorescence after addition of the REEs (Figure 1C). The addition of calcium or TRIS buffer caused a decrease in fluorescence, showing the effect is specific to REEs and GCaMP functionality is no longer present. Although this showed an increase in fluorescence, we decided to modify this protein to attempt to create a more optimized version of GLamouR. Instead of exchanging the entire calmodulin for lanmodulin as was done in GLamouR 1.0, we decided to only replace the calcium binding sites with the lanmodulin binding sites, which is shown in the schematic of second-generation GLamouR 2.2 (Figure 1B). It was hypothesized since the GCaMP had been optimized, swapping smaller parts would allow for a greater response to REEs. Our hypothesis was proven correct as

the GLamouR 2.2 exhibited over 100% increase in fluorescent signal in response to REEs and still had a negative response to both calcium and TRIS buffer (Figure 1D).

After discovering the more optimal design of GLamouR, we wanted to further learn the capabilities of this protein. We tested the saturation kinetics of this protein and saw a linear relationship up to 50μM of gadolinium (Figure 2A). To test the lower bounds of the protein, we were able to detect a 40% change in fluorescence using 200nM of gadolinium (Figure 2B). These results show GLamouR can be used to bind and detect gadolinium from 200nM up to 50 μM.

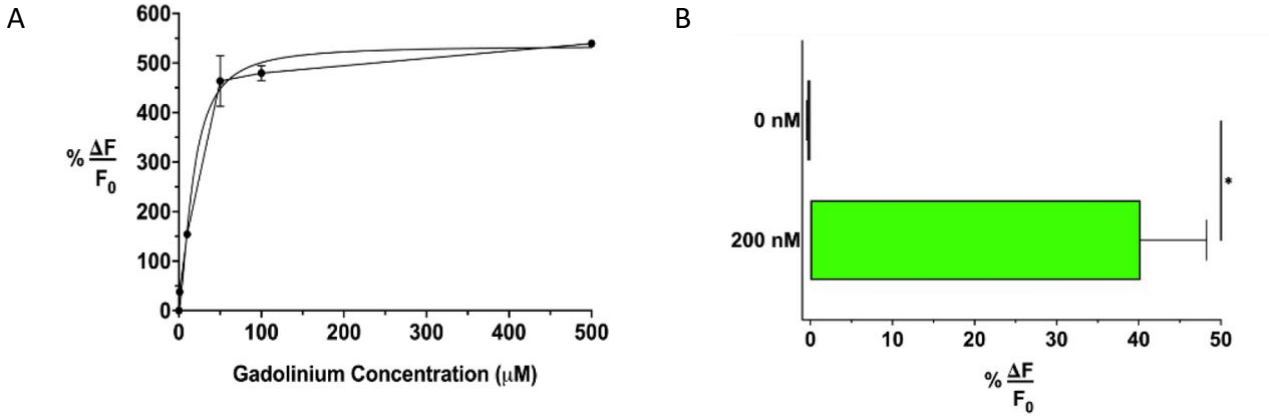

Figure 2: Fluorescence properties of GLamouR. (A) Fluorescence saturation curve for GLamouR with gadolinium shows a linear response up to 50 µM. (B) 200 nM concentrations of gadolinium were detectable with GLamouR with a 40% increase in fluorescence upon injection. Experiment was performed with n=3 replicates. Statistical significance was calculated by an unpaired t-test with Welch's correction, p value=0.0128.

To expand this system further, we wanted to see if we could create a red shifted version of this protein. To do this, we exchanged the EGFP for the red-shifted mApple (Figure 3A). The mApple was chosen due to its prevalence in the red shifted genetically encoded calcium indicators[8]. This construct was tested with gadolinium and saw a 200% increase in fluorescent signal (Figure 3B). After the initial testing of this construct, we tested 11 different REEs to see if both GLamouR and the red shifted version would be able to detect these REEs. It was shown both

constructs were able to detect all REEs, apart from lanthanum which the red shifted variant did not detect.

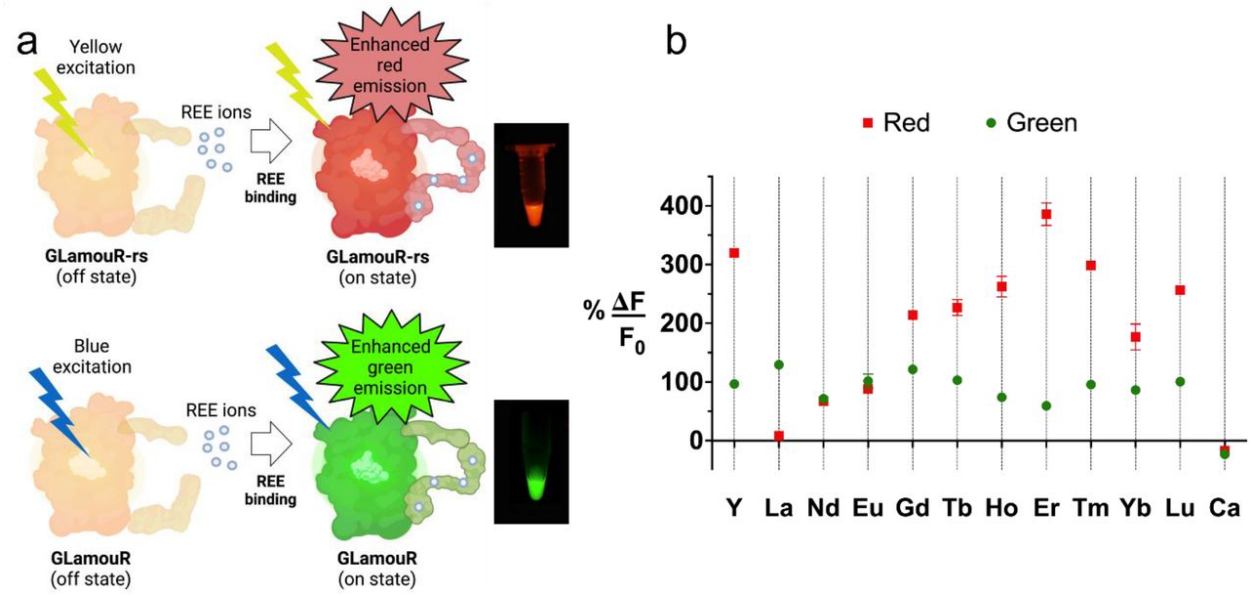

Figure 3: (A) Schematic of the red-shifted GLamouR and original GLamouR binding REEs, with their corresponding fluorescence images to the right. (B) Fluorescence increase of green and red shifted GLamouR upon addition of eleven different REEs (calcium added as negative control).

For the future directions of this project, it has been hypothesized GLamouR could be a tool for bioremediation of REEs. Although the initial plan was to create a protein-based MRI agent, which we have shown the ability of GLamouR to act as a contrast agent[9], though due to proteases and other degradation possibilities in cells, it may be not a good candidate and could deposit gadolinium in cells leading to future problems. The prospect of concentrating and potentially extracting REEs could lead to a more fruitful endeavor. Having the protein in a bound in a column, can allow for concentrating the REEs. The other option is to have bacteria express the GLamouR and use them to extract REEs from soil or recycle from other products containing REEs.

CHAPTER 2: Calcium-inducible Promoters for Creation of Gene Circuit

2.1: c-fos promoter

EPG has been shown to cause an influx of calcium in response to magnetic fields. Using this mechanism, we sought to create a genetic circuit utilizing the EPG protein as the activator, and a calcium sensitive promoter incorporated to express the reporter or gene of interest. One candidate for the calcium sensitive promoter is the c-fos promoter. The c-fos gene, part of the immediate early gene family (IEG), is a transcription factor is transcribed within minutes of activation. This system is normally found in neurons and has been shown to be activated by calcium influx as well as neurotransmitters and growth factors such as NGF, PDGF, and EGF[63]. The promoter for this gene has both serum response elements as well as cyclic AMP response elements[64]. Because of this, the promoter needs to be characterized for both elements so to see the effect under each condition.

To test the c-fos promoter and the effects of both calcium activation as well as serum activation, tdTomato was cloned downstream of the c-fos promoter as the reporter for the system. A calcium response was induced by using phorbol 12-myristate 13-acetate (PMA). To control the serum response, cells was media exchanged to Opti-MEM media, which has reduced serum in comparison to complete media. HEK 293FT cells transfected with c-fos tdTomato plasmid using Lipofectamine 3000 transfection reagent. Cells were washed 48 hours post transfection and media replaced the stimuli of the group. Stimuli was given 24 hours pre-recording. PMA was given at a concentration of 25mM. Serum was altered by using complete media (DMEM with 10%FBS 1%P/S) and OptiMEM reduced serum media. Recording done using BD Accuri™ C6 Flow Cytometer. Figure 4 shows results of 3 separate experiments in each

of the four conditions. When the replicates were averaged, we see the group receiving both complete media and PMA having the highest percent of cells expressing the tdTomato at 58.4% of cells, followed by the PMA only group at 46.5%, the serum only group at 38.7% and the no stimulus group at 26.2% of cells (Figure 5). An image of the cells before a cytometry read showing the fluorescence of the cells (Figure 5).

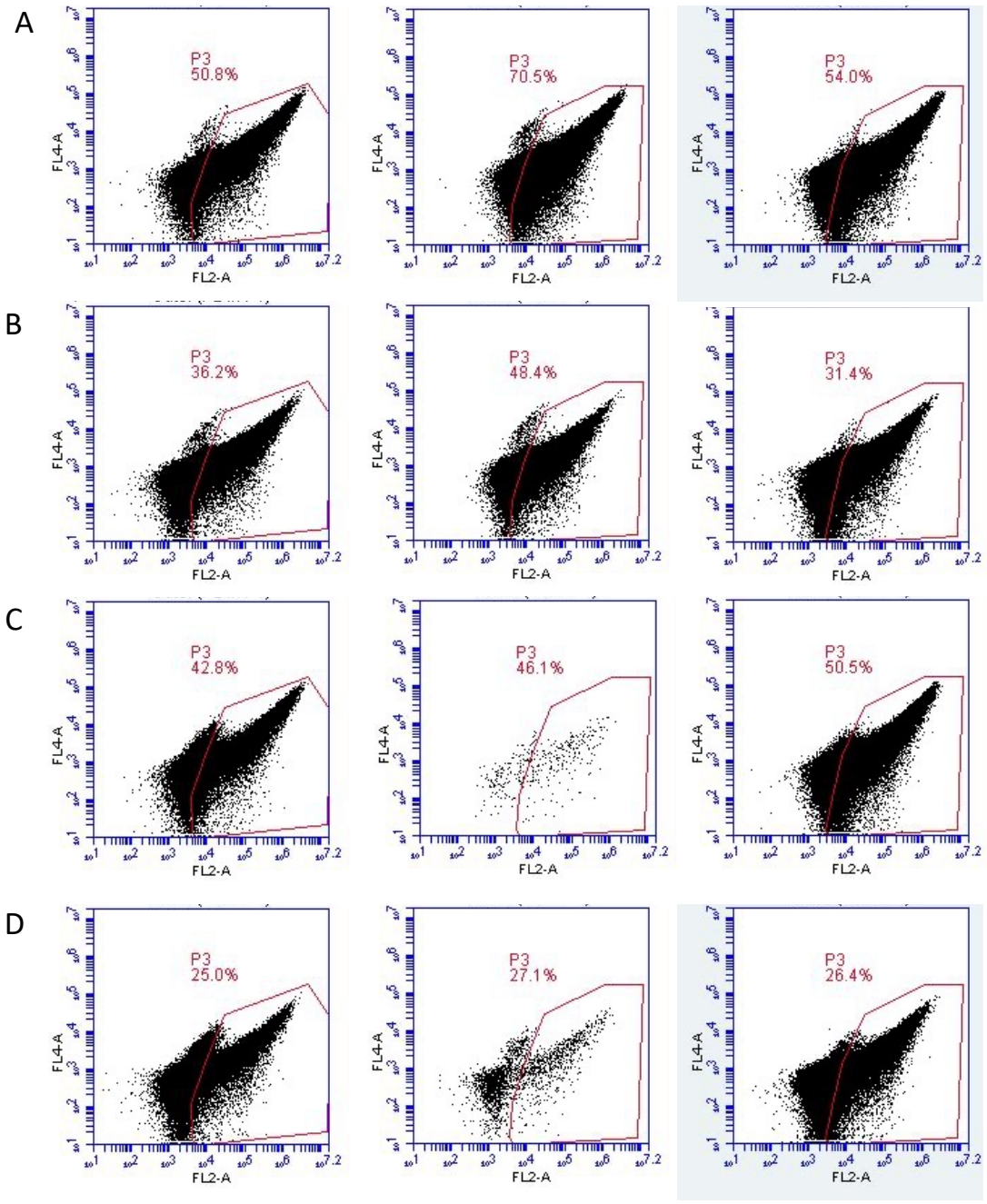

Figure 4: Flow Cytometry of HEK cells expression c-fos driven tdTomato. Graphs of triplicate experiments of cells treated with PMA and serum (A), serum only (B), PMA only (C) and control cells with no treatment (D). Activation of the c-fos promoter was shown to be most induced by PMA and serum, then the single treatments of PMA or serum.

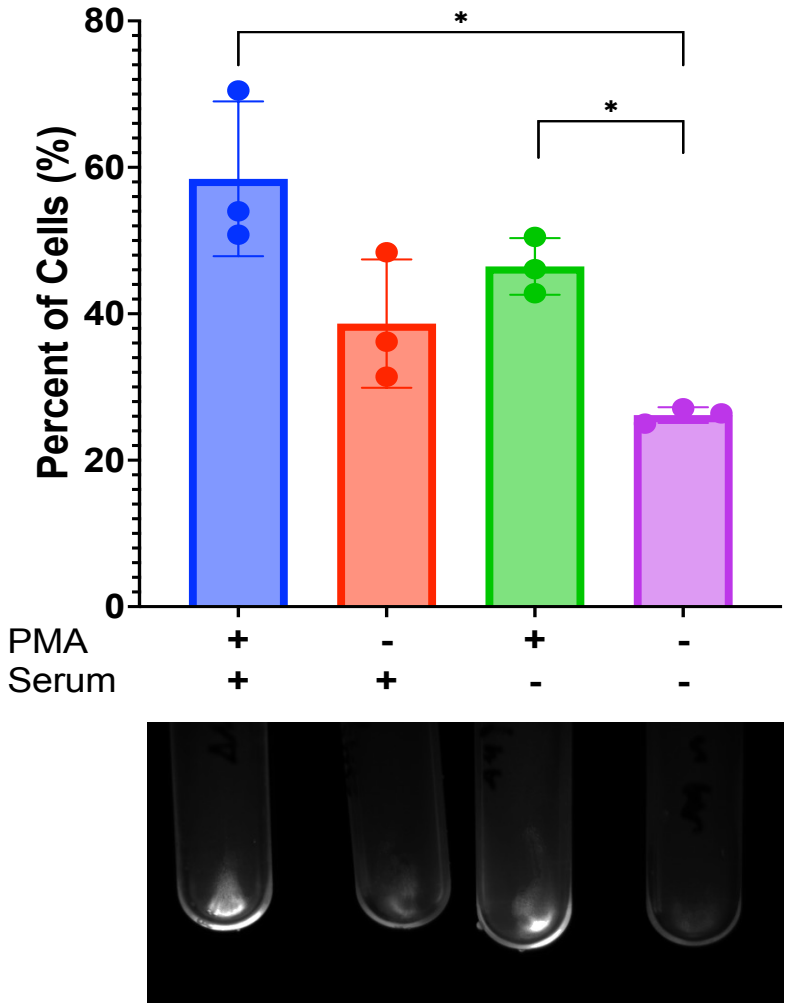

Figure 5: Averages of the flow cytometry experiments with c-fos tdTomato. Bar graph of averages as well as standard deviation of each condition in triplicate experiments (Top). Fluorescent image of cells after before read on cytometer (Bottom). Statistical analysis was with a t-test with Welch's correction and a p-value threshold <0.05.

To test whether this could be used in a circuit with EPG as the activator, we set up two experiments. The first experiment was to transiently co-transfect both the EPG plasmid with the c-fos tdTomato plasmid. The second experiment would be to use a lentiviral transduced line that expressed EPG IRES EGFP, which would then be transfected with c-fos tdTomato. For each of these experiments, non-transfected cells were used for the initial gating (Figures 6A and 7A).

Another control for these groups was the c-fos tdTomato only group to see what the baseline activity of the promoter without co-transfection or stimulation. This c-fos tdTomato only group had 9.5% of cells expressing in the gated region. (Figure 6B). The co-transfected group with EPG and the c-fos tdTomato constructs with no magnetic stimulus had 17.4% of cells expression tdTomato (Figure 6C). The same group under static magnetic stimulus had 17.9% of cells expressing tdTomato reporter (Figure 6D). Although this was a very small difference in percent of cells, it was promising toward a potential use in future experiments.

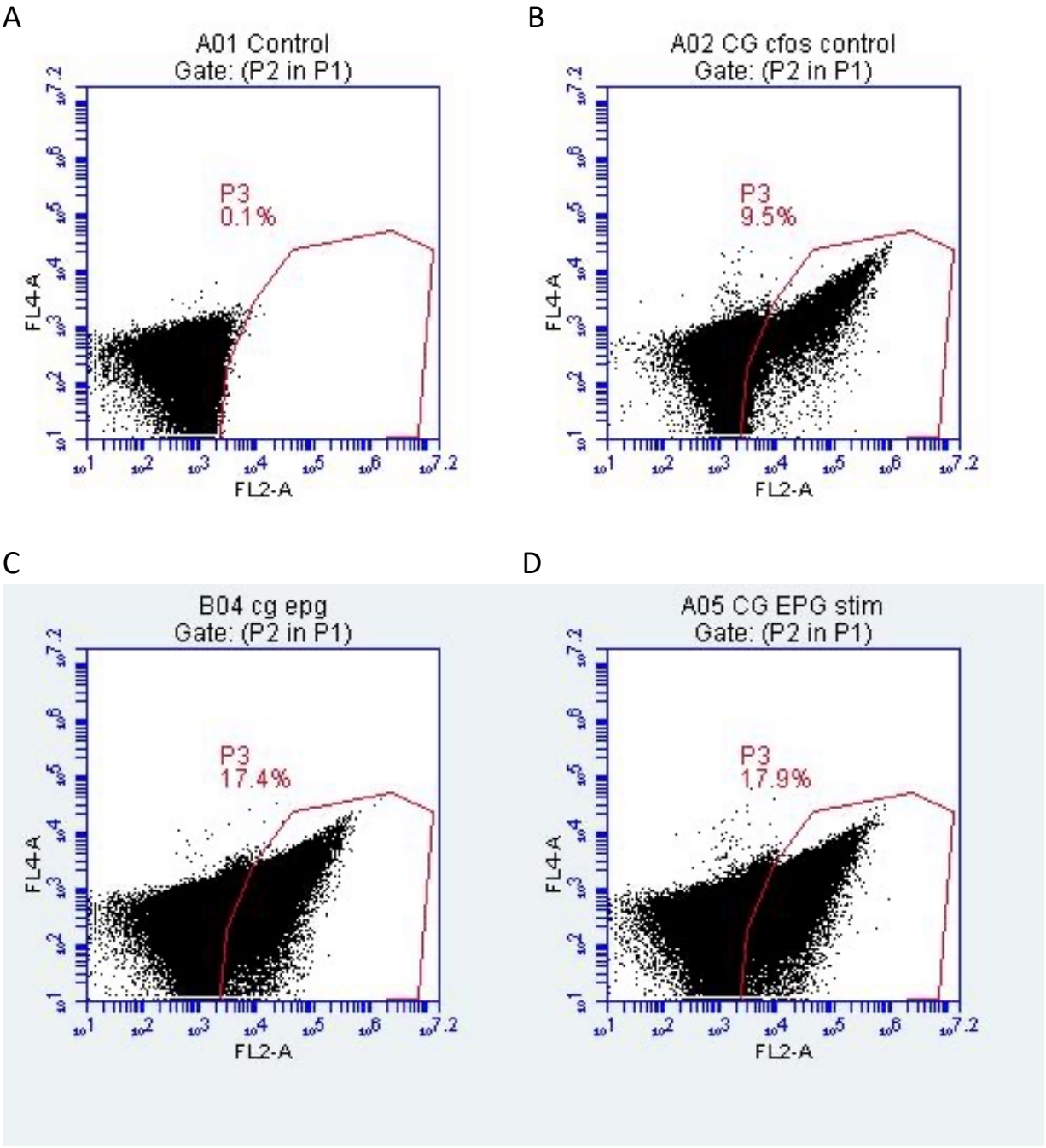

Figure 6: EPG activation of c-fos tdTomato circuit measured with flow cytometry. Initial gating was performed using untransfected cells (A). Cells transfected with only the c-fos tdTomato construct (B). Cells transfected with both EPG and c-fos tdTomato constructs with no magnetic stimulation (C) and static magnetic stimulation (D). Cells transfected with both constructs stimulated with magnetic field show a slight increase in tdTomato expression.

To test the lentiviral transduced cells in this construct we added a EGFP transfected cell line to see the expression. This was especially important due to the instrument used only having one laser which was a 488nm laser, which is optimal for GFP or other green fluorophores. The GFP transfected group showed 71.1% of cells expressing (Figure 7B). When comparing the EPG groups, the non-magnetic stimulated group had 62.6% of cells expressing (Figure 7C) compared to the magnetic stimulated group showing 69.7% of cells expressing (Figure 7D). This result showed a much greater response in the magnetic stimulated group compared to the control. The lentiviral transduced also had a better difference (7.1%) than the co-transfected (0.5%) EPG groups.

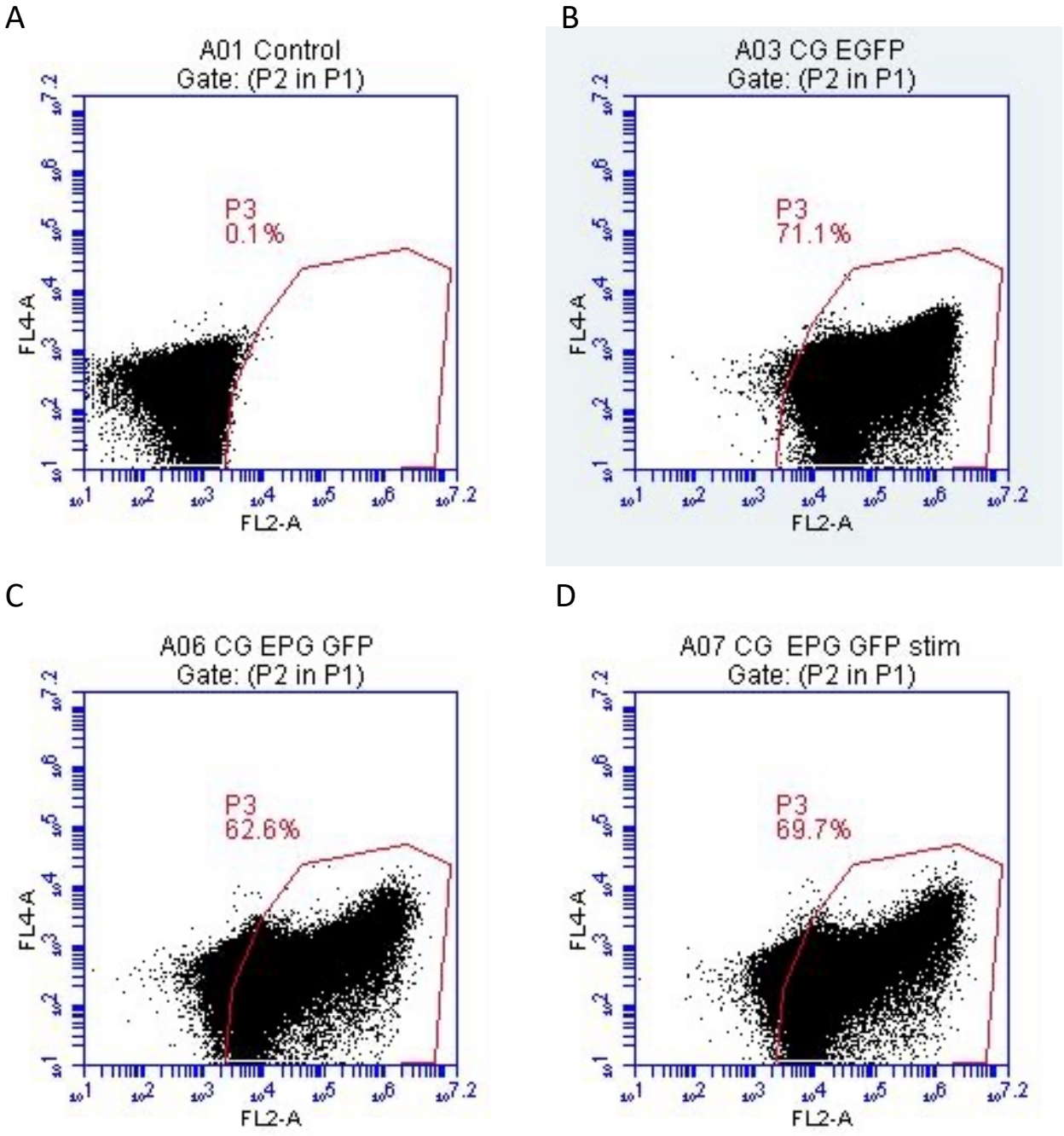

Figure 7: EPG activation of c-fos tdTomato circuit measured with flow cytometry using viral transduced EPG. Initial gating was performed using untransfected cells (A). Cells transfected with CMV EGFP plasmid (B) . Viral transduced cells transfected with c-fos tdTomato with no magnetic stimulus (C) or static magnetic stimulus (D). Cells with magnetic stimulus showed a greater increase in tdTomato expression compared to control cells with no stimulation.

The c-fos promoter showed promise a possibility to be used in a genetic circuit with the EPG protein. It has rapid response to calcium influx and has shown some promise in activation in conjunction with EPG. It does appear lentiviral transduced EPG cells work better in activation of the promoter, but this could also be due to the number of cells that each have both constructs. The c-fos does have its disadvantages as it can be activated by other stimuli other than calcium. This could lead to a less controllable system and therefore not very implementable into other systems. Overall, the initial experiments of the EPG activation of the c-fos promoter at least set up for future experiments to create a gene circuit with EPG's ability to cause calcium influx and therefore activate calcium sensitive promoters.

2.2: Synthetic calcium dependent promoter

It was shown that the c-fos promoter could be a potential tool in creation a calcium sensitive synthetic circuit, but due to its susceptibility to changes in serum we wanted to see if we could create a synthetic calcium promoter. There were two approaches that were taken to create this synthetic promoter. One was to take a *de novo* approach combining various different calcium or cyclic AMP (cAMP) responses elements and putting them together to create a new promoter. The second approach was to take two know calcium responsive promoters of c-fos and NFAT, perform various mutagenesis and cloning methods to make a synthetic conglomerate promoter sensitive to calcium.

The design of the *de novo* promoter was made using 12 reported calcium or cAMP responsive elements (CREs) in DNA from various promoters. These include elements from mammalian systems such as CREs from the c-fos, ABRE and BDNF promoters. Also included was the NFAT responsive element, yeast CDRE, Arabidopsis ABRE and the serum response element from c-fos. These elements are all associated upstream of a minimal promoter. The locations of these elements were positioned in locations as close as possible to their location to the transcriptional start site in their native state. Although this was not possible due for all elements as we limited the size of the promoter to 300bp in size. The design of this promoter, named CaRE, was shown in Figure 8.

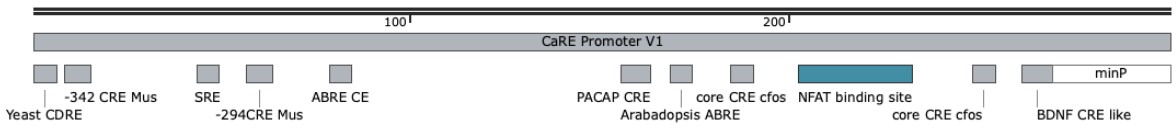

Figure 8: Design of synthetic calcium sensitive promoter. Each element added to the promoter is labeled with a box designating the size of the element.

The CaRE promoter was cloned into the pGlow TOPO vector, which is a promoterless vector used to analyze promoter systems. This construct was transfected into HEK 293FT cell and stimulated with the calcium ionophore ionomycin. Fluorescent images were taken every hour for 8 hours. Unfortunately, the CaRE promoter design had no expression of fluorescent signal throughout the 8 hours of ionomycin stimulation. After this experiment, the decision was to then shift focus towards creating a synthetic promoter from the two calcium sensitive promoters of c-fos and NFAT rather than the completely de novo approach.

The approach to create a synthetic promoter utilizing the NFAT and c-fos promoters was to use gene shuffling. This method is an evolution technique that has been used on genes such as LacZ[65], and involves fragmenting genes into small pieces where they can be randomly reassembled into a new gene. To perform this, the initial promoters were amplified out of their respective plasmids (Figure 9A) and then the bands were excised and gel purified. The purified bands then underwent DNase I digestion to create small fragments. This step was optimized using different concentrations of DNase I U/µl per µg of DNA. The digestion progressed for 4 min at 15C with a dilution scheme of U/µl for DNase I (Figure 9B). This resulted in adequate digestion of DNA with concentrations of DNase I 1/10 U/µl or higher. Once the DNA was digested, the fragments were run through two filtration steps using Amicon centrifugal filters. The first filter used was a 100k molecular weight cutoff and was used to eliminate larger fragments or non-digested fragments in the filter allowing the smaller fragments to proceed into the flowthrough. The second centrifugal filter was a 3k molecular weight filter and was used to concentrate the fragments for use the future steps. After centrifugation, the fragments underwent a procedure called primerless PCR. This process is as the name implies PCR without the use of primers. This

allows for random amplification of fragments by using varying annealing temperatures. A serial dilution of the concentrated fragments was run, and a smear was shown in lanes 5-7 showing random amplification of the fragments (Figure 9C). The last step of the procedure is known as rescue PCR. A set of primers were used to amplify random fragments that could be used to clone into expression vectors, which can be tailored to the preferred cloning method. The vector used was once again the pGlow TOPO, allowing for easy sub-cloning of the mutant synthetic promoters. After the rescue PCR was performed, in each of the dilutions, two dominant sized bands appeared around 200bp and 500bp along with smears in between (Figure 9D). The constructs that were successfully scrambled were tested with ionomycin stimulation and measure every hour for 8 hours. Although they were scrambled, effectively none of the constructs produced any fluorescence with or without ionomycin stimulus.

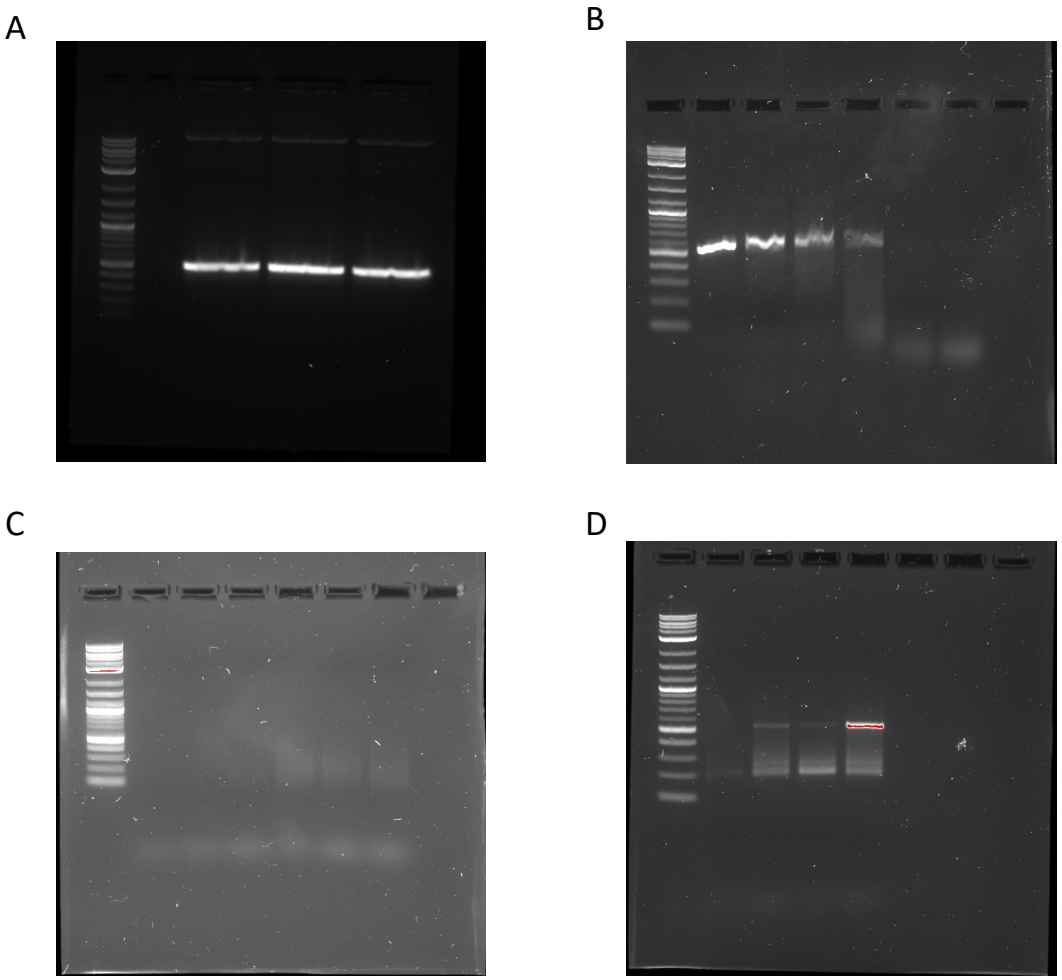

Figure 9: Gene shuffling procedure using NFAT and c-fos promoters. (A) Amplification of the NFAT promoter to use for gel extraction. (B) DNase I dilution scheme digestion of promoters using no DNase (lane 2), 1/100 U/µl of DNase I (lane 3), 1/50 U/µl of DNase I (lane 4), 1/10 U/µl of DNase I (lane 5), 1/2 U/µl of DNase I (lane 6) 1 U/µl of DNase I (lane 7). (C) Primerless PCR of promoters using DNA serial dilution scheme. (D) Rescue PCR from primerless PCR reactions. Each reaction was run with a 1Kb plus MW ladder for size comparison. The final reactions were TOPO cloned into a primerless vector for evaluation of function.

Although creating a synthetic promoter through the means attempted here did not lead to any positive results it led to some knowledge that could be leveraged if this was attempted in future EPG circuits. Looking back at some of the evolutionary methods may not have been the best methods, as transcription factors recognize specific sequences and breaking those

sequences apart leads to no binding of the transcription factors. For the *de novo* approach, using elements that are not cell specific was an lack of knowledge at the time. It has been shown synthetic NFAT promoters with various repeats of the NFAT binding domains[7, 66] could be a better option to optimize. The other option that has shown promise in the field is to modify existing NFAT transcription factors to bind synthetic promoters[67]. This has the potential of less crosstalk with natural systems in the cells and less off target effects.

CHAPTER 3: Bioluminescence resonance energy transfer using EPG

3.1: BRET studies of EPG

To effectively use EPG as a tool for synthetic biology, it would be helpful to understand more about the protein's response to magnetic stimulation. While the EPG protein had been shown to have calcium influx due to magnetic field activation, the mechanism to which this occurs remains unclear. One hypothesis is the EPG undergoes a conformational change or forms a complex with itself in the presence of magnetic fields. Previous studies have shown there was no change in conformation with 25mTesla when EPG was in a purified form[49], but this could also be due to not having potential cofactors to help facilitate this change. Because of this, we decided to test this hypothesis in cells. We used bioluminescence resonance energy transfer (BRET) studies which have been used for indicating or determining if conformational changes occur within a protein[68, 69]. The idea is if there is a conformational change in EPG, the distance between donor and acceptor will also change causing a change in the BRET ratio.

Using this BRET design, we studied if EPG has a conformational change due to static magnetic field (10 mTesla). To design the construct we decided to fuse EPG to the blue emitting bioluminescent protein NanoLuc and the yellow emitting fluorescent protein mVenus on the N and C terminals respectively and was expressed in HeLa cells. Figure 10A shows the transfected cells showed a 2.5% signal increase in the group stimulated by magnetic field over the non-stimulated group. The response seen is comparable to other BRET studies of single protein conformational changes[68, 70] and there was a significant difference at the saturation point of the two curves (T=2).

We then designed a BRET construct to test if the protein underwent a dimerization event

due to magnetic stimulus. This has the EPG fused to NanoLuc on the C terminal followed by an IRES site followed by EPG fused to mVenus (EPG-NanoLuc IRES EPG-mVenus). The group stimulated with the static magnet had a 1.5% increase compared to the control group (Figure 10B). The response from the EPG IRES experiment is not consistent with the standard BRET studies for protein-protein interaction[71] and data was not significant at point of saturation (T=7). The low response implies that dimerization of EPG is not the mechanism by which EPG works. Collectively, these findings suggests that magnetic stimulation led to conformational change of the EPG protein.

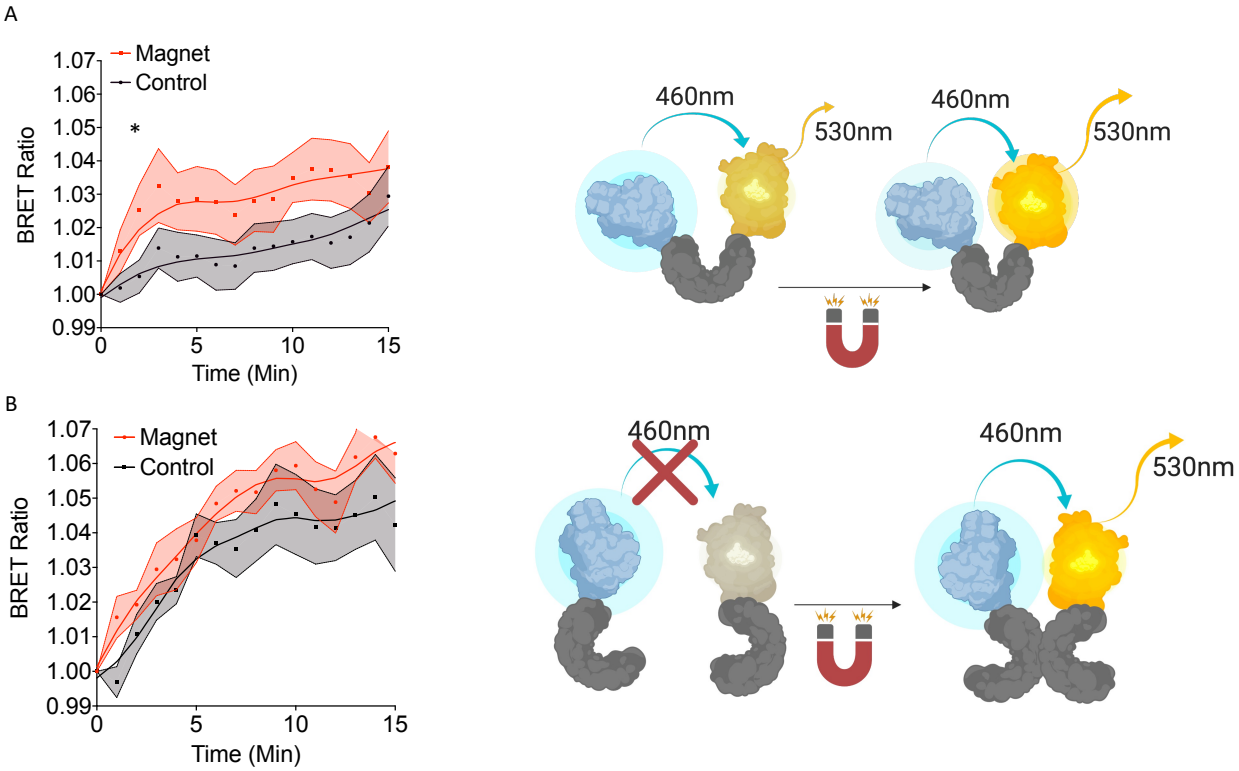

Figure 10: Bioluminescent Resonance Energy Transfer studies of EPG conformational changes in HeLa cells. (A) A single copy of EPG cloned between NanoLuc and mVenus. (B) A copy of the EPG was fused to Nanoluc followed by an internal ribosome entry site (IRES) and an EPG fused to an mVenus to express both constructs on the same plasmid. Readings were taken at 530 nm and 460 nm every minute for 30 minutes with or without constant static magnetic stimulation. Readings were normalized to the last read before stimulation. Fit line in each graph is a Lowess smoothing to show the relationship between the groups. Data is shown as mean ± s.e.m. N=15 wells were analyzed for the single and N=9 for the EPG IRES experiments. Statistical analysis was performed using unpaired t-test with Welch's correction at saturation timepoint of each experiment (T=2, A; T=7, B). A (*) denotes a p-value < 0.05.

3.2: Localization of EPG BRET construct

After performing the BRET study on the EPG protein we noticed an interesting aspect on the way the way the BRET constructs were cloned. These constructs were cloned in a way that should block the signal sequence and the membrane anchor sequence of the EPG. Therefore, we anticipated cytoplasmic expression. To test this, we co-expressed the EPG BRET construct as well as the EPG HaloTag construct that was previously shown to be membrane anchored in mammalian cells. Fluorescent images show the BRET construct was likely expressed in the cytoplasm as opposed to the EPG HaloTag fusion protein that is mostly observed on the cellular membrane. Figure 11 demonstrates the EPG BRET construct to be a cytoplasmic protein providing evidence to support that the membrane and signal sequences were blocked. The conformational change that occurs in the cytoplasm also indicates that the magnetoreception of EPG is not dependent of its cellular localization.

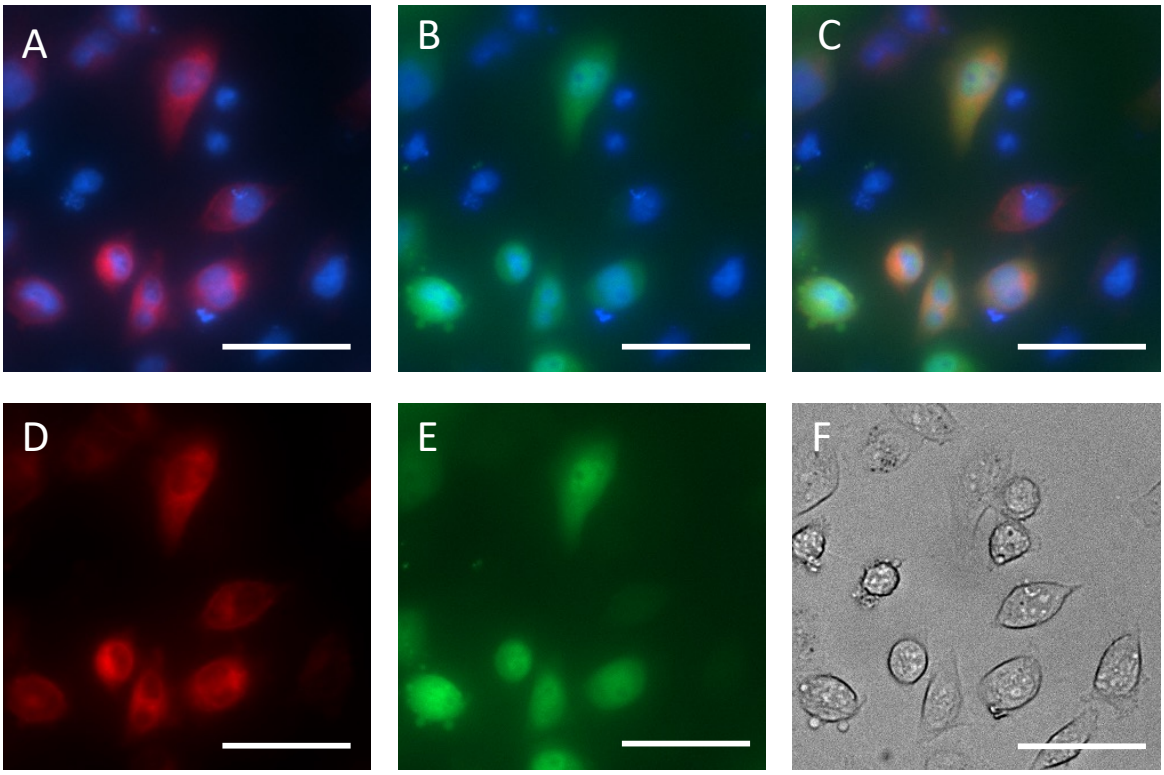

Figure 11: EPG BRET Fluorescent Imaging for Cell Localization. Hela cells cotransfected with EPG BRET construct and EPG N terminus HaloTag construct and imaged with 40x magnification. Hoechst dye was used as nuclear marker and imaged using the DAPI filter (Blue; A, B, and C). The EPG HaloTag construct was imaged using a JFX 650 dye with the Cy5 filter overlayed with nuclear marker (A) and without nuclear marker (D). EPG BRET construct was imaged using the GFP filter overlayed with nuclear marker (B) and without nuclear marker (E). Merged image of the three channels (C) shows expression of the EPG BRET construct in the cytoplasm and the EPG HaloTag construct on the cell membrane. (F) Phase contrast image of cells. Scale bar = 50 µm.

CHAPTER 4: Establishment of EPG split proteins

4.1: EPG Split EGFP

Due to the finding of EPG's magentoresponsiveness not being depending on cellular location, we sought to explore useful technologies for the cytosolic EPG. Split proteins, or fragmenting proteins or enzymes in a way that can be re-functionalized with a specific stimulus, was proposed as a tool to incorporate with EPG. Building upon the split protein concept and on the magnetoresponsive properties of the EPG, we looked to develop a new platform that allows remote activation of a protein or enzyme using electromagnetic fields (EMF). The principle for this tool is cloning the EPG between two parts of a split protein or between two enzymes/proteins that need close proximity for activation. The first construct to test this concept with EPG was the split EGFP. The design of this split construct was using the 144/149 split site of EGFP and fusing EPG in between the two parts of EGFP (Figure 12). This construct was transfected into HEK 293FT cells and stimulated with magnetic fields. After stimulation there was no measurable effect of the magnetic field.

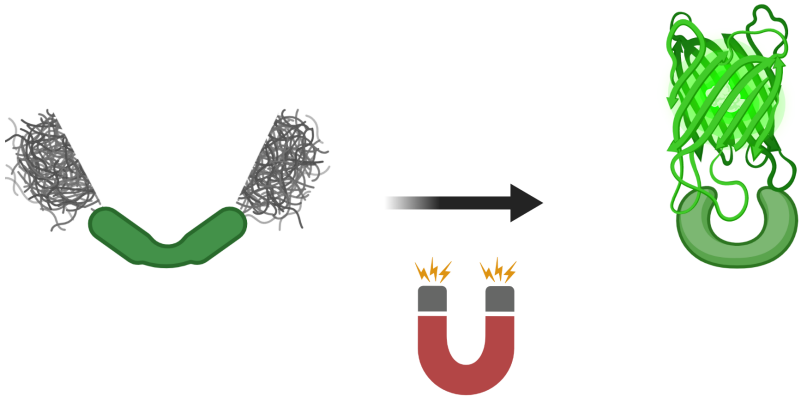

Figure 12: Schematic of EPG split protein concept using a green fluorescent protein. Under standard conditions the fluorescent protein should be inactive. With the addition of a magnetic field the split fragments would reconstitute and regain fluorescence.

This construct has a few flaws in the design of the protein and was probably not the ideal choice for the initial testing of the EPG split protein constructs. The split site chosen has been shown more with circularly permutated GFPs rather than true split protein constructs. Also, since the chromophore of the EGFP has to be in the correct geometry to become fluorescent, a design that allows for more stability of the beta barrel may be a more efficient choice for creating an EPG split fluorescent protein.

4.2: EPG Split NanoLuc

After the initial testing of the split GFP, we decided to test another split protein design. Here we split NanoLuc (171 amino acids) into two fragments at amino acid sites 65 and 66. The 1-65 and 66-171 fragments were fused to the N and C termini of EPG respectively (Figure 13A). We chose this split site based on previous reports[72] (Figure 13B). A truncated version of this construct was created by removing the signal sequence and membrane anchor sequence of EPG. Another construct was created by using the reverse nucleotide sequence of the truncated EPG and this was referred to as flipped trEPG.

When exposed to EMF, the EPG construct when measured in cell extract, the EPG construct displayed a 39.4±41.4% compared to control truncated or reverse truncated EPG (Figure 13C). Under the same condition but when measured in the intact cells showed up to 68.7±24.6% increase in luminescence in contrast to controls constructs (Figure 13D). We quantified the change in luminescence due to magnetic stimulation by subtracting the luminescence at the last read of stimulation by the last read before stimulation; then dividing by the last read before stimulation. Results of the changes in luminescence from each well from the lystate (Figure 13E) and whole cell (Figure 13F) groups show significant increases in luminescence from the EPG group when compared to the trEPG and Flipped trEPG groups. These results are the first demonstration that a split protein can be brought together by the conformational change of EPG. Thus, EPG can act as a magnetically activatable hinge.

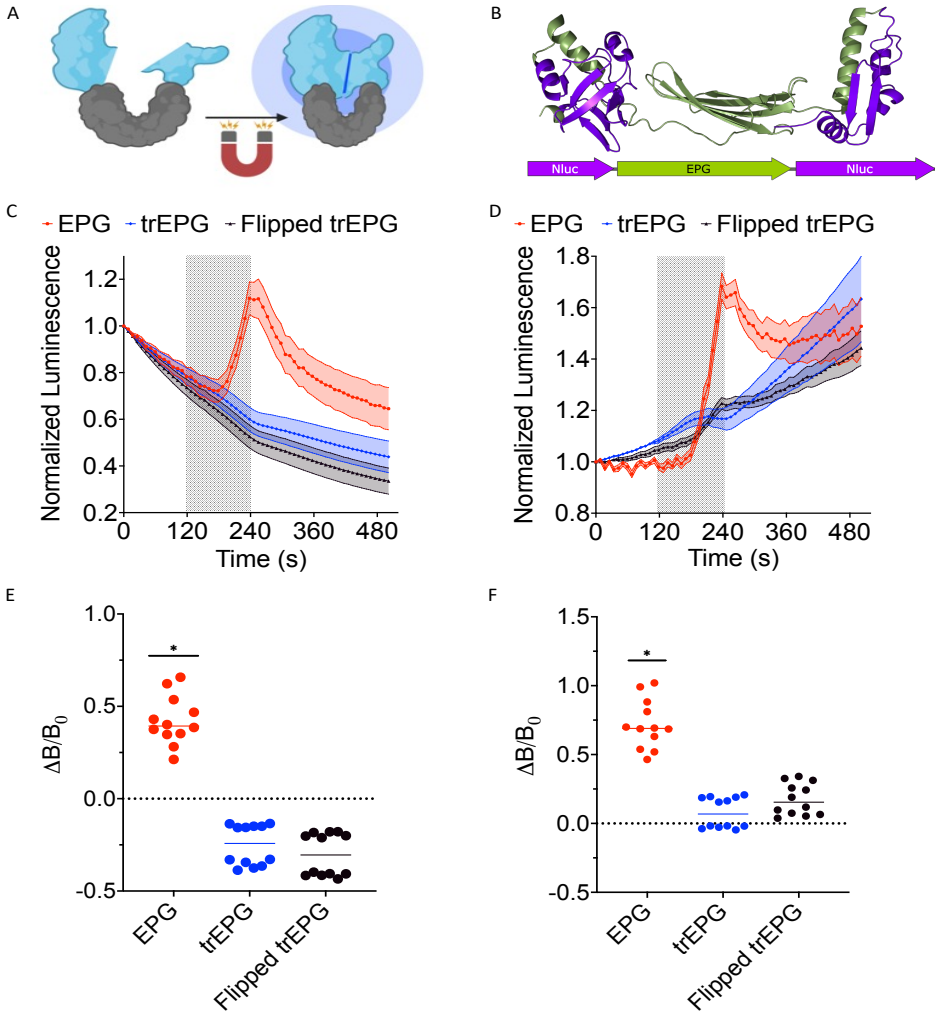

Figure 13: EPG split NanoLuc experiments in E. coli BL21 cells**.** Readings were taken on the IVIS every 10 seconds with an open filter. Electromagnetic stimulus was applied to the cells for 2 minutes and shown as shaded region. (A) Illustration of EPG split NanoLuc construct. (B) A model of the EPG split NanoLuc construct. E. coli Lysate (C) and whole cell E. coli (D) containing EPG split NanoLuc showed an increase in luminescence in contrast to EPG truncated and Flipped EPG. Data is shown as mean ± s.e.m. Change in luminescence from before and end of stimulus of each well in lysate (E) and whole cell (F) groups are shown with line at median. Results shown are duplicate experiments with N=6 wells in each trial. Statistical significance was calculated by an unpaired t-test with Welch's correction; A (*) denotes p-value <0.05.

EPG split NanoLuc was shown to work, but we wanted to see if we could make a more effective version of this construct. While it had a good response to magnetic fields, the overall brightness of the construct was not ideal. It was decided to use the NanoBiT[73] split site to create

new EPG split NanoLuc constructs. This site creates a large bit (LgBiT) which is around 18KDa and a small bit (SmBiT) which is around 1 KDa. NanoBiT constructs have been shown to be effective reporters for PCA assays by fusing the LgBiT to one protein of interest and SmBiT to the other.

Because it is not known what the mechanism of EPG's response to magnetic fields, multiple designs of the EPG split NanoBiT were created. The main aspects to look into when designing this construct were determining which terminus of EPG to fuse each of the BiTs (Large and Small) and determining if the transmembrane sequence is necessary for function of the protein. The signal sequence was not considered in this construct design due to its likelihood of being cleaved off and therefore not involved in the magnetoreception. With these considerations, four constructs were made. Two of which having no signal sequence or transmembrane domains with one having SmBiT on the N-terminus of EPG and the LgBiT on the C-terminus (SmLg) and one with the opposite configuration and the LgBiT on the N-terminus and SmBiT on the C-terminus (LgSm). The process was repeated using the EPG protein without the signal sequence but leaving the transmembrane domain in the protein creating two other constructs (SmLg TM and LgSm TM). A tandem copy of EPG (no signal sequence or transmembrane domain) was also cloned into the NanoBiT system with the LgBiT on the N-terminus of the tandem repeat and the SmBiT on the C-terminus. As a control a flipped DNA sequence of the truncated form of EPG was cloned into the NanoBiT system with the LgBiT on the N-terminus and the SmBiT on the C-terminus. These constructs were expressed in HEK 293FT cells then imaged on the IVIS and exposed to electromagnetic stimulation for two minutes followed by 2 minutes of reads without stimulation then another 2 minutes of stimulation. As shown in Figure 14A, the LgSm construct appears to have to best response to magnetic

stimulation compared to the rest of the groups. The change in bioluminescence during the first electromagnetic stimulation and the period between stimulations was significant compared to the Flip EPG control group (Figure 14B). The other groups did not show a response to magnetic stimulation until the second stimulation period. The exception to this trend was the dEPG construct which showed no response to stimulation. This could be due to a greater distance between the split fragments not allowing them to come together or counteracting of tandem EPG proteins. The one construct that is concerning is the Flip EPG construct which showed a small change in signal after the second stimulation indicating this change could be due to things other than magnetic activation such as heating of cells from constant electric current through coil.

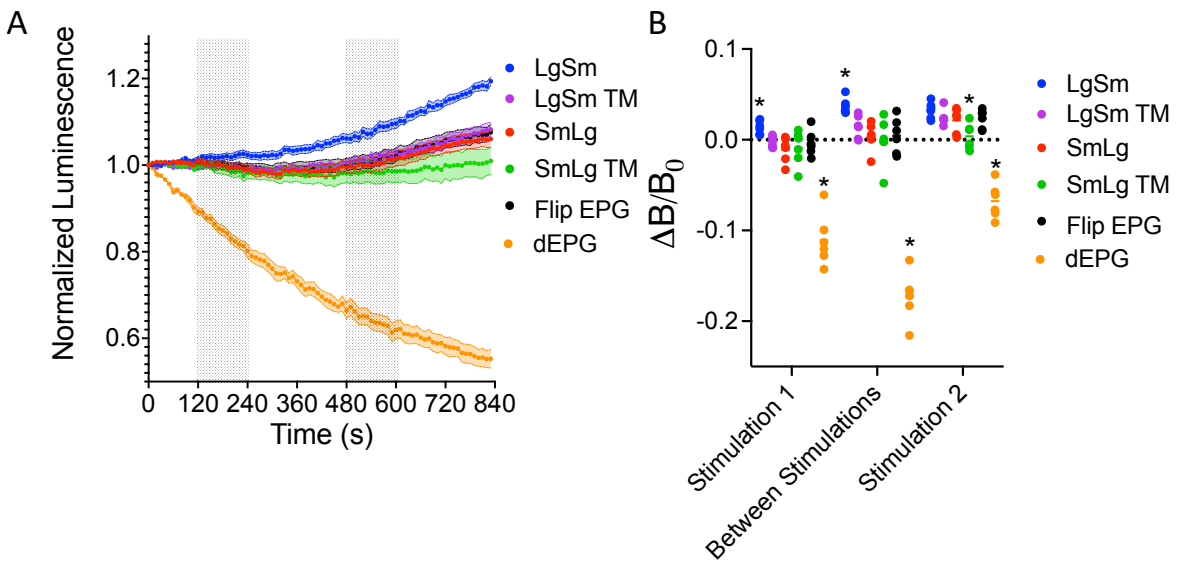

Figure 14: EPG NanoBiT variant testing in HEK 293FT cells. The screening was done with a combination of EPG constructs without the signal sequence. The TM represents the predicted transmembrane domain of EPG. The Sm and Lg denote the order of the small and large bits fused to EPG. dEPG is a consecutive repeat of the EPG gene and Flip EPG is a flipped DNA sequence of EPG. (A) Reads from 14 minute experiment taking reads every 10 seconds. Shaded regions are the times at which the electromagnetic stimulation was applied (2 minutes). Each construct was with N=6 biological replicates (wells) and data is shown as mean ± s.e.m on the graph. (B) Change in bioluminescent signal due to 1st and 2nd magnetic stimulation as well as the time between the stimulations. Statistical analysis was performed on the change in luminescence using an unpaired t-test and a Welch's corrections. A (*) denotes a p-value < 0.05.

To attempt to further optimize the split NanoBiT construct, we decided to explore different SmBiT variants. A higher affinity peptide called peptide 86 or HiBiT[74] was developed that would produce greater activity of the split enzyme. Since the LgSm orientation seemed to produce the best results, it was used as the template for the HiBiT constructs. Four variants were cloned using a combination of flexible (GGGGS) or rigid (PAPAP) linkers. For each of constructs, the letter that comes first designates the linker composition between the LgBiT and N-terminus of EPG and the second letter designates the linker between the C-terminus of EPG and peptide 86. A construct that obtained a point mutation in the cloning process was also included (mRF) as

it showed promise in preliminary screening. The two controls for this experiment were the Flip construct, which was cloned with flexible linkers and NanoLuc. Due to the apparent response of the EPG constructs to multiple segments of electromagnetic stimulation, we decided to have an experiment which incorporated four two-minute stimulation periods. After each stimulation there was 6 minutes of rest. When expressed in HEK 293 FT cells and imaged on the IVIS, each of the EPG constructs increases their bioluminescent output after the second stimulation and almost recovers the initial luminescence at the final read (Figure 15). Upon the conclusion of this experiment though, we noticed the electromagnetic coil and plate were abnormally warm.

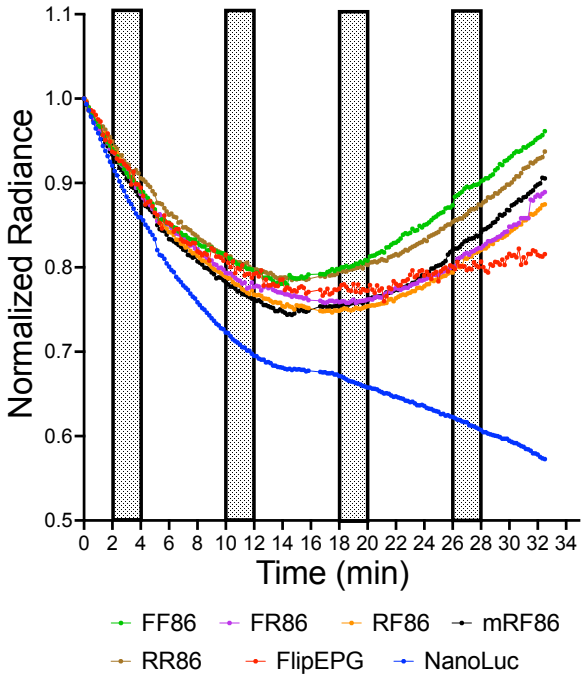

Figure 15: EPG NanoBiT constructs bioluminescence with four electromagnetic pulses. Each electromagnetic stimulus was given for 2 minutes followed by 6 minutes of no stimulus. Increases during and after 3rd stimulus likely due to increases in coil temperature.

We decided to test if this increase was due to heating and ran a temperature experiment on the coil with the same parameters as the EPG NanoBiT experiment. Figure 16 shows a rapid increase in temperature of the coil each time the current is run through the coil. Although the temperature dissipates slightly during the off period, at the end of the experiment the exterior of the coil reached a final temperature of 51.2 C after starting at 22.4 C. The interior of the plate had a similar trend but not as drastic starting at 22.6 C and rising to 24.5 C. There is a key difference in this experiment and the in the IVIS. This experiment was done at room temperature out on the bench with room temperature liquid in the plate. The IVIS experiment was performed in a closed instrument and heated staged (37C). With this in mind we believe this would not allow for heat to dissipate as quickly as it did on the benchtop, and therefore more than likely cause a

greater increase in cellular temperatures than the 1.9C increase on the benchtop. With this information we believe the effects that are seen in the EPG split NanoBiT were likely due to temperature increases rather than magnetic activation.

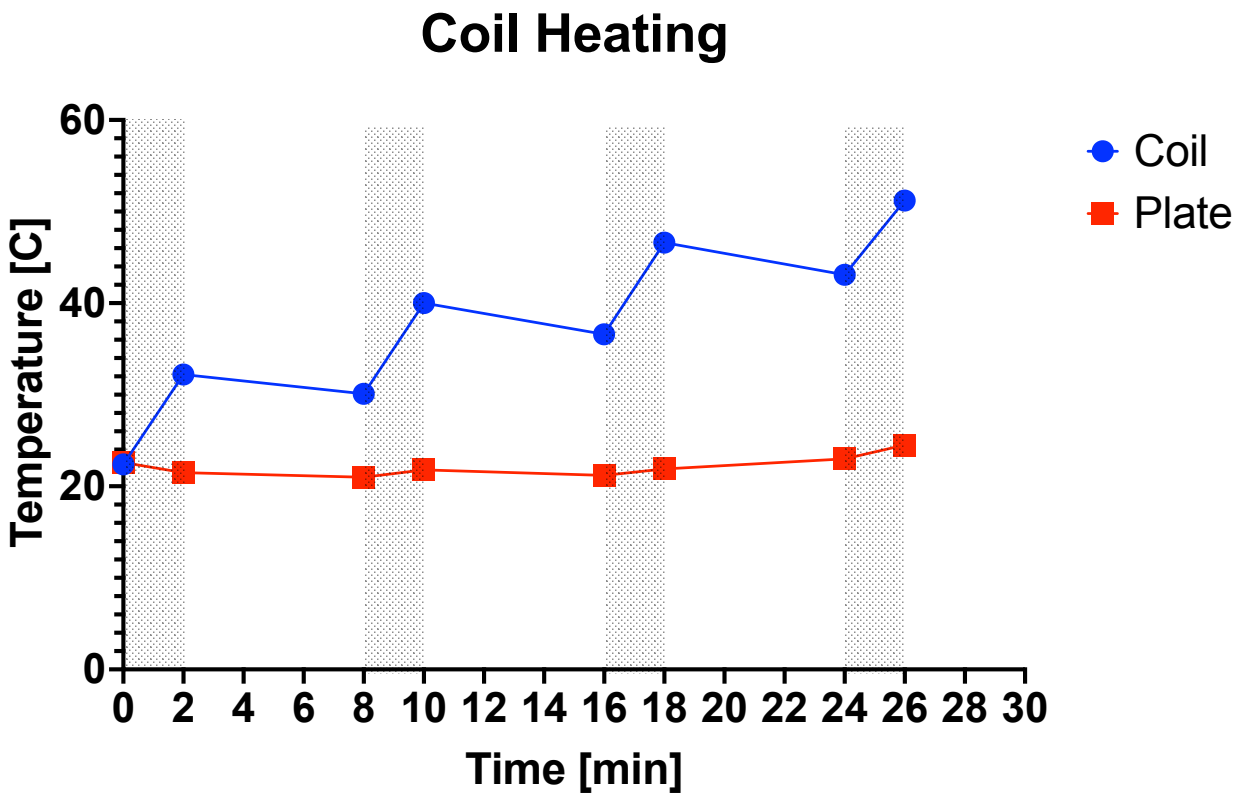

Figure 16: Temperature measurements of electromagnetic coil. Measurements were performed with a handheld infrared thermometer before and after electromagnetic stimulation. Coil was run at 15A for a 2-minute period shown in shaded region. Coil represents reads taken on the copper wire of the coil on the exterior of electromagnet. Plate represents temperature readings taken from a well filled with water in the center of the plate.

For the future of this project, I believe the linker optimization has to be further considered. With the starting brightness of these constructs, I believe the NanoBiT fragments have already reassembled and therefore should have no response to magnetic fields. If rationally designed linkers are not used, temporarily using the signal sequence and transmembrane domains has shown promise acting as helical linkers. While they may not be ideal, they could be

a starting point for optimization of other aspects. This could be potential of using a lower affinity variant of the SmBiT. This may cause less spontaneous reconstitution of the enzyme and still allow for a brighter construct than the original EPG split NanoLuc.

4.3: EPG Split APEX2

To demonstrate that the EPG split approach can be used as a platform technology, we used a Split APEX2 Peroxidase[75]. This system allows simplified demonstration of the concept that EMF can control an enzymatic reaction and the output can be measured directly with colorimetric or fluorescent reaction with any standard plate reader or potentially even a microscope. HEK 293FT cells expressing EPG split APEX2 treated with both static magnetic stimulus and hydrogen peroxide displayed a clear increase in fluorescence (150±16%; Figure 17) compared to the cells that did not experience magnetic stimulation. These results show a statistically significant increase in peroxidase activity in response to 30 minutes of exposure to static magnetic field. We also repeated this experiment at room temperature and 37°C and found similar results (Figure 18). These findings indicate that the EPG protein can be used as magneto-switch to activate multiple enzymes.

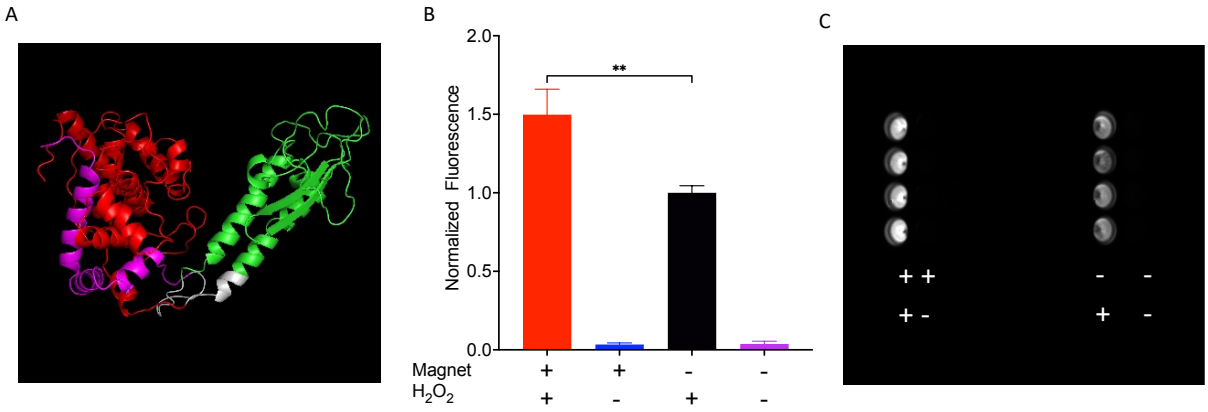

Figure 17: HEK 293FT cells expressing EPG split APEX2 show an increase in fluorescence in response to magnetic field. All wells were treated with Amplex UltraRed reagent and the four combinations of with or without magnetic stimulus and H2O2 for 30 minutes. (A) Predicted structure of EPG split APEX2 with EPG (green), AP fragment (red), EX fragment (magenta), and linkers (white). (B) Endpoint results of cells treated with all combinations of static magnetic stimulus and hydrogen peroxide (N=4 independent experiments with n=4 replicates per experiment). (C) Image of a plate taken with Cy3 filter after experiment for detection of resorufin

Figure 17 (cont'd)
accumulation. Statistical analysis was performed using an unpaired t-test with Welch's correction. The (**) denotes p-value <0.01.

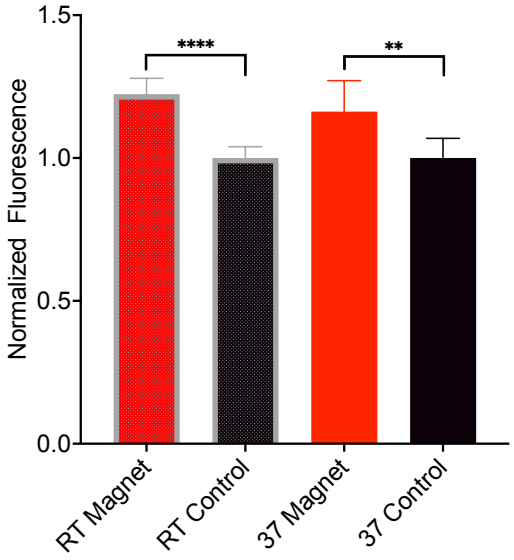

Figure 18: EPG split APEX2 temperature variation. Comparison of the EPG split APEX2 system at room temperature and 37C. Cells were either subjected to magnetic field (red) or no stimulus (black). N=8 biological replicates per group. Statistical analysis was performed using an unpaired t-test with Welch's correction. The (**) denotes p-value <0.01 and the (****) denotes a p-value <0.0001.

After the initial establishment of this EPG split protein, we again wanted to see if we could optimize the construct in a similar way to the EPG split NanoLuc constructs utilizing the split APEX2 platform. For this we created one construct with no signal sequence EPG (NoSS), one with No transmembrane sequence EPG (NoTM), a tandem repeat of the full EPG (dEPG) and a tandem repeat of no signal or transmembrane sequence EPG (dEPG NoSSTM). Another aspect we wanted to explore with these constructs is whether light plays a factor in the magnetoreception of EPG, since it plays a major factor in the magnetoreception in proteins such as Cry4. To test this, we ran the same stimulation of a static magnet at the top and bottom of cells as well as control cell with no stimulus. Two additional groups were added that were stimulated with an LED light as

well as a group stimulated with an LED light a magnet under the plate.

When the original EPG split APEX2 group was put under the magnet and control conditions, we see the same trend as before. When this group was exposed to LED light, we maintain the trend of the magnetically stimulated group having a higher fluorescence than the light only group with both groups higher than the magnet only group (Figure 19A). The NoSS group also showed the magnetic stimulation having a greater increase in signal when comparing the magnet stimulated group to the control. This group showed slightly more fluorescent signal in the light only group compared to the magnet and light stimulated group with both groups being higher than the magnet only (Figure 19B). The NoTM group had the opposite trend compared to the NoSS, with the magnet group showing the lowest response, but the magnet and light stimulated showing the greatest overall response (Figure 19C). The dEPG groups had the same trend as the EPG group with both magnetic stimulated groups producing more fluorescent signal than the controls of their groups and light stimulation producing more signal overall (Figures 19D and 19E). All constructs, with the exception of the NoTM construct, have shown the ability of EPG to control the split APEX2 construct (Figure 20). Although LED lights did create greater conversion of the substrate, it does not appear to have enhanced the activity of EPG.

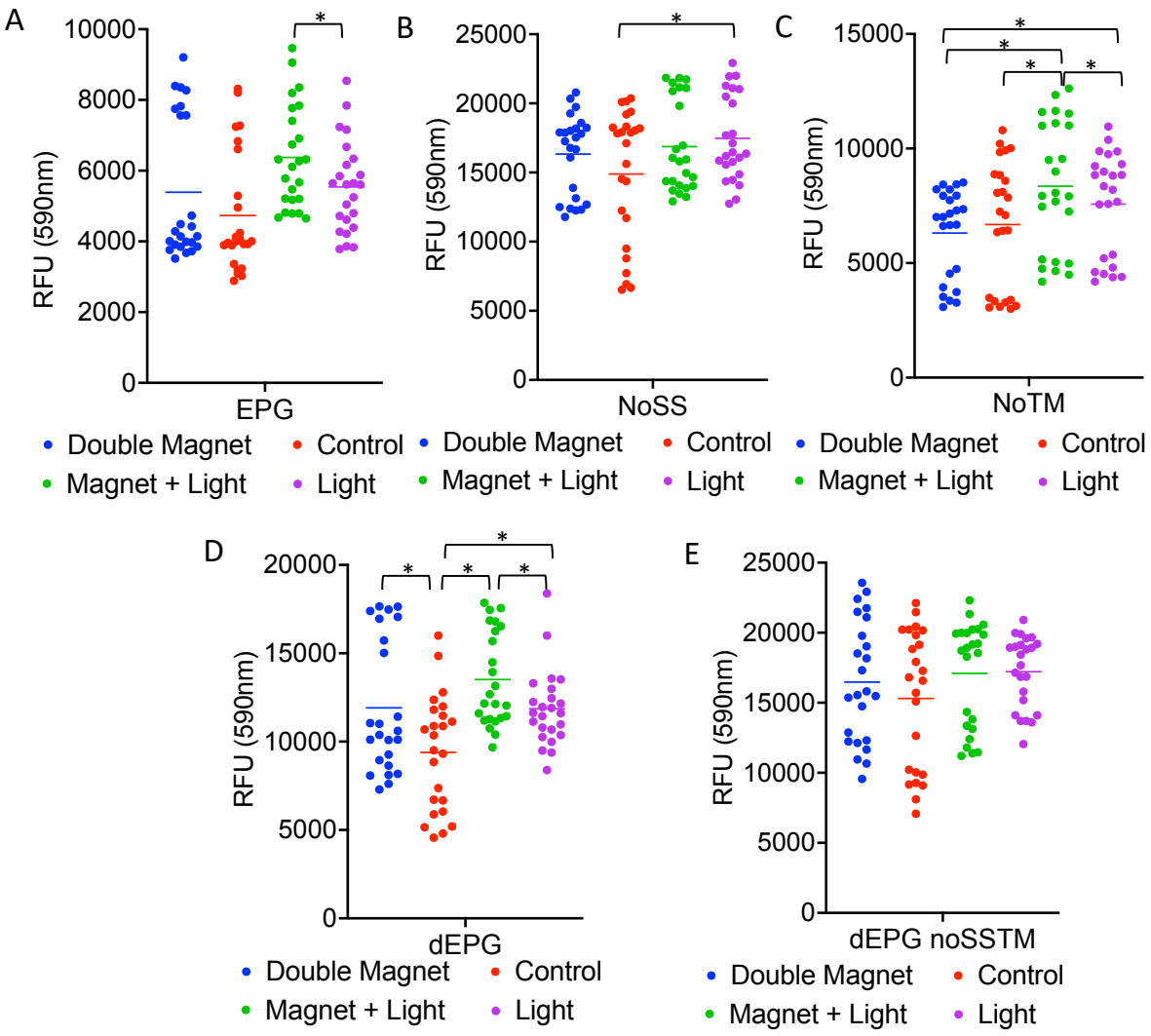

Figure 19: EPG split APEX2 variants stimulation by magnetic fields and LED lights. Stimulation with a magnet on top and bottom of plate (Double Magnet), no stimulation (Control), a single magnet under the plate with LED lights above well (Magnet + Light) or LED lights only (Light). The five EPG constructs were tested under these conditions were the full EPG (A), no signal sequence EPG (B), no transmembrane EPG (C), tandem repeat EPG (D), and tandem repeat of no signal or transmembrane sequence EPG (E). Graphs show the results of triplicate experiments with N=8 replicates per experiments. Statistical analysis was performed using an unpaired t-test with Welch's correction. The (*) denotes p-value <0.05.

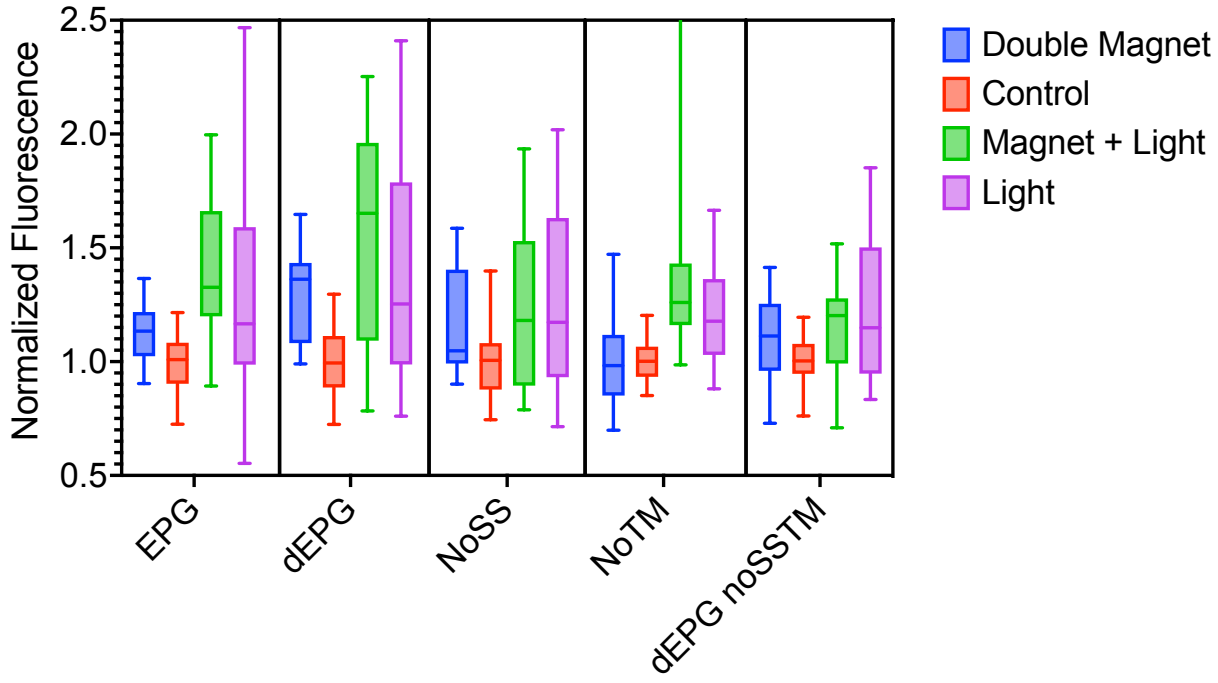

Figure 20: Normalized EPG APEX2 variants stimulation by magnetic fields and LED lights. Each construct was normalized to the control of their perspective group. The data shown is a of triplicate experiments with N=8 replicates per experiments.

We then wanted to explore the time dependency of the EPG split APEX2 variants. All the constructs other than the dEPG NoSSTM were analyzed for their activity at 5, 15, and 30 minutes. Figure 21A shows the EPG split APEX2 group with magnet consistently had higher fluorescence signal at each of the time point. An interesting outcome of this experiment was the dEPG group showed the opposite trend of the previous experiment, having the control group consistently higher fluorescence than the magnet stimulated group (Figure 21B). The NoSS group showed a similar trend to the EPG group with the magnet stimulated groups having higher fluorescence at each time point (Figure 21C). The NoTM group showed a different trend. The magnet stimulated group showed greater fluorescence at the 5-minute time point, and there was no difference between the groups at the 15 minute mark, and the control group with greater fluorescence at

the 30 minute time point (Figure 21D). This was interesting because it shows the possibility of an 'off' type functionality of the EPG split constructs rather than the activation we have previously shown.

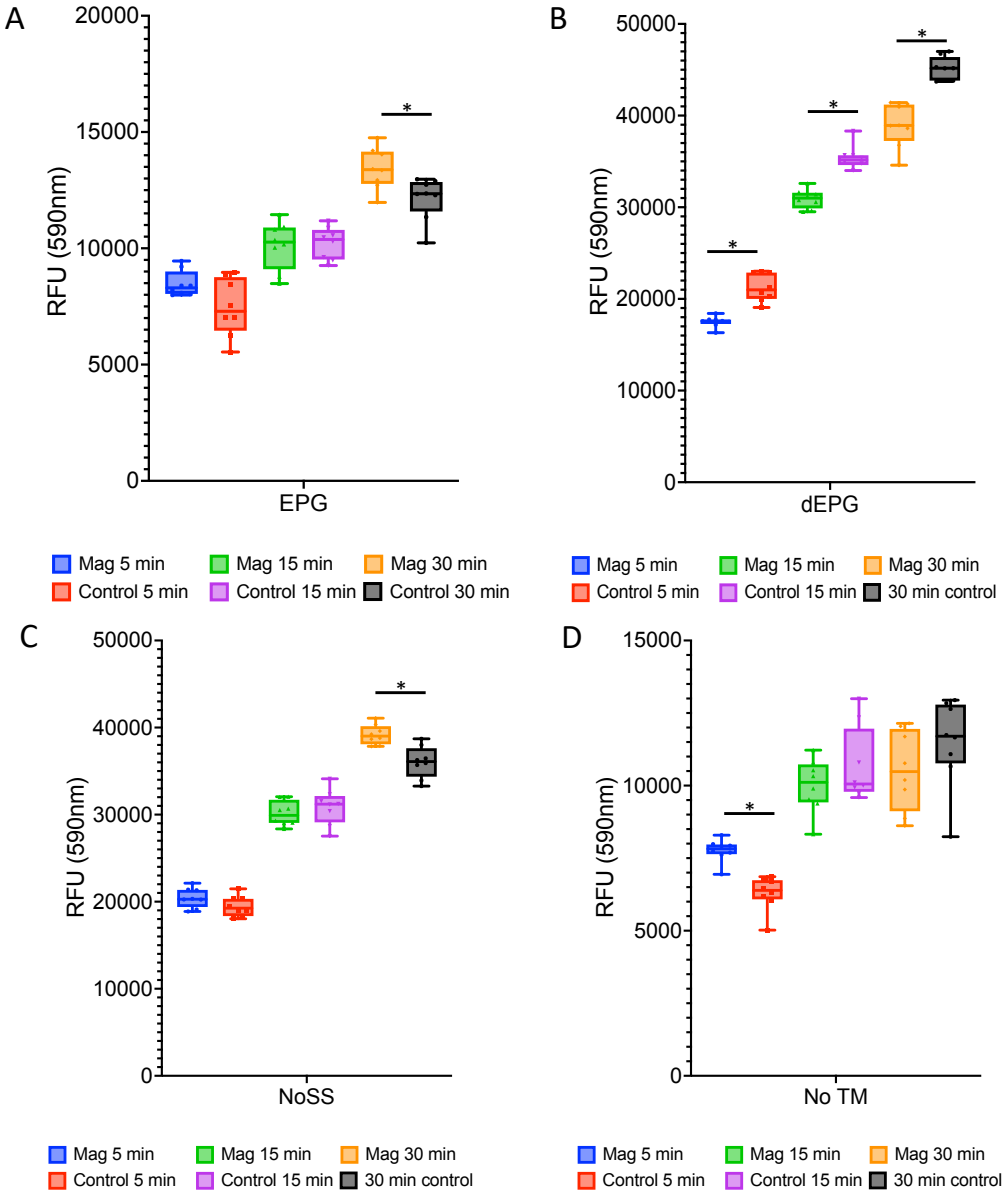

Figure 21: EPG split APEX2 variants at different time points. EPG (A) tandem EPG (B), No signal sequence EPG (C), and no transmembrane sequence (D) were measure at 5, 15 and 30 minutes under magnetic stimulation and control conditions. This data was run with N=8 biological replicates. Statistical analysis was performed using an unpaired t-test with a Welch's correction. A (*) denotes a p-value < 0.05.

For the future of the EPG split APEX2, I believe this project has mostly reached a good conclusion. This protein was never intended to serve a future application and was used to further establish the EPG split protein system. It did provide insights to designing split constructs that could be useful in future applications. Due to split APEX2 ease of use we can establish the signal sequence and transmembrane sequences are not needed for the magnetoreception but can contribute to the control of split proteins by acting as linkers or spaces between EPG and the split fragments. It does not seem like light plays a factor in this system but could be further validated in other systems that do not use fluorescent reporters to further confirm this hypothesis. This was also the first time we were able to show EPG being able to act as both an activator and repressor of the system depending on the composition of EPG in relation to the split fragments.

4.4: EPG Split HSV1-TK

The herpes simplex virus type-1 thymidine kinase (HSV1-tk) is a protein that has been using for both therapeutic and molecular imaging studies. One therapeutic example is the use of HSV1-tk with antiviral nucleosides such as ganciclovir or acyclovir for suicide gene therapy. This works due to normal cellular enzymes not being able to phosphorylate the nucleosides, which protects healthy cells. Cancer cells which can drive and express the HSV1-tk will uptake the antiviral nucleosides and the HSV1-tk can phosphorylate them which allows the natural cellular mechanisms to further phosphorylate the nucleosides and eventually get incorporated into the cell's DNA. Once incorporated, these nucleosides prevent DNA replication leading to cell death. This method has been previously shown in cells transduced with a HSV1-tk plasmid[76], but we wanted to see if we could produce similar results with using transiently transfected cells. To do this we transfected HEK 293FT cells with a HSV1-tk plasmid and subjected them to a range of ganciclovir concentrations for 24, 48 or 72 hours. Cell viability was measure using Cell Titer Blue (Promega). As expected after each day the viability of the cells drop compared to the control and their prospective groups on previous days (Figure 22). With these results, we found the best time and concentration combination would be 0.15mg/mL of ganciclovir for 72 hours.

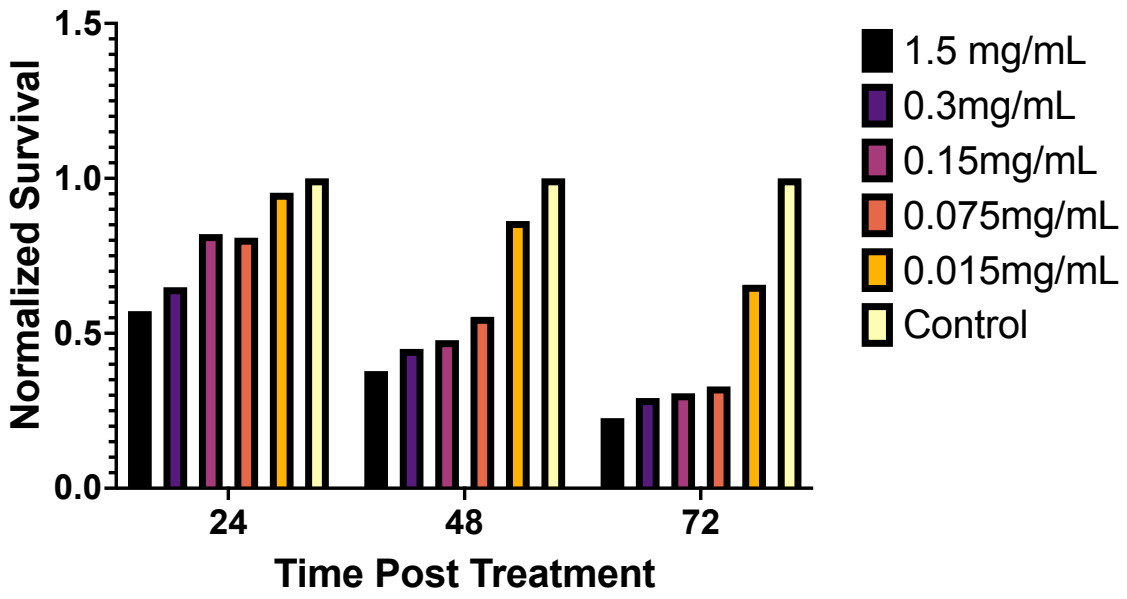

Figure 22: HEK 293FT cell survival with HSV1-tk ganciclovir treatment. Survival was normalized to control cells receiving no ganciclovir treatment. Cells were treated with varying concentrations of ganciclovir and measured at 24, 48, and 72 hours post treatment. Results are shown as single experiment with a bar corresponding to a single well.

After characterization of the HSV1-tk, we wanted to incorporate it into the EPG split protein family. The sr39 mutant of the HSV1-tk enzyme had been split previously[25] and was used at the template for creating the EPG split HSV1-tk. Two design approaches were taken to creating the initial EPG split HSV1-tk constructs. The first was to use the linkers from the original split tk which were 3 repeats of the GGGGS motif. From this the first construct was designed with N-terminus HSV1-tk-$GGGGS_3$-EPG-$GGGGS_3$-C-terminus HSV1-tk. This construct was deemed inconsistent most likely due to the size and flexibility of the linker so we decided to use a random linker library method to create better variants. For this method, we decided to use a BCT mutagenic primer method to create new variants. By using this we limit the choices in amino acids to only serine (UCT), proline (CCT) and alanine (GCT). This method has been shown to help optimize linkers and performance of genetically encoded sensors[77]. We decided to shorten the

linkers to 8 amino acids and use 8 repeats of the BCT primers. For the initial screening 5 colonies were tested against the positive control of HSV1-tk, negative control of cells with no plasmid, and the original EPG split HSV1-tk. When viability was examined after 72 hours all groups other than the control, showed lowered viability due to magnetic field stimulation (Figure 23).

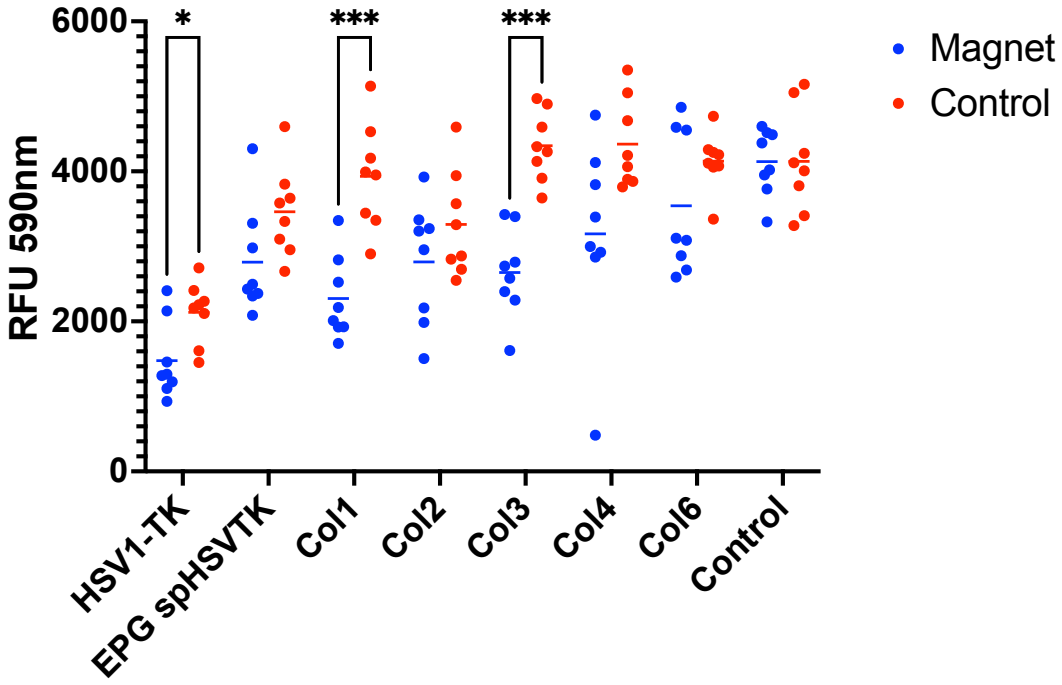

Figure 23: Initial test EPG HSV-tk linker variant screening. Viability was measured using Cell Titer Blue and fluorescence measurements were performed at 590nm. Each construct was treated with ganciclovir for 72 hours before viability reads. Magnetic stimulated groups were treated for the entire duration of ganciclovir treatment. Data shows means and all N=8 replicates. Statistical analysis was performed using an unpaired t-test with a Welch's correction. A (*) denotes a p-value < 0.05 and a (***) denotes a p-value <0.001.

The initial screening showed promising results, so we scaled up the amount of colonies screened to 16. Each of these variants were miniprepped and transfected into 4 wells of a 384 well plate of HEK 293FT cells. Figure 24 shows the results of this initial screen. This screen had a good distribution of low to high enzyme activity as well as activation and deactivation due to magnetic fields.

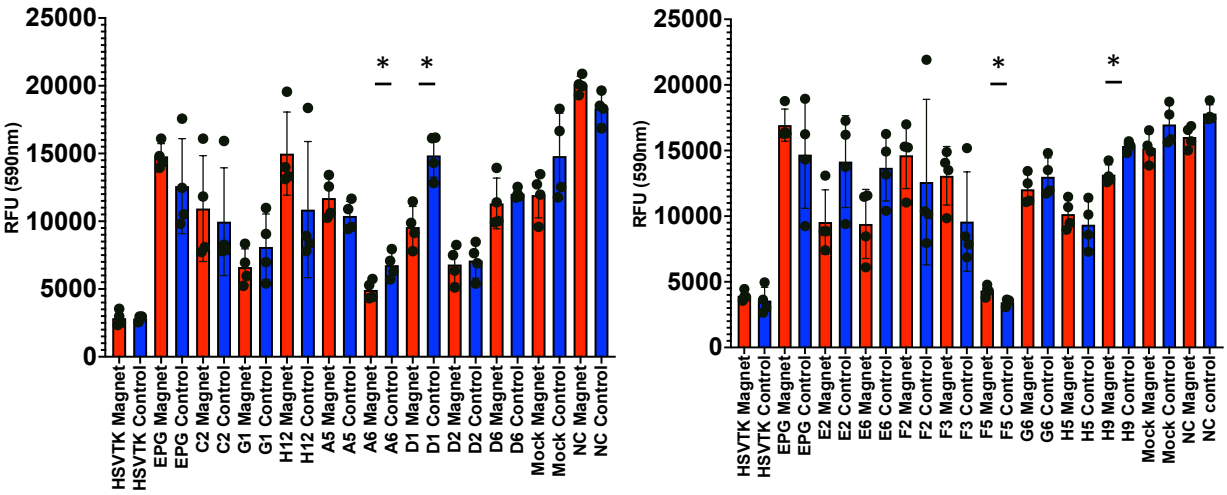

Figure 24: First round of EPG HSV1-tk linker screening in HEK 293FT cells. Groups were subjected to magnetic stimulation for 72 hours and compared to group with no stimulation. Viability measurements with Cell Titer Blue and 590nm fluorescent reads. Data shown is mean and individual with N=4 for each group. Statistical analysis was performed using an unpaired t-test with a Welch's correction. A (*) denotes a p-value < 0.05.

To verify these results, the experiment was repeated and the results can be seen in Figure 25. The constructs that showed the same or similar activity to the first screen were further sent to sequencing. Unfortunately, after analysis of the sequencing results, only one construct came back without a mutation. This result showed the BCT cloning method may not be a suitable method for linkers larger 8 amino acids or with a low sensitivity screening tool.

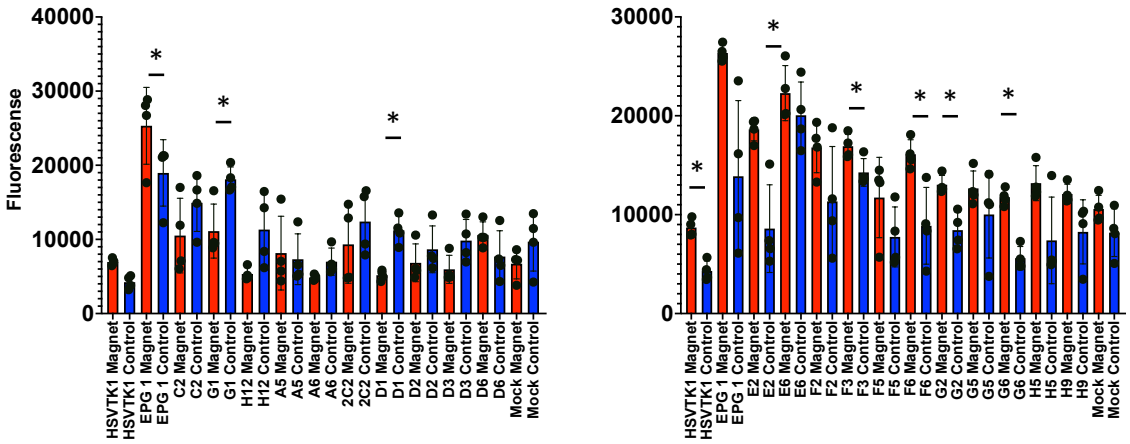

Figure 25: Repeat of EPG HSV1-tk linker screening in HEK 293FT cells. Groups were subjected to magnetic stimulation for 72 hours and compared to group with no stimulation. Viability measurements with Cell Titer Blue and 590nm fluorescent reads. Data shown is mean and individual with N=4 for each group. Statistical analysis was performed using an unpaired t-test with a Welch's correction. A (*) denotes a p-value < 0.05.

The next step with these constructs was to move to a rational design approach to linkers as we did with the NanoBiT variants adding the flexible (GGGGS) and rigid (PAPAP) linkers. These constructs were transfected to cells and split 24 hours post transfections at two cell dilutions. Figures 26A and 26B show the magnet stimulated group had a lower viability than that of the control groups. The surprising result was some of the EPG split HSV-tk groups having a higher viability than the control.

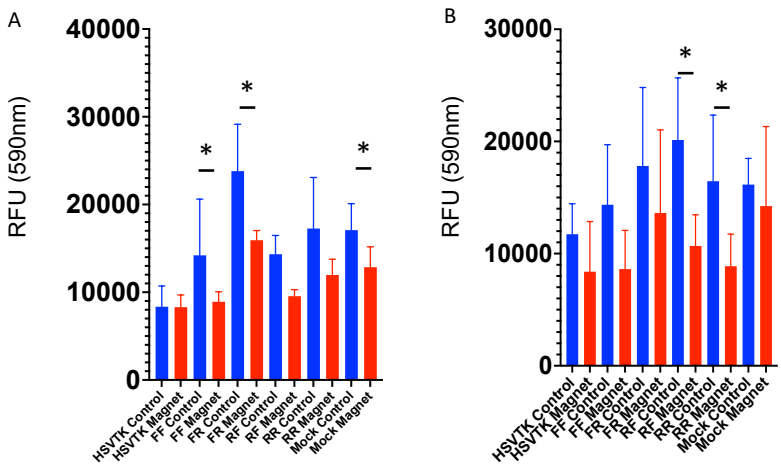

Figure 26: Rational linker design screen of EPG split HSV1-tk with ganciclovir in HEK 293FT cells. Cells were plated at (A) 1x concentration and (B) 1/2x concentration. Fluorescent readouts from constructs after 72 hours of GCV treatment with and without magnetic stimulation. Data is shown as mean of N=4 wells. Statistical analysis was performed using an unpaired t-test with a Welch's correction. A (*) denotes a p-value < 0.05.

We expanded the EPG groups to add the shortened versions of EPG without signal and transmembrane sequences. When the experiment was repeated with these additional constructs, we noticed a difference in the groups along with groups showing higher viability than the control (Figure 27). This is likely to do with too high of a number of cells seeding into the well. This causes the control cells to overgrow and thus be less viable, whereas the groups with low enzyme activity can still have room to continue to grow. After this was discovered a lower seeding number of cells was used and we were able to effectively screen these constructs to obtain reasonable results.

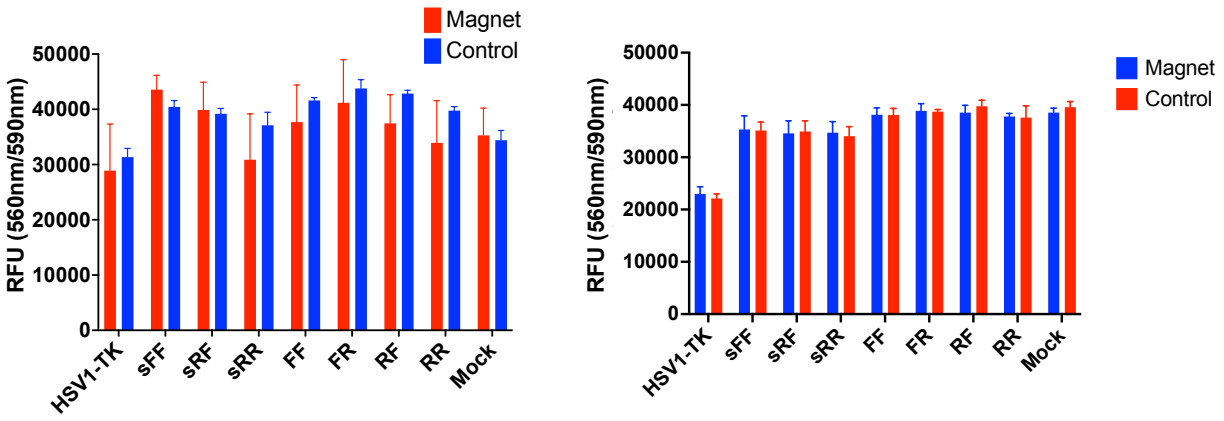

Figure 27: EPG variants screening of EPG split HSV1-tk in HEK293FT cells. Fluorescent readouts from constructs after 72 hours of GCV treatment with and without magnetic stimulation. The lowercase "s" denotes EPG without signal sequence and membrane sequences. The capital "F" denotes a flexible linker and capital "R" denotes a rigid linker. Statistical analysis was performed using an unpaired t-test with a Welch's correction. No constructs were found to be significant.

We decided to switch cell lines 4T1 cell line that constitutively expresses firefly luciferase. This is advantageous as the luciferase is an ATP dependent enzyme and thus can be used to assess cell viability. Figure 28 shows these results with two of the groups, sRR and FR, having statistical significance between the magnetic stimulated and the control group. Due to having less background than the sRR, we decided to move forward the FR group for future experiments.

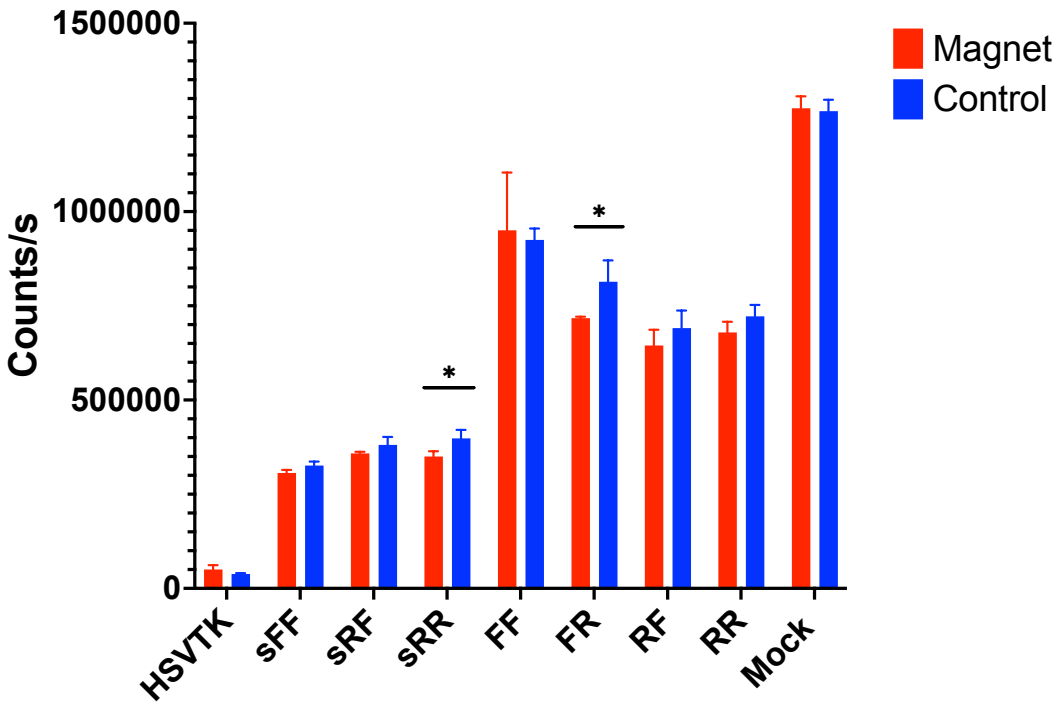

Figure 28: Linker Screening of EPG-HSVTK constructs in 4T1 Cells. Bioluminescent readouts from constructs after 72 hours of GCV treatment with and without magnetic stimulation. The lowercase "s" denotes EPG without signal sequence and membrane sequences. The capital "F" denotes a flexible linker and capital "R" denotes a rigid linker. Statistical analysis was performed using an unpaired t-test with a Welch's correction . The (*) denotes a p-value <0.05.

To further aid in this experimental design, the majority of the protocol was then moved toward a liquid handling robot for all cell plating and transfections. This not only helped to remove bias from manual pipetting, but also allowed us to shorten the protocol as cells were transfected in the 96 well plate rather than split after transfection in larger (6 or 12 well) plate. From this improved protocol we ran 8 more replicate experiments with the FR version of the EPG split HSV1-tk construct. Eight experimental replicates were performed comparing magnetic stimulated cells and non-stimulated cells. In each of these replicates the mean of luminescence of the EPG-HSV1-tk magnetic stimulated cells was lower than the control EPG-HSV1-TK cells with the average percent change between these groups of 10% (Figures 29B and 30A-H), the

probability for such event is 0.00039; (see methods for statistical calculation). This was not the case with the HSV1-TK (Figures 29B and 30I-P) and mock transfected (Figs. 29B and 30Q-X) groups which have an average of 3.6% and 1.3% respectively. In both these control groups there was no consistent trend of cell viability due to magnetic stimulation as both groups showed three experiments with lower average cell viability and five experiments of increased in cell viability in the presence of magnetic field (Fig 29B; the probability for such event is 0.375). Therefore, it appears that even in a complex system such as EPG split HSV1-TK and GCV, a significant yet small effect of magnetic field can be measured (Figures 31-33). Together with the other experiments, our finding implies that EPG can be used as a bio-magnetic switch for remote magnetic activation of enzymes.

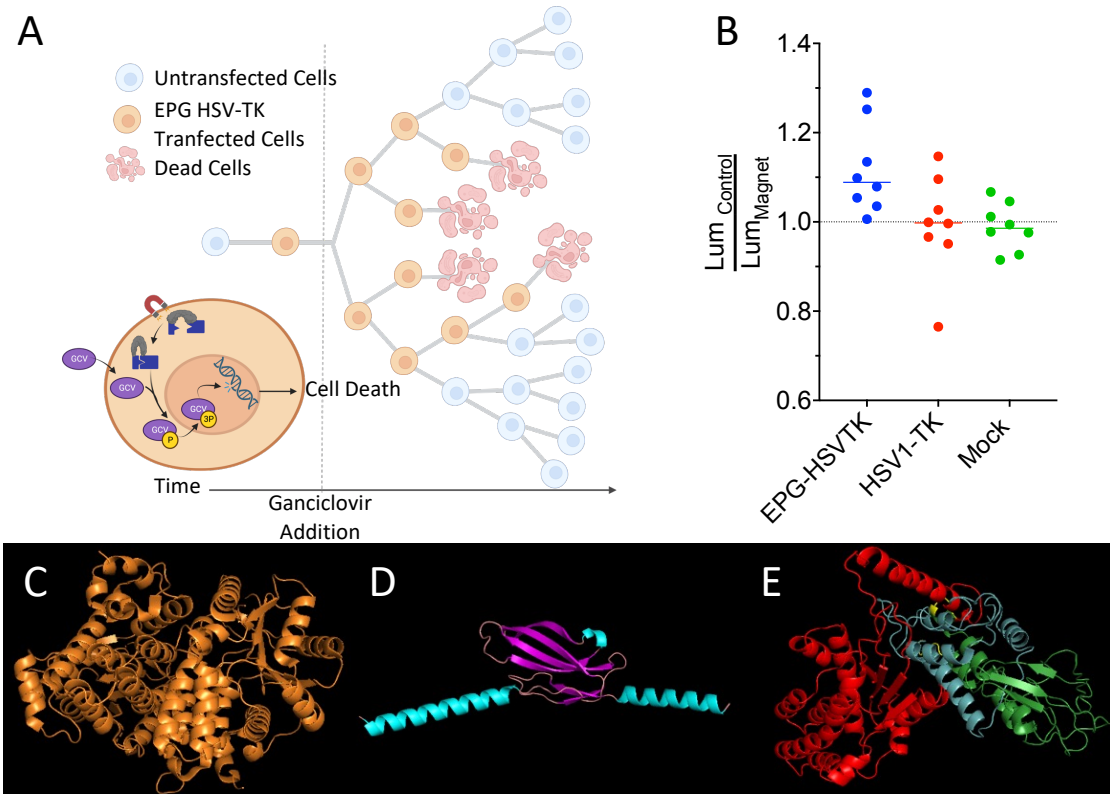

Figure 29: Ganciclovir Mediated Cell Death; Control vs Magnet. (A) Schematic of the experimental process and design. (B) The ratio of average control cell luminescence to magnetic stimulated cell luminescence over the course of eight experimental replicates. (C) Structure of HSV1-TK; (D) predicted structure of EPG with core structure (purple) and signal sequence and membrane anchor sequence (teal), (E) and predicted structure of EPG split HSV1-TK with N-terminal HSV1-TK (red), EPG (green), and C-terminal HSV1-TK (blue).

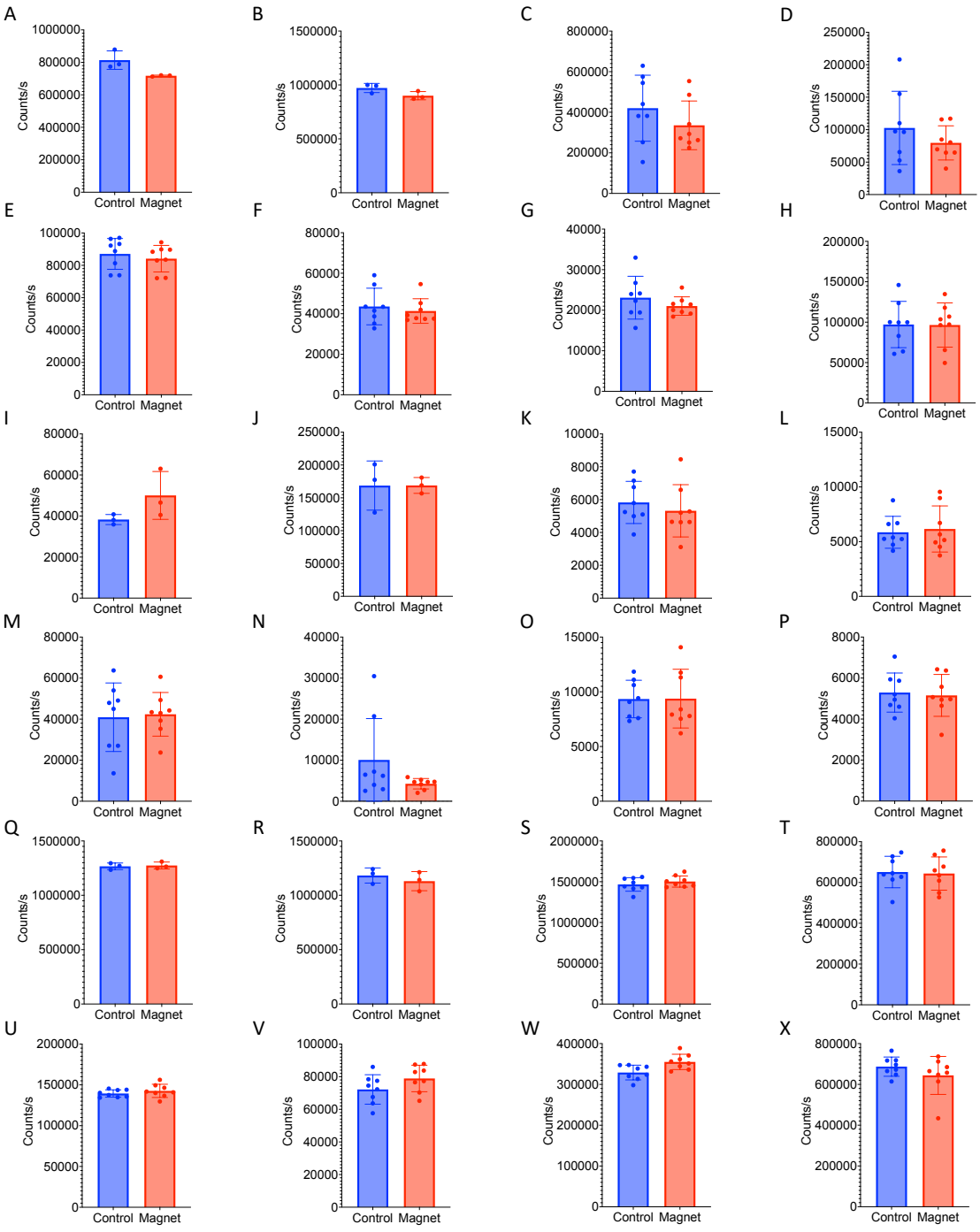

Figure 30: Ganciclovir mediated cell death in 4T1 cells. Cells expressed the EPG split HSV1-TK construct (A-H), HSV1-TK construct (I-P), or were mock transfected (Q-X) and cell viability in either a magnetic stimulated or control conditions.

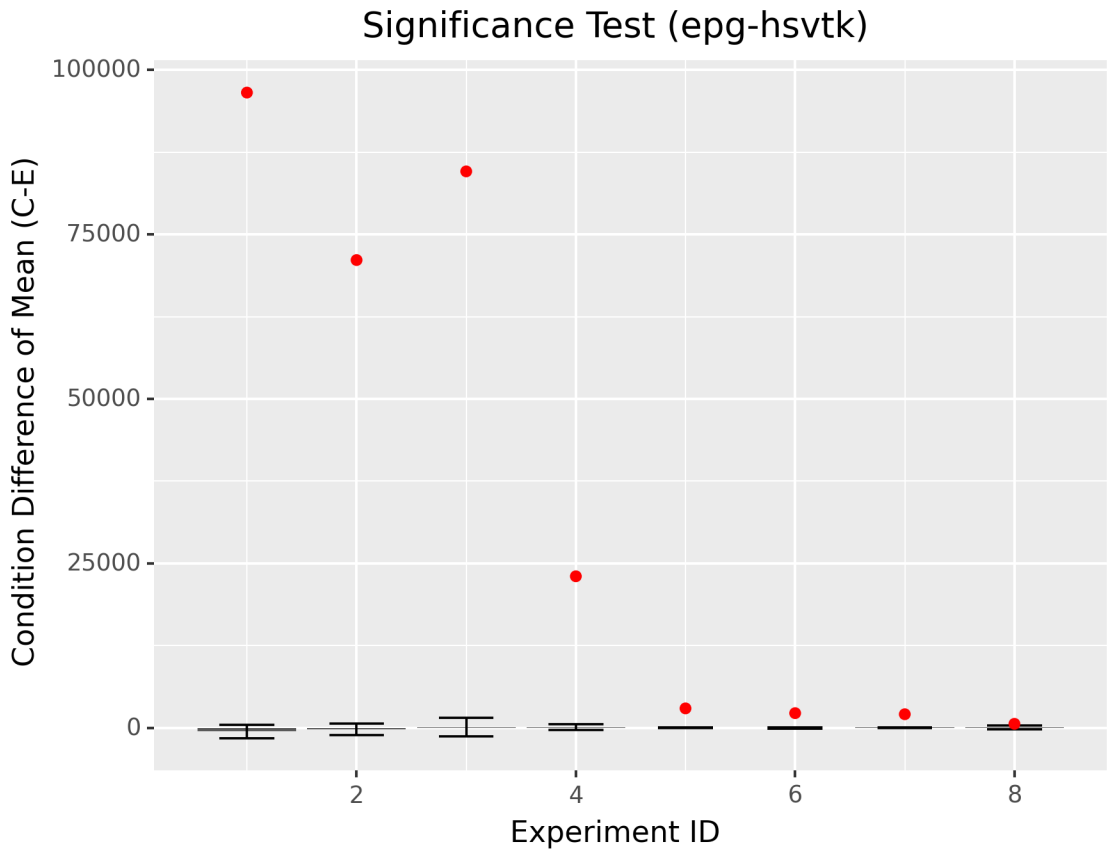

Figure 31: Significance Testing of EPG-HSV1-TK construct for Ganciclovir mediated cell death in 4T1 cells.

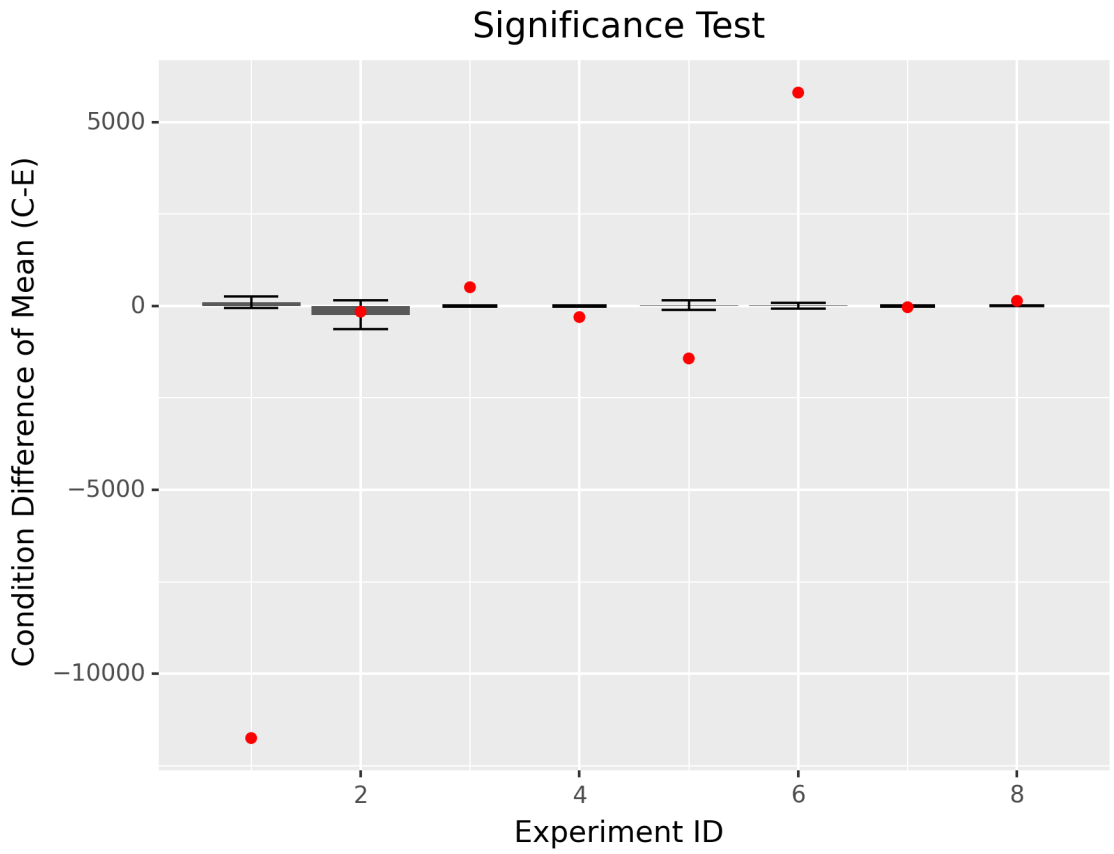

Figure 32: Significance Testing of HSV1-TK construct for Ganciclovir mediated cell death in 4T1 cells.

Figure 33: Significance Testing of Mock construct for Ganciclovir mediated cell death in 4T1 cells.

The final experiment we wanted to test is to see whether this EPG split HSV-tk could be used in molecular imaging to selectively trap imaging agents. One compound that has been used in conjunction with HSV1-tk for molecular imaging purposes is the I-124 labeled FIAU. This radionuclide is a PET agent with a half-life over 4 days. An uptake experiment was attempted on consecutive days with each of the EPG constructs and controls. The results after 2, 4 and 6 hours of uptake and stimulation are shown in Figure 34. This experiment did not show effective uptake of the radionuclide in any of the groups. All EPG groups showed lower uptake than the control. This experiment was done before the move to the liquid handler and EPG groups could have had lower cell counts attributing to the appeared lowered enzymatic activity.

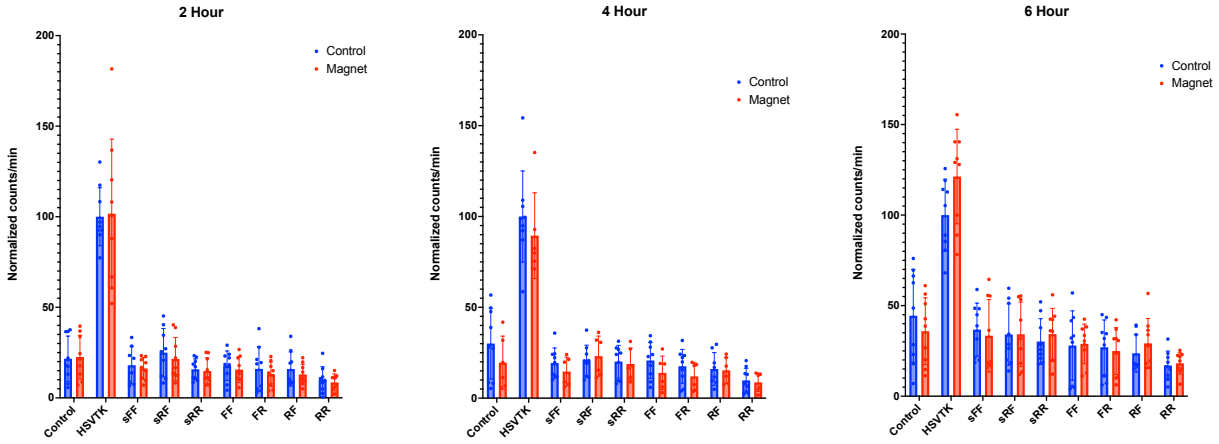

Figure 34: Uptake of I-124 FIAU in 4T1 cells. Uptake was measured at 2, 4 and 6 hours after the addition of the radionuclide. Stimulation was given with magnet for the entire duration. Results are shown as mean and standard deviation of 3 experiments with points for replicates N=3 per experiment. Statistical analysis was performed using an unpaired t-test with a Welch's correction. No data was found to be statistically significant.

The future of this project seems very promising. I believe to get more consistent results, using a stable or transduced cell line could lead to lower variability and better results. Because the ganciclovir experiments were done with transient transfection, after time the cells have the ability to lose the plasmid and the untransfected cells could become the majority of the well. The stable/transduced line would also allow for the ease of translating into rodent models for *in vivo* imaging applications. Currently we are working to test EPG split HSV-tk with F-18 FHBG as an alternative to the I-124 FIAU because of price and ability to manufacture in house with collaborators.

4.5: EPG Split Beta Lactamase

The final split protein that is currently a work in progress is EPG split beta lactamase. This protein is most known for resistance to beta lactam antibiotics such as ampicillin. The EPG split

beta lactamase was cloned using the split site from a currently split version. Once designed we expressed it in a pLacIQ vector for characterization. We wanted to determine what the OD600 to antibiotic ratio should be for effective use of this construct. Figure 35 shows the effect of different concentrations of antibiotics on different starting OD600 of bacteria cultures overnight. This graph shows the 50ug ampicillin/mL is most effective at selection of the EPG split beta lactamase.

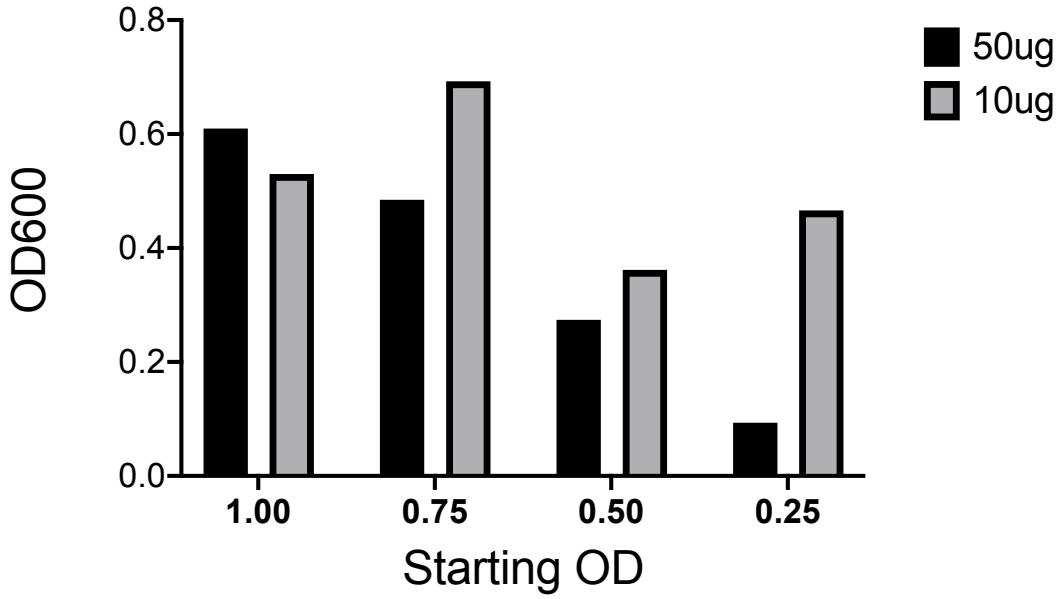

Figure 35: Growth of EPG Beta Lactamase with Ampicillin. Overnight OD600 of EPG beta lactamase at different starting OD600s and concentrations of ampicillin. Results are shown as a single culture (n=1) for each condition.

To further explore this starting OD range, we ran a second experiment and found a significant drop in overnight OD600 after a starting OD600 of 0.6 (Figure 36). This data suggests a max OD600 of 0.5 in combination with 50ug/mL ampicillin would be the best way for selection of EPG split beta lactamase to see if magnetic fields can activate the system.

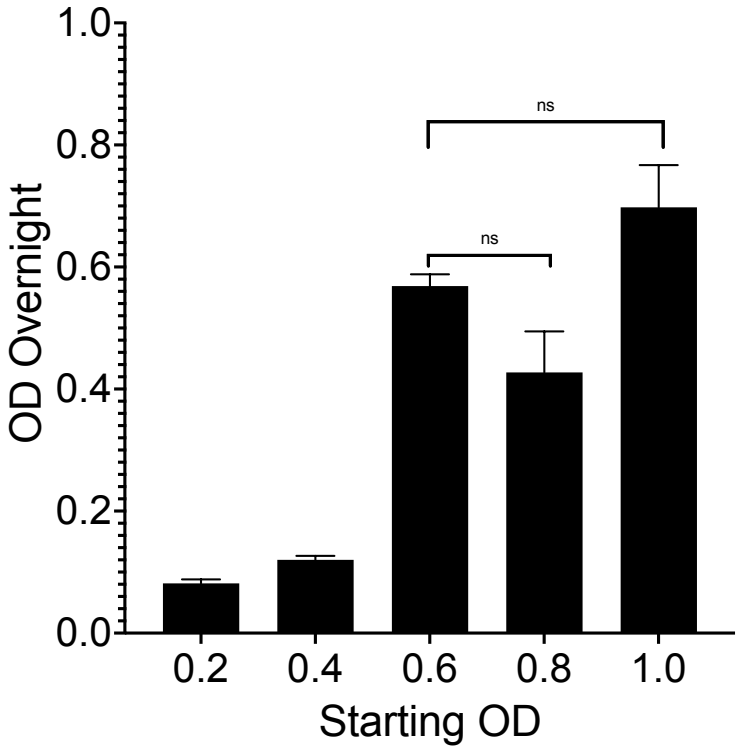

Figure 36: Overnight OD600 Measurements of EPG Beta Lactamase with varying starting concentrations. Results are shown as mean ± standard deviation and N=3 biological replicates. All columns were statistically significant to each other unless noted as 'ns'. Statistics were performed using unpaired t-test with a Welch's correction.

To further analyze this system, we used a colorimetric substrate nitrocefin to evaluate the EPG beta lactamase activity and can be read at 486nm. To test the EPG beta lactamase construct with the colorimetric assay we used overnight cultures and serial diluted them into wells on separate ends of a plate. Half the plate was stimulated with magnetic field and reads were taken 15 minutes for one hour. As shown in Figure 37 the magnetic stimulated groups at each cell dilution converted more of the nitrocefin substrate.

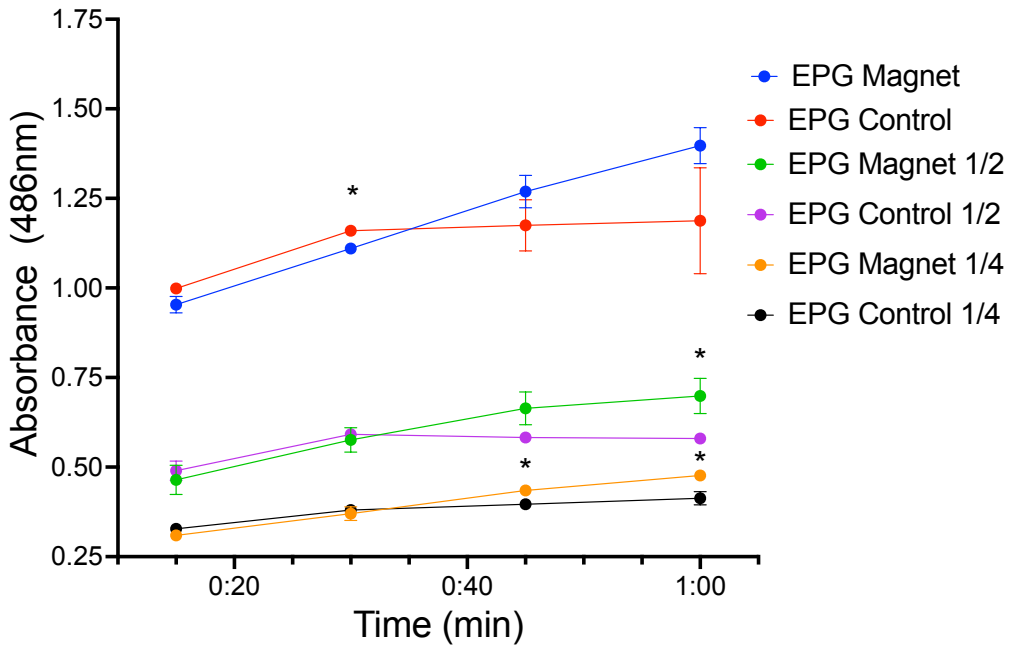

Figure 37: Colorimetric Assay for EPG beta lactamase activity. Data shown is a single experiment with mean ± standard deviation and N=3 biological replicates. Statistics were performed using unpaired t-test with a Welch's correction. A (*) denotes a p-value < 0.05.

This project is very early in development. It does provide a good platform for the potential of EPG mutagenesis screening. It can eliminate the nonresponding variants while amplifying the highly responsive mutants. Much more work needs to go into developing this further and establishing an optimal version of this construct, but the initial groundwork has been established and could lead to interesting discoveries of EPG.

CHAPTER 5: CONCLUSIONS AND FURTHER DIRECTIONS

The use of gene and protein engineering techniques to create tools for synthetic biology was the overarching goal of this thesis. While there was a range of success shown throughout, it should provide a good basis on future designs and applications of these technologies. An important aspect of this work is that there was very little optimization of the constructs made. Many were just made from linkers and backbones of the existing systems they were cloned from. Because of this, more work can be done on each of these constructs to create a more optimal design and response.

EPG has been shown to be an effective tool in various systems. To expand the use of this protein more work can be done on the functionality of the protein. This should be done with identifying the calcium signaling pathway as well as the magnetoreceptive properties. Determining what the mechanism of the magnetoreception is likely the most important thing to study in the future. The understanding of this mechanism will allow for better use of both EPG and EPG split systems. In terms of the magnetoreception, much should be explored on the biophysical aspects of the EPG. Work to discover potential cofactors that allow for the conformational change would greatly help in use of this protein in split systems. This would also allow for the characterization of the split systems in purified systems. Identifying the interacting protein(s) of EPG can help to better utilize EPG and perhaps learn the limitations of this protein. Since it is likely taking the place of its closest homologs, it can lead to insights on which cells EPG would or would not work well in depending on use of its interacting partner. The final aspect I believe will be very important to moving this project forward will be the generation of the crystal structure of the EPG protein. This will allow for better creation of EPG split proteins as the linkers

and split fragments will be able to be rationally designed, which should save time and resources.

A future direction of the EPG split systems is to move into *in vivo* (rodent) models. The reasons magneto-activation could be a better alternative to light or chemical stimulus are amplified with *in vivo* models. Cell culture work does not have issues of penetration depth or equal distribution to the extent that a rodent model would have. Moving the EPG split protein work could be very important to providing evidence magneto-activation could be a viable alternative.

CHAPTER 6: METHODS

6.1: Statement of rigor and transparency

We adhere to the following principles and good laboratory practices. The statistical analysis associated with this project will be performed with senior biostatistician faculties at the "Biocomputation and Biostatistics Core" at MSU. Briefly, all in vitro biological experimentation is conducted using a minimum of three or more independent biological repeats and referred here as n for the data shown unless stated otherwise. For data with $n < 3$, further repeats will be conducted, or the key conclusions will be verified by alternative means. Statistical analyses are carried out using t-test and ANOVA using the Graphpad Prism statistical software. P values less than 0.05 will be regarded as statistically significant. To diminish bias, we rely on objective quantitative analyses, repeats of the data processing by multiple members of the lab and/or by collaborators. Authentication of key resources is provided separately. All personnel are informed of potential health risks and monitored closely according to established best practices.

6.2: Engineering Novel Synthetic Protein for Binding Gadolinium

6.2.1: Protein Expression

Proteins were expressed by E. coli (BL21*) that had been transformed with the cloned pET101 vectors containing the GLamouR constructs. Cells were incubated with ampicillin-spiked (100 µg/mL) Magic Media for 24hrs at 30C, shaking at 300-360 RPM. Expression and purification were verified via Western Blot against the V5 tag.

6.2.2: Protein Purification and buffer exchange

Purification was performed via HIS-tag purification with cobalt resin. For small (<50 mL) cultures, 200 uL columns were used, whereas larger volumes (>400 mL) were purified via FPLC

(AKTA by Cytiva). Buffer exchange was done with either centrifugal filtration units (3-10kD, 4-15 mL), desalting columns (7kD), or dialysis cassettes (10kD) at least three consecutive times with 25 mM TRIS buffer at pH 7.0. Further purification via size exclusion was performed as necessary, with HiLoad 16/600 Superdex 200pg columns connected to the FPLC system.

6.2.3: Fluorescence Measurements

Fluorescence was measured with the Cytation5 (Biotek) with excitation at 488 nm and emission at 510 nm, with monochromators and/or filters. Wells were prepared with a 10-200 nM concentration of GLamouR (quantified via sequence-specific a205) in TRIS buffer (25 mM, pH7); after the second read, REEs/negative controls were introduced to reach desired concentrations (with ten averages per read).

6.3: c-fos promoter

6.3.1: Cell Culture

HEK 293FT cells were maintained using DMEM with 10% FBS and 1% Penicillin-Streptomycin at 37C and 5% CO_2. Cells were routinely subcultured once culture reached 80-90% confluency. Transfections were performed using Lipofectamine 3000 (Invitrogen) according to manufacturer's procedure.

6.3.2: Flow Cytometry

To perform flow cytometry cells were put into a starvation state by replacing complete media with Opti-MEM™ Reduced Serum Medium (Thermo Scientific) 18-24 hours before experimental stimulus added. HEK 293FT cells transfected with c-fos tdTomato plasmid using Lipofectamine 3000 transfection reagent. Cells were washed 48 hours post transfection and media replaced the stimuli of the group. Stimuli was given 24 hours pre-recording. PMA was given

at a concentration of 25mM. Serum was altered by using complete media (DMEM with 10%FBS 1%P/S) and OptiMEM reduced serum media. Magnetic stimulus was performed with 150mTesla static magnet on top of well plate. Cells were spun down and fixed using 1% paraformaldehyde and strained using a cell strainer. Recording and analysis performed using Accuri C6.

6.4: Synthetic calcium dependent promoter

6.4.1: Promoter Shuffling

6.4.1.1: Preparation of DNA Fragments

To shuffle the promoters to create a new promoter starts with amplification using PCR of the parental DNA fragments to shuffle with a high-fidelity polymerase. Full PCR reaction was run on an agarose gel where desired fragments were gel excised and purified. To determine the optimal time and concentration of DNase I for fragment digestion, 1ug of purified fragments were used with a dilution scheme of DNA I. This was further optimized with timepoints of digestion from 2-8 minutes of digestion. Optimal digestion should appear as blurry band rather than a smear on a 1.8% agarose gel.

6.4.1.2: Size Fractionation and Purification

Amicon filtration was used to separate digested and non-digested fragments. The first step to eliminate the non-digested fragments was to use a 100k Amicon filtration unit (Sigma). The sample was spun at 500 x g for 10 minutes. Then we used a 3k Amicon filtration unit (Sigma) to concentrate digested fragments where they were spun at 14,000 x g until almost all liquid had passed through. TE buffer was added and process was repeated for a buffer exchange and spun down again. After this 100ul of TE buffer was added to lift fragments from membrane. Filter was then inverted and liquid was collected in a new tube. Concentration of fragments were measured

using a NanoDrop.

6.4.1.3: Reassembly Protocol

Serial dilutions of DNA were prepared for primerless PCR reactions from 50ng/ul of DNA and using 2x Taq Master Mix (NEB). Cycles were 2 minutes of initial denaturation followed by 40 cycles of denaturation at 95Cfor 20 seconds, annealing at 50C for 30 seconds (-0.2C/cycle), and extension at 72C for 30 seconds (+1sec/cycle) with no final extension. Sample ran on 1% agarose gel with significant amount of smearing.

Rescue PCR.

Newly assembled fragments were rescued from the Primeless PCR use primers associated with downstream cloning process or specific to each parent used. 1-5ul of a 1/100-1/50 dilution was used for reassembly PCR mix. PCR was then done according to the manufacturer's protocol. Cloning was performed using either TOPO cloning or Gibson Assembly and following each transformation protocol.

6.5: BRET studies of EPG

HeLa cells were split to 70% confluency in a 6 well plate. The following day cells were transfected with plasmid DNA according to Lipofectamine 3000 protocol. The transfection efficiency was checked under the Keyence microscope using the GFP filter. Cells were then split to black walled clear bottom plastic 96 well plates. A stock solution (50 mM) of h-Coelenterazine (h-CTZ, NanoLight Technologies) was prepared by adding 25uL of solution to dried h-CTZ powder. A working concentration of 5uM was made by diluting the h-CTZ stock solution in FluoroBrite DMEM (Gibco).

Prior to measurements, culture media was aspirated from cells and replaced with h-CTZ

containing media. The plate was then put into a Victor Nivo (Perkin Elmer) plate reader. Reads were taken every minute for 15 minutes from the bottom of the plate using 480/30nm and 540/30nm filters. The plate was then taken out and static magnets were put into wells for magnet samples and then the plate was placed back in the reader and readings were taken every minute for 15 minutes. A ratio of the 540/480 was used to calculate BRET efficiency.

6.6: Localization of EPG BRET construct

HeLa cells were co-transfected with the EPG BRET and EPG HaloTag constructs using Lipofectamine 3000 (Thermo Scientific). The following day cells were labeled with 200nM Janelia Fluor 646 HaloTag ligand (Promega). After Labeling, cells were imaged using the Keyence BZX-700 microscope. Imaged were captured using the GFP (Ex 470/40nm, Em 525/50nm) and Cy5 (Ex 620/60nm, Em 700/75nm) filter cubes. Images were overlaid using the Keyence Image Analyzer software.

6.7: EPG Split NanoLuc

6.7.1: Nanoluciferase Assay in *E. coli*

Plasmids containing NanoLuciferase constructs were transformed into BL21 E. coli cells. Colonies were picked and grown in Magic Media (Invitrogen) expression media overnight at 37°C. After overnight expression, cells were pelleted by centrifugation followed by resuspension in PBST and were sonicated using 10 sec on 20 second on pulses for 2-3 minutes to create cell lysates.

For IVIS (Perkin Elmer) imaging 25 uL of cells or cell lysate were added to the 96 well plate followed by 150uL of LB broth with 5uM h-CTZ. 15 min after the addition of h-CTZ, IVIS images were captured using a 1 second exposure time with an open emission filter and an F stop of 1

which allowed us to capture an image every 10 seconds. After 2 minutes of imaging, an electromagnetic coil (35 mTesla field strength) surrounding the 96 well plate was turned on and samples were under electromagnetic stimulation for a 2-minute period at which the magnet was turned off and images were captured for another 6 minutes. Images were analyzed using the Living Image Software (Perkin Elmer).

6.7.2: Nanoluciferase Assay in HEK 293FT cells

Plasmids containing the EPG split NanoLuc/NanoBiT constructs were transfected into HEK 293FT cells 24 hours before experiment. For IVIS imaging, media was exchanged to Fluorbrite Media containing 5uM of h-CTZ. 15 minutes post media exchange cells were imaged on the IVIS using a 1 second exposure time with an open emission filter and an F stop of 1 which allowed us to capture an image every 10 seconds. After 2 minutes of imaging, an electromagnetic coil (35 mTesla field strength) surrounding the 96 well plate was turned on and samples were under electromagnetic stimulation followed by a period at which the magnet was turned off. This was repeated for one or 3 times depending on the experiment. After acquisition, images were analyzed using the Living Image Software (Perkin Elmer).

6.8: EPG Split APEX2

6.8.1: Amplex Ultrared Assay

HEK 293FT cells were grown to 70-90% confluency and transfected in a 6 well plate according to manufacturer's protocol (Lipofectamine 3000). After 24 hours post transfection, cells were split into black walled 96 well plates and left for to grow for 18-24 hours. Cells were then moved to ice and media was replaced with a solution of 50uM Amplex UltraRed (Life Technologies) with 0.02% (6.7mM) H202 in PBS. Cells with magnet stimulation had static magnets

(150-200 mTesla) on top and bottom of well plate over the stimulated wells. Stimulation occurred for 30 minutes and then were read on Cytation 5 plate reader (BioTek) using 530 excitation and 590 emission read settings.

6.9: EPG Split HSV1-TK

6.9.1: Ganciclovir Mediated Cell Death

4T1 Luc2 (ATCC) cells were plated at 10,000-20,000 cells per well into 96 well plates. After 8 hours, cells were transfected according to manufacturer's protocol (Lipofectamine 3000). The following day media was exchanged with media containing 0.15mg/mL ganciclovir (InvivoGen). Magnet stimulated cells were then placed under constant magnetic stimulation (~150mT) for 72 hours. After 72 hours viability was measured by exchanging media with Fluorobrite (Invitrogen) supplemented with 0.15 mg/mL d-Luciferin (Gold Biotechnology). Luminescent reads were then taken on a Spark (Tecan) plate reader. Experiments performed with HEK 293 FT cells were handled in the same way except viability was measured with Cell Titer Blue (Promega) and 530em/590ex fluorescent reads were used to measure conversion.

6.9.2: Statistical analysis of the HSV1-TK Ganciclovir experiments:

The experiment includes 8 replicates from which we observed that the average cell growth was inhibited when under magnetic influence compared to the non-magnetic condition and compared to each of 8 replicates of controls expecting cell growth, and cell death. There are 2 questions about the statistical significance of this observation: 1) "How likely is it to again observe the 8 replicate outcomes of reduced average cell growth if the magnetic condition actually had no effect?" 2) "How likely is it to again observe in each replicate the particular difference of averages, if the magnetic condition actually had no effect?" These can be thought

of as condition and replicate significance testing, respectively.

For the condition significance testing, we investigated how likely it is to observe all 8 replicates of average cell growth showing inhibition if the experimental magnetic condition had no effect. To test this, we simulated how often we observe all 8 replicates with inhibited cell growth if we were to perform the growth and death control replicates many more times. This test is simulated because more replicate data becomes costly and laborious to gather. To simulate more control replicates we sampled our existing control replicates with replacement, counting how many samples of 8 contain all 8 showing inhibited cell growth. By chance, we observe our experimental results from the simulated sampling of the control conditions with a probability of 0.00039 (see Equation 1). This is sufficiently low to suggest significance of inhibition between replicate conditions. Probability density for the binomial distribution is shown in Equation 1, where n is the number of trials, p is the probability of success, and N is the number of successes.

$$P(N) = \binom{n}{N} p^N (1-p)^{n-N}$$

Equation: 1. Our control conditions both have 3 replicates with average inhibited cell growth or death, and 5 replicates with invigorated cell growth or death. Assuming this outcome was the most common outcome to observe of the underlying distribution, then the probability of inhibition in the controls then becomes 3/8 or p=0.375, and N=8. Using the binomial formula yields P (8)=0.00039.

For the replicate significance testing, we investigated how likely it is to observe, for each

replicate, the particular difference of means if the experimental magnetic condition had no effect and the data for both conditions had come from the same distribution. To test this, we used a Randomization Test[78] wherein the data comprising each replicate for both magnetic and non-magnetic conditions are assumed to originate from the same source. We randomize the "magnetic" and "non-magnetic" labels from the collected data for each replicate, then recalculate the difference of means. When performed many times (1,000,000), this process creates a distribution of differences, from which we can calculate how often the actual observed means difference or better can arise. All experimental condition replicates (EPG-HSV1-TK) showed statistical significance that the observed difference of means was far greater than the 95% confidence interval of the mean in which the differences of the means were sampled from randomized data assuming no effect of the magnetic condition.

6.9.3: HSV1-TK Mediated Uptake of I124-FIAU

4T1 Luc2 cells (ATCC) were grown in 6 well plates to 70-80% confluency then transfected with HSV1-tk, EPG split HSV-tk, or mock transfection using Lipofectamine 3000. 24 hours post transfection, cells were split into 96 well plates. 48 hours post transfection, cells were exchanged with media containing 10 uCi/mL of I124-FIAU. Cells were placed under constant magnetic stimulation (~200mTesla) or control conditions for 2, 4 or 6 hours with radionuclide. After each timepoint cells were washed 3 times with PBS. After washing cells were lysed with NaOH and collected in PCR tubes for radioactivity reads. Radioactivity was measured using the Wizard Gamma Counter (Perkin Elmer).

6.10: EPG Split Beta Lactamase

6.10.1: Antibiotic Sensitivity

The EPG split Beta Lactamase construct was cloned into a pLacIQ vector and expressed in BL21 (DE3) *E. coli*. To determine the sensitivity of the system we first grew an overnight culture in LB broth. This culture was diluted until an OD600 of 1.0 was reached on a NanoDrop. Once this was obtained, cultures with corresponding OD600 were made from the 1.0 culture. These were grown from one hour in fresh LB broth to allow for protein production to start. After this initial hour corresponding amounts of ampiciilin (50ug/mL or 10ug/mL) were added to the culture tube and grown overnight. Overnight cultures were then measured using either Spark (Tecan) or NanoDrop for OD600 reads.

6.10.2: Beta Lactamase Nitrocefin Assay

EPG split Beta Lactamase cultures were grown overnight in LB broth. Culture was then serial diluted to 1/2 and 1/4 dilutions of overnight culture and allowed to grow for an additional hour. Nitrocefin (BioVision) was made into a 1mM stock solution and used added to cultures for a final concentration of 0.1mM. Cultures were divided into 6 wells, 3 for magnetic stimulation (~200mTesla) and 3 for control. Reads were taken every 15 minutes at 486nm for one hour on the Spark (Tecan).

REFERENCES

1. Gibson, D.G. et al. Enzymatic assembly of DNA molecules up to several hundred kilobases. *Nat Methods* **6**, 343-345 (2009).

2. Engler, C., Kandzia, R. & Marillonnet, S. A One Pot, One Step, Precision Cloning Method with High Throughput Capability. *PLOS ONE* **3**, e3647 (2008).

3. Hughes, R.A. & Ellington, A.D. Synthetic DNA Synthesis and Assembly: Putting the Synthetic in Synthetic Biology. *Cold Spring Harb Perspect Biol* **9** (2017).

4. Ausländer, S. & Fussenegger, M. From gene switches to mammalian designer cells: present and future prospects. *Trends Biotechnol* **31**, 155-168 (2013).

5. Gossen, M. et al. Transcriptional activation by tetracyclines in mammalian cells. *Science* **268**, 1766-1769 (1995).

6. Cronin, C.A., Gluba, W. & Scrable, H. The lac operator-repressor system is functional in the mouse. *Genes Dev* **15**, 1506-1517 (2001).

7. Xie, M. et al. β-cell-mimetic designer cells provide closed-loop glycemic control. *Science* **354**, 1296-1301 (2016).

8. Zhao, Y. et al. An expanded palette of genetically encoded Ca^{2+} indicators. *Science* **333**, 1888-1891 (2011).

9. Lee, H.D. et al. A Novel Protein for the Bioremediation of Gadolinium Waste. *bioRxiv* (2023).

10. Petersen, E.D. et al. Bioluminescent Genetically Encoded Glutamate Indicator for Molecular Imaging of Neuronal Activity. *bioRxiv*, 2021.2006.2016.448690 (2022).

11. Liu, Z. et al. Sustained deep-tissue voltage recording using a fast indicator evolved for two-photon microscopy. *Cell* **185**, 3408-3425.e3429 (2022).

12. Nihongaki, Y., Otabe, T., Ueda, Y. & Sato, M. A split CRISPR-Cpf1 platform for inducible genome editing and gene activation. *Nat Chem Biol* **15**, 882-888 (2019).

13. Ye, H., Daoud-El Baba, M., Peng, R.W. & Fussenegger, M. A synthetic optogenetic transcription device enhances blood-glucose homeostasis in mice. *Science* **332**, 1565-1568 (2011).

14. Nagel, G. et al. Light activation of channelrhodopsin-2 in excitable cells of Caenorhabditis elegans triggers rapid behavioral responses. *Current biology* **15**, 2279-2284 (2005).

15. Vierock, J., Grimm, C., Nitzan, N. & Hegemann, P. Molecular determinants of proton selectivity and gating in the red-light activated channelrhodopsin Chrimson. *Scientific Reports* **7**, 1-15 (2017).

16. Zhang, F. et al. Multimodal fast optical interrogation of neural circuitry. *Nature* **446**, 633-639 (2007).

17. Polesskaya, O. et al. Optogenetic regulation of transcription. *BMC neuroscience* **19**, 3-13 (2018).

18. Atasoy, D. & Sternson, S.M. Chemogenetic Tools for Causal Cellular and Neuronal Biology. *Physiol Rev* **98**, 391-418 (2018).

19. Urban, D.J. & Roth, B.L. DREADDs (Designer Receptors Exclusively Activated by Designer Drugs): Chemogenetic Tools with Therapeutic Utility. *Annual Review of Pharmacology and Toxicology* **55**, 399-417 (2015).

20. Vlasov, K., Van Dort, C.J. & Solt, K. Optogenetics and Chemogenetics. *Methods Enzymol* **603**, 181-196 (2018).

21. Romei, M.G. & Boxer, S.G. Split Green Fluorescent Proteins: Scope, Limitations, and Outlook. *Annu Rev Biophys* **48**, 19-44 (2019).

22. Paulmurugan, R. & Gambhir, S.S. Monitoring protein-protein interactions using split synthetic renilla luciferase protein-fragment-assisted complementation. *Anal Chem* **75**, 1584-1589 (2003).

23. Galarneau, A., Primeau, M., Trudeau, L.E. & Michnick, S.W. Beta-lactamase protein fragment complementation assays as in vivo and in vitro sensors of protein protein interactions. *Nat Biotechnol* **20**, 619-622 (2002).

24. Shekhawat, S.S. & Ghosh, I. Split-protein systems: beyond binary protein-protein interactions. *Curr Opin Chem Biol* **15**, 789-797 (2011).

25. Massoud, T.F., Paulmurugan, R. & Gambhir, S.S. A molecularly engineered split reporter for imaging protein-protein interactions with positron emission tomography. *Nat Med* **16**, 921-926 (2010).

26. Zetsche, B., Volz, S.E. & Zhang, F. A split-Cas9 architecture for inducible genome editing and transcription modulation. *Nat Biotechnol* **33**, 139-142 (2015).

27. Cubillos-Ruiz, A. et al. An engineered live biotherapeutic for the prevention of antibiotic-induced dysbiosis. *Nat Biomed Eng* **6**, 910-921 (2022).

28. Gao, X.J., Chong, L.S., Kim, M.S. & Elowitz, M.B. Programmable protein circuits in living cells. *Science* **361**, 1252-1258 (2018).

29. Mouritsen, H. Long-distance navigation and magnetoreception in migratory animals. *Nature* **558**, 50-59 (2018).

30. Wiltschko, W. & Wiltschko, R. Magnetic orientation and magnetoreception in birds and other animals. *J Comp Physiol A Neuroethol Sens Neural Behav Physiol* **191**, 675-693 (2005).

31. Wiltschko, R. & Wiltschko, W. Magnetoreception in birds. *J R Soc Interface* **16**, 20190295 (2019).

32. Beason, R.C., Wiltschko, R. & Wiltschko, W. Pigeon homing: effects of magnetic pulses on initial orientation. *The Auk* **114**, 405-415 (1997).

33. Pinzon-Rodriguez, A. & Muheim, R. Zebra finches have a light-dependent magnetic compass similar to migratory birds. *Journal of Experimental Biology* **220**, 1202-1209 (2017).

34. Hart, V. et al. Magnetic alignment in carps: evidence from the Czech christmas fish market. *PLoS One* **7**, e51100 (2012).

35. Blakemore, R. Magnetotactic bacteria. *Science* **190**, 377-379 (1975).

36. Bellini, S. On a unique behavior of freshwater bacteria. *Chinese Journal of Oceanology and Limnology* **27**, 3 (2009).

37. Guo, F.F. et al. Magnetosomes eliminate intracellular reactive oxygen species in Magnetospirillum gryphiswaldense MSR-1. *Environmental Microbiology* **14**, 1722-1729 (2012).

38. Lin, W., Kirschvink, J.L., Paterson, G.A., Bazylinski, D.A. & Pan, Y. On the origin of microbial magnetoreception. *National Science Review* **7**, 472-479 (2019).

39. Zadeh-Haghighi, H. & Simon, C. Magnetic field effects in biology from the perspective of the radical pair mechanism. *J R Soc Interface* **19**, 20220325 (2022).

40. Xu, J. et al. Magnetic sensitivity of cryptochrome 4 from a migratory songbird.

41. Naisbett-Jones, L.C. & Lohmann, K.J. Magnetoreception and magnetic navigation in fishes: a half century of discovery. *J Comp Physiol A* **208** (2022).

42. Johnsen, S. & Lohmann, K.J. The physics and neurobiology of magnetoreception. *<i data-test="journal-title" style="box-sizing: inherit;">Nature Reviews Neuroscience* **6** (2005).

43. Nimpf, S. et al. A Putative Mechanism for Magnetoreception by Electromagnetic Induction in the Pigeon Inner Ear. *Curr Biol* **29**, 4052-4059.e4054 (2019).

44. Huang, H., Delikanli, S., Zeng, H., Ferkey, D.M. & Pralle, A. Remote control of ion channels and neurons through magnetic-field heating of nanoparticles. *Nat Nanotechnol* **5**, 602-606 (2010).

45. Wheeler, M.A. et al. Genetically targeted magnetic control of the nervous system. *Nat Neurosci* **19**, 756-761 (2016).

46. Barbic, M. Possible magneto-mechanical and magneto-thermal mechanisms of ion channel activation in magnetogenetics. *eLife* **8**, e45807 (2019).

47. Ng, H.H. & Kottelat, M. After eighty years of misidentification, a name for the glass catfish (Teleostei: Siluridae). *Zootaxa* **3630**, 308-316 (2013).

48. Wachtel, A.W. & Szamier, R.B. Special cutaneous receptor organs of fish: IV. Ampullary organs of the nonelectric catfish, Kryptopterus.

49. Krishnan, V. et al. Wireless control of cellular function by activation of a novel protein responsive to electromagnetic fields. *Sci Rep* **8**, 8764 (2018).

50. Ricker, B. et al. Proposed three-phenylalanine motif involved in magnetoreception signaling of an Actinopterygii protein expressed in mammalian cells. *bioRxiv*, 2022.2012.2008.519643 (2022).

51. Cywiak, C. et al. Non-invasive neuromodulation using rTMS and the Electromagnetic-Perceptive Gene (EPG) facilitates plasticity after nerve injury. *bioRxiv*, 851444 (2019).

52. Metto, A.C., Gilad, A.A. & Pelled, G. Magnetogenetic closed-loop reduction of seizure activity in a rat model of epilepsy. *bioRxiv*, 2022.2008. 2019.504501 (2022).

53. Hwang, J. et al. Regulation of Electromagnetic Perceptive Gene Using Ferromagnetic Particles for the External Control of Calcium Ion Transport. *Biomolecules* **10** (2020).

54. Lohrke, J. et al. 25 Years of Contrast-Enhanced MRI: Developments, Current Challenges and Future Perspectives. *Adv Ther* **33**, 1-28 (2016).

55. Runge, V.M. Commentary on T1-Weighted Hypersignal in the Deep Cerebellar Nuclei After Repeated Administrations of Gadolinium-Based Contrast Agents in Healthy Rats: Difference Between Linear and Macrocyclic Agents. *Investigative Radiology* **50**, 481-482 (2015).

56. Louie, A.Y. et al. In vivo visualization of gene expression using magnetic resonance imaging. *Nature Biotechnology* **18**, 321-325 (2000).

57. Gilad, A.A., Bar-Shir, A., Bricco, A.R., Mohanta, Z. & McMahon, M.T. Protein and peptide engineering for chemical exchange saturation transfer imaging in the age of synthetic biology. *NMR in Biomedicine* **n/a**, e4712.

58. Yang, C., Tian, R., Liu, T. & Liu, G. MRI Reporter Genes for Noninvasive Molecular Imaging. *Molecules* **21** (2016).

59. Skovran, E. & Martinez-Gomez, N.C. Just add lanthanides. *Science* **348**, 862-863 (2015).

60. Cotruvo, J.A., Jr., Featherston, E.R., Mattocks, J.A., Ho, J.V. & Laremore, T.N. Lanmodulin: A Highly Selective Lanthanide-Binding Protein from a Lanthanide-Utilizing Bacterium. *J Am Chem Soc* **140**, 15056-15061 (2018).

61. Mattocks, J.A., Cotruvo, J.A. & Deblonde, G.J.-P. Engineering lanmodulin's selectivity for actinides over lanthanides by controlling solvent coordination and second-sphere interactions. *Chemical Science* **13**, 6054-6066 (2022).

62. Chen, T.W. et al. Ultrasensitive fluorescent proteins for imaging neuronal activity. *Nature* **499**, 295-300 (2013).

63. Sheng, M. & Greenberg, M.E. The regulation and function of c-fos and other immediate early genes in the nervous system. *Neuron* **4**, 477-485 (1990).

64. Fisch, T.M., Prywes, R., Simon, M.C. & Roeder, R.G. Multiple sequence elements in the c-fos promoter mediate induction by cAMP. *Genes Dev* **3**, 198-211 (1989).

65. Stemmer, W.P. Rapid evolution of a protein in vitro by DNA shuffling. *Nature* **370**, 389-391 (1994).

66. Tastanova, A. et al. Synthetic biology-based cellular biomedical tattoo for detection of hypercalcemia associated with cancer. *Science Translational Medicine* **10**, eaap8562 (2018).

67. Meško, M., Lebar, T., Dekleva, P., Jerala, R. & Benčina, M. Engineering and Rewiring of a Calcium-Dependent Signaling Pathway. *ACS Synth Biol* **9**, 2055-2065 (2020).

68. Audet, N. et al. Bioluminescence resonance energy transfer assays reveal ligand-specific conformational changes within preformed signaling complexes containing delta-opioid receptors and heterotrimeric G proteins. *J Biol Chem* **283**, 15078-15088 (2008).

69. Inagaki, S. et al. Genetically encoded bioluminescent voltage indicator for multi-purpose use in wide range of bioimaging. *Sci Rep* **7**, 42398 (2017).

70. Pétigny, C. et al. Monitoring TRPC7 Conformational Changes by BRET Following GPCR Activation. *Int J Mol Sci* **23** (2022).

71. Machleidt, T. et al. NanoBRET—A Novel BRET Platform for the Analysis of Protein–Protein Interactions. *ACS Chemical Biology* **10**, 1797-1804 (2015).

72. Zhao, J., Nelson, T.J., Vu, Q., Truong, T. & Stains, C.I. Self-Assembling NanoLuc Luciferase Fragments as Probes for Protein Aggregation in Living Cells. *ACS Chem Biol* **11**, 132-138 (2016).

73. Dixon, A.S. et al. NanoLuc Complementation Reporter Optimized for Accurate Measurement of Protein Interactions in Cells. *ACS Chem Biol* **11**, 400-408 (2016).

74. Pereira, G.C. et al. A High-Resolution Luminescent Assay for Rapid and Continuous Monitoring of Protein Translocation across Biological Membranes. *J Mol Biol* **431**, 1689-1699 (2019).

75. Han, Y. et al. Directed Evolution of Split APEX2 Peroxidase. *ACS Chem Biol* **14**, 619-635 (2019).

76. Alon, L. et al. Molecular Imaging of CXCL12 Promoter-driven HSV1-TK Reporter Gene Expression.

77. Farhana, I., Hossain, M.N., Suzuki, K., Matsuda, T. & Nagai, T. Genetically Encoded Fluorescence/Bioluminescence Bimodal Indicators for Ca2+ Imaging. *ACS Sensors* **4**, 1825-1834 (2019).

78. Manly, B.F.J. Randomization Tests, 4th Edition by Eugene S. Edgington, Patrick Onghena.

79. Bar-Shir, A., Liu, G., Greenberg, M.M., Bulte, J.W. & Gilad, A.A. Synthesis of a probe for monitoring HSV1-tk reporter gene expression using chemical exchange saturation transfer MRI. *Nat Protoc* **8**, 2380-2391 (2013).

80. Bar-Shir, A. et al. Transforming thymidine into a magnetic resonance imaging probe for monitoring gene expression. *J Am Chem Soc* **135**, 1617-1624 (2013).

81. Schymkowitz, J. et al. The FoldX web server: an online force field. *Nucleic Acids Res* **33**, W382-388 (2005).

82. Baek, M. et al. Accurate prediction of protein structures and interactions using a three-track neural network. *Science* **373**, 871-876 (2021).

APPENDIX

Table 1: Sequences of Constructs

Construct	Vector	Amino Acid Sequence (*Denotes DNA sequence)
DPD	pET-28(a)+	MAPVLSKDSADIESILALNPRTQTHATLCSTSAKKLDKKHWKRNPDK NCFNCEKLENNFDDIKHTTLGERGALREAMRCLKCADAPCQKSCPT NLDIKSFITSIANKNYYGAAKMIFSDNPLGLTCGMVCPTSDLCVGGC NLYATEEGPINIGGLQQFATEVFKAMSIPQIRNPSLPPPEKMSEAYSA KIALFGAGPASISCASFLARLGYSDITIFEKQEYVGGLSTSEIPQFRLPYD VVNFEIELMKDLGVKIICGKSLSVNEMTLSTLKEKGYKAAFIGIGLPEP NKDAIFQGLTQDQGFYTSKDFLPLVAKGSKAGMCACHSPLPSIRGVV IVLGAGDTAFDCATSALRCGARRVFIVFRKGFVNIRAVPEEMELAKEE KCEFLPFLSPRKVIVKGGRIVAMQFVRTEQDETGKWNEDEDQMVH LKADVVISAFGSVLSDPKVKEALSPIKFNRWGLPEVDPETMQTSEAW VFAGGDVVGLANTTVESVNDGKQASWYIHKYVQSQYGASVSAKPE LPLFYTPIDLVDISVEMAGLKFINPFGLASATPATSTSMIRRAFEAGW GFALTKTFSLDKDIVTNVSPRIIRGTTSGPMYGPGQSSFLNIELISEKTA AYWCQSVTELKADFPDNIVIASIMCSYNKNDWTELAKKSEDSGADA LELNLSCPHGMGERGMGLACGQDPELVRNICRWVRQAVQIPFFAK LTPNVTDIVSIARAAKEGGANGVTATNTVSGLMGLKSDGTPWPAVG IAKRTTYGGVSGTAIRPIALRAVTSIARALPGFPILATGGIDSAESGLQF LHSGASVLQVCSAIQNQDFTVIEDYCTGLKALLYLKSIEELQDWDGQS PATVSHQKGKPVPRIAELMDKKLPSFGPYLEQRKKIIAENKIRLKEQN VAFSPLKRSCFIPKRPIPTIKDVIGKALQYLGTFGELSNVEQVVAMIDE EMCINCGKCYMTCNDSGYQAIQFDPETHLPTITDTCTGCTLCLSVCPI VDCIKMVSRTTPYEPKRGVPLSVNPVC
GLamouR 1.0	pET101	MVDSSRRKWNKTGHAVRAIGRLSSLENVYIKADKQKNGIKANFKIR HNIEDGGVQLAYHYQQNTPIGDGPVLLPDNHYLSVQSKLSKDPNEK RDHMVLLEFVTAAGITLGMDELYKGGTGGSMVSKGEELFTGVVPIL VELDGDVNGHKFSVSGEGEGDATYGKLTLKFICTTGKLPVPWPTLVT TLTYGVQCFSRYPDHMKQHDFFKSAMPEGYIQERTIFFKDDGNYKT RAEVKFEGDTLVNRIELKGIDFKEDGNILGHKLEYNLPMAFRLSSAVLL AALVAAPAYAAPTTTTKVDIAAFDPDKDGTIDLKEALAAGSAAFDKL DPDKDGTLDAKELKGRVSEADLKKLDPDNDGTLDKKEYLAAVEAQF KAANPDNDGTIDARELASPAGSALVNLIRKGELNSKLEGKPIPNPLLG LDSTRTGHHHHHH
GLamouR 2.2	pET101	MVDSSRRKWNKTGHAVRAIGRLSSLENVYIKADKQKNGIKANFKIR HNIEDGGVQLAYHYQQNTPIGDGPVLLPDNHYLSVQSKLSKDPNEK RDHMVLLEFVTAAGITLGMDELYKGGTGGSMVSKGEELFTGVVPIL VELDGDVNGHKFSVSGEGEGDATYGKLTLKFICTTGKLPVPWPTLVT TLTYGVQCFSRYPDHMKQHDFFKSAMPEGYIQERTIFFKDDGNYKT RAEVKFEGDTLVNRIELKGIDFKEDGNILGHKLEYNLPDQLTEEQIAEF

Table 1 (cont'd)

		KEAFSLFDKDGTIDLKELGTVMRSLGQNPTEAELQDMINEVDPDKD GTLDAKEFLTMMARKGSYRDTEEEIREAFGVFDPDNDGTLDKKELR HVMTNLGEKLTDEEVDEMIREANPDNDGTIDAREFVQMMTAKKG ELNSKLEGKPIPNPLLGLDSTRTGHHHHHH
GLamouR-rs	pET101	MVDSSRRKWNKAGHAVRAIGRLSSPVVSERMYPEDGALKSEIKKGL RLKDGGHYAAEVKTTYKAKKPVQLPGAYIVDIKLDIVSHNEDYTIVEQ CERAEGRHSTGGMDELYKGGTGGSLVSKGEEDNMAIIKEFMRFKVH MEGSVNGHEFEIEGEGEGRPYEAFQTAKLKVTKGGPLPFAWDILSP QFMYGSKAYIKHPADIPDYFKLSFPEGFRWERVMNFEDGGIIHVNQ DSSLQDGVFIYKVKLRGTNFPPDGPVMQKKTMGWEATRDDLTEEQ IAEFKEAFSLFDPDKDGTIDLKELGTVFRSLGQNPTEAELQDMINEVD PDKDGTLDAKEFLTMMARKMNDTDSEEEIREAFRVFDPDNDGTLD KKELRHVMTDLGEKLTDEEVDEMIRVANPDNDGTIDAREFVQMMT AKGKPIPNPLLGLDSTRTGHHHHHH
c-fos tdTomato*		CCTCCCTCCTTTACACAGGATGTCCATATTAGGACATCTGCGTCAG CAGGTTTCCACGGCCGGTCCCTGTTGTCCTGGGGGGAACCATCCC CGAAATCCTACATGCGGAGGGTCCAGGAGACCTTCTAAGATCCCA ATTGTGAACACTCATAGGTGAAAGTTACAGACTGAGACGGGGGT TGAGAGCCTGGGGCGTAGAGTTGATGACAGGGAGCCCGCAGAG GGCATTCGGGAGCGCTTTCCCCCCTCCAGTTTCTCTGTTCCGCTCA TGACGTAGTAAGCCATTCAAGCGCTTCTATAAAGCGGCCAGCTGA GGCGCCTACTACTCCAACCGCGATTGCAGCTAGCAACTGAGAAG ACTGGATAGAGCCGGCGGAGCCGCGAACGAGCAGTGACCGCGC TCCCACCCAGCTCTGCTCTGCAGCTCCCACCAGTGTCTACCCCTGG ACCCAAGGGCGAATTCGACCCAAGTTTGTACAAAAAAGCAGGCT CCGCGGCCGCCCCTTCACCATGGTGAGCAAGGGCGAGGAGGTCA TCAAAGAGTTCATGCGCTTCAAGGTGCGCATGGAGGGCTCCATG AACGGCCACGAGTTCGAGATCGAGGGCGAGGGCGAGGGCCGCC CCTACGAGGGCACCCAGACCGCCAAGCTGAAGGTGACCAAGGGC GGCCCCCTGCCCTTCGCCTGGGACATCCTGTCCCCCCAGTTCATGT ACGGCTCCAAGGCGTACGTGAAGCACCCCGCCGACATCCCCGATT ACAAGAAGCTGTCCTTCCCCGAGGGCTTCAAGTGGGAGCGCGTG ATGAACTTCGAGGACGGCGGTCTGGTGACCGTGACCCAGGACTC CTCCCTGCAGGACGGCACGCTGATCTACAAGGTGAAGATGCGCG GCACCAACTTCCCCCCCGACGGCCCCGTAATGCAGAAGAAGACCA TGGGCTGGGAGGCCTCCACCGAGCGCCTGTACCCCCGCGACGGC GTGCTGAAGGGCGAGATCCACCAGGCCCTGAAGCTGAAGGACG GCGGCCACTACCTGGTGGAGTTCAAGACCATCTACATGGCCAAG AAGCCCGTGCAACTGCCCGGCTACTACTACGTGGACACCAAGCTG GACATCACCTCCCACAACGAGGACTACACCATCGTGGAACAGTAC GAGCGCTCCGAGGGCCGCCACCACCTGTTCCTGGGGCATGGCAC CGGCAGCACCGGCAGCGGCAGCTCCGGCACCGCCTCCTCCGAGG

Table 1 (cont'd)

		ACAACAACATGGCCGTCATCAAAGAGTTCATGCGCTTCAAGGTGC GCATGGAGGGCTCCATGAACGGCCACGAGTTCGAGATCGAGGGC GAGGGCGAGGGCCGCCCCTACGAGGGCACCCAGACCGCCAAGC TGAAGGTGACCAAGGGCGGCCCCCTGCCCTTCGCCTGGGACATC CTGTCCCCCCAGTTCATGTACGGCTCCAAGGCGTACGTGAAGCAC CCCGCCGACATCCCCGATTACAAGAAGCTGTCCTTCCCCGAGGGC TTCAAGTGGGAGCGCGTGATGAACTTCGAGGACGGCGGTCTGGT GACCGTGACCCAGGACTCCTCCCTGCAGGACGGCACGCTGATCTA CAAGGTGAAGATGCGCGGCACCAACTTCCCCCCCGACGGCCCCG TAATGCAGAAGAAGACCATGGGCTGGGAGGCCTCCACCGAGCGC CTGTACCCCCGCGACGGCGTGCTGAAGGGCGAGATCCACCAGGC CCTGAAGCTGAAGGACGGCGGCCACTACCTGGTGGAGTTCAAGA CCATCTACATGGCCAAGAAGCCCGTGCAACTGCCCGGCTACTACT ACGTGGACACCAAGCTGGACATCACCTCCCACAACGAGGACTACA CCATCGTGGAACAGTACGAGCGCTCCGAGGGCCGCCACCACCTG TTCCTGTACGGCATGGACGAGCTGTACAAGTAA
EPG	pcDNA 3.1(+)	MKCVLLGFAAVIGFFAIAESLTCNTCSVSLIGICLNPATATCSTNTSVC TTGRASFTGVLGFLGFNSQGCTEGAQCNGTVSGSILGASYTVTQTCC STNNCNPVTSGASYVQISVSAALSAALLACVWGQSVY
EGFP	pcDNA 3.1(+)	MVSKGEELFTGVVPILVELDGDVNGHKFSVSGEGEGDATYGKLTLKF ICTTGKLPVPWPTLVTTLTYGVQCFSRYPDHMKQHDFFKSAMPEGY VQERTIFFKDDGNYKTRAEVKFEGDTLVNRIELKGIDFKEDGNILGHK LEYNYNSHNVYIMADKQKNGIKVNFKIRHNIEDGSVQLADHYQQNT PIGDGPVLLPDNHYLSTQSALSKDPNEKRDHMVLLEFVTAAGITLGM DELYK
CaRE Promoter*	pGlow	AGCCTCAGCCCGTCAATCCCTCCCTCCTTTAGTCAGGATGTGGATA TTACCACATCTGCGTCAGCAGGTTTCCACGGCCACGCGTCTAGAG TTCGAGCTGCAGCCGGACTGCACTAGGAAGTACTGCTTGCGGAA GACATACTTTGTACTGAAGCTGACGTCTAGGAACACGTGTTCCGC CCAGTGACGTAGGGATCCCGGGACGCCTTCTGTATGAAACAGTTT TTCCTCCACCGGTGAATTCCCAGTGACGTCAGAAGTTCACGTCAA GAGGGTATATAATGGAAGCTCGACTTCCAG
EPG BRET	pcDNA 3.1(+)	MVFTLEDFVGDWRQTAGYNLDQVLEQGGVSSLFQNLGVSVTPIQRI VLSGENGLKIDIHVIIPYEGLSGDQMGQIEKIFKVVYPVDDHHFKVILH YGTLVIDGVTPNMIDYFGRPYEGIAVFDGKKITVTGTLWNGNKIIDER LINPDGSLLFRVTINGVTGWRLCERILAMKCVLLGFAAVIGFFAIAESL TCNTCSVSLIGICLNPATATCSTNTSVCTTGRASFTGVLGFLGFNSQG CTEGAQCNGTVSGSILGASYTVTQTCCSTNNCNPVTSGASYVQISVS AALSAALLACVWGQSVYMVSKGEELFTGVVPILVELDGDVNGHKFS VSGEGEGDATYGKLTLKLICTTGKLPVPWPTLVTTLGYGLQCFARYPD HMKQHDFFKSAMPEGYVQERTIFFKDDGNYKTRAEVKFEGDTLVN RIELKGIDFKEDGNILGHKLEYNYNSHNVYITADKQKNGIKANFKIRH

Table 1 (cont'd)

		NIEDGGVQLADHYQQNTPIGDGPVLLPDNHYLSYQSALSKDPNEKR DHMVLLEFVTAAGITLGMDELYK
EPG NanoLuc BRET	pcDNA 3.1(+)	MKCVLLGFAAVIGFFAIAESLTCNTCSVSLIGICLNPATATCSTNTSVC TTGRASFTGVLGFLGFNSQGCTEGAQCNGTVSGSILGASYTVTQTCC STNNCNPVTSGASYVQISVSAALSAALLACVWGQSVYMVFTLEDFV GDWRQTAGYNLDQVLEQGGVSSLFQNLGVSVTPIQRIVLSGENGLK IDIHVIIPYEGLSGDQMGQIEKIFKVVYPVDDHHFKVILHYGTLVIDGV TPNMIDYFGRPYEGIAVFDGKKITVTGTLWNGNKIIDERLINPDGSLL FRVTINGVTGWRLCERILA
EPG mVenus BRET	pcDNA 3.1(+)	MKCVLLGFAAVIGFFAIAESLTCNTCSVSLIGICLNPATATCSTNTSVC TTGRASFTGVLGFLGFNSQGCTEGAQCNGTVSGSILGASYTVTQTCC STNNCNPVTSGASYVQISVSAALSAALLACVWGQSVYMVSKGEELF TGVVPILVELDGDVNGHKFSVSGEGEGDATYGKLTLKLICTTGKLPVP WPTLVTTLGYGLQCFARYPDHMKQHDFFKSAMPEGYVQERTIFFKD DGNYKTRAEVKFEGDTLVNRIELKGIDFKEDGNILGHKLEYNYNSHN VYITADKQKNGIKANFKIRHNIEDGGVQLADHYQQNTPIGDGPVLLP DNHYLSYQSALSKDPNEKRDHMVLLEFVTAAGITLGMDELYK
EPG HaloTag	pcDNA 3.1(+)	MKCVLLGFAAVIGFFAIAESMAEIGTGFPFDPHYVEVLGERMHYVDV GPRDGTPVLFLHGNPTSSYVWRNIIPHVAPTHRCIAPDLIGMGKSDK PDLGYFFDDHVRFMDAFIEALGLEEVVLVIHDWGSALGFHWAKRNP ERVKGIAFMEFIRPIPTWDEWPEFARETFQAFRTTDVGRKLIIDQNVF IEGTLPMGVVRPLTEVEMDHYREPFLNPVDREPLWRFPNELPIAGEP ANIVALVEEYMDWLHQSPVPKLLFWGTPGVLIPPAEAARLAKSLPNC KAVDIGPGLNLLQEDNPDLIGSEIARWLSTLEISGEPTTEDLYFQSDNL TCNTCSVSLIGICLNPATATCSTNTSVCTTGRASFTGVLGFLGFNSQG CTEGAQCNGTVSGSILGASYTVTQTCCSTNNCNPVTSGASYVQISVS AALSAALLACVWGQSVYDYKDDDDKDYKDDDDKDYKDDDDK
EPG split EGFP	pcDNA 3.1(+)	MVSKGEELFTGVVPILVELDGDVNGHKFSVSGEGEGDATYGKLTLKF ICTTGKLPVPWPTLVTTLTYGVQCFSRYPDHMKQHDFFKSAMPEGY VQERTIFFKDDGNYKTRAEVKFEGDTLVNRIELKGIDFKEDGNILGHK LEYNYNSHNVYIMADKQGGGGSKCVLLGFAAVIGFFAIAESLTCNTC SVSLIGICLNPATATCSTNTSVCTTGRASFTGVLGFLGFNSQGCTEGA QCNGTVSGSILGASYTVTQTCCSTNNCNPVTSGASYVQISVSAALSA ALLACVWGQSVYGGGGSKNGIKVNFKIRHNIEDGSVQLADHYQQN TPIGDGPVLLPDNHYLSTQSKLSKDPNEKRDHMVLLEFVTAAGITLG MDELYK
EPG split NanoLuc	pET101	MVFTLEDFVGDWRQTAGYNLDQVLEQGGVSSLFQNLGVSVTPIQRI VLSGENGLKIDIHVIIPYEGGSKCVLLGFAAVIGFFAIAESLTCNTCSVSL IGICLNPATATCSTNTSVCTTGRASFTGVLGFLGFNSQGCTEGAQCN GTVSGSILGASYTVTQTCCSTNNCNPVTSGASYVQISVSAALSAALLA CVWGQSVYGGSGLSGDQMGQIEKIFKVVYPVDDHHFKVILHYGTLV

Table 1 (cont'd)

		IDGVTPNMIDYFGRPYEGIAVFDGKKITVTGTLWNGNKIIDERLINPD GSLLFRVTINGVTGWRLCERILA
trEPG split NanoLuc	pET101	MVFTLEDFVGDWRQTAGYNLDQVLEQGGVSSLFQNLGVSVTPIQRI VLSGENGLKIDIHVIIPYEGGSLTCNTCSVSLIGICLNPATATCSTNTSV CTTGRASFTGVLGFLGFNSQGCTEGAQCNGTVSGSILGASYTVTQTC CSTNNCNPVTSGASGGSGLSGDQMGQIEKIFKVVYPVDDHHFKVIL HYGTLVIDGVTPNMIDYFGRPYEGIAVFDGKKITVTGTLWNGNKIIDE RLINPDGSLLFRVTINGVTGWRLCERILA
Flipped trEPG split NanoLuc	pET101	MVFTLEDFVGDWRQTAGYNLDQVLEQGGVSSLFQNLGVSVTPIQRI VLSGENGLKIDIHVIIPYEGGSGGAAGHGVAVVCAAAGLSDRVRRTQ DGPGHGAITLSSLRAALGVEAQEAEDARETGSSCGADGCVGGASRC CGIQTYSNQTHGACVTGKGGSGLSGDQMGQIEKIFKVVYPVDDHH FKVILHYGTLVIDGVTPNMIDYFGRPYEGIAVFDGKKITVTGTLWNG NKIIDERLINPDGSLLFRVTINGVTGWRLCERILA
EPG SmLg NanoBiT	pcDNA 3.1(+)	MVTGWRLCERILAGGGGSLTCNTCSVSLIGICLNPATATCSTNTSVCT TGRASFTGVLGFLGFNSQGCTEGAQCNGTVSGSILGASYTVTQTCCS TNNCNPVTSGASGGGGSVFTLEDFVGDWEQTAAYNLDQVLEQGG VSSLLQNLAVSVTPIQRIVRSGENALKIDIHVIIPYEGLSADQMAQIEE VFKVVYPVDDHHFKVILPYGTLVIDGVTPNMLNYFGRPYEGIAVFDG KKITVTGTLWNGNKIIDERLITPDGSMLFRVTIN
EPG SmLg TM NanoBiT	pcDNA 3.1(+)	MVTGWRLCERILAGGGGSLTCNTCSVSLIGICLNPATATCSTNTSVCT TGRASFTGVLGFLGFNSQGCTEGAQCNGTVSGSILGASYTVTQTCCS TNNCNPVTSGASYVQISVSAALSAALLACVWGQSVYGGGGSVFTLE DFVGDWEQTAAYNLDQVLEQGGVSSLLQNLAVSVTPIQRIVRSGEN ALKIDIHVIIPYEGLSADQMAQIEEVFKVVYPVDDHHFKVILPYGTLVI DGVTPNMLNYFGRPYEGIAVFDGKKITVTGTLWNGNKIIDERLITPD GSMLFRVTIN
EPG LgSm NanoBiT	pcDNA 3.1(+)	MVFTLEDFVGDWEQTAAYNLDQVLEQGGVSSLLQNLAVSVTPIQRI VRSGENALKIDIHVIIPYEGLSADQMAQIEEVFKVVYPVDDHHFKVIL PYGTLVIDGVTPNMLNYFGRPYEGIAVFDGKKITVTGTLWNGNKIID ERLITPDGSMLFRVTINGGGGSLTCNTCSVSLIGICLNPATATCSTNTS VCTTGRASFTGVLGFLGFNSQGCTEGAQCNGTVSGSILGASYTVTQT CCSTNNCNPVTSGASGGGGSVTGWRLCERILA
EPG LgSm TM NanoBiT	pcDNA 3.1(+)	MVFTLEDFVGDWEQTAAYNLDQVLEQGGVSSLLQNLAVSVTPIQRI VRSGENALKIDIHVIIPYEGLSADQMAQIEEVFKVVYPVDDHHFKVIL PYGTLVIDGVTPNMLNYFGRPYEGIAVFDGKKITVTGTLWNGNKIID ERLITPDGSMLFRVTINGGGGSLTCNTCSVSLIGICLNPATATCSTNTS VCTTGRASFTGVLGFLGFNSQGCTEGAQCNGTVSGSILGASYTVTQT CCSTNNCNPVTSGASYVQISVSAALSAALLACVWGQSVYGGGGSVT GWRLCERILA

Table 1 (cont'd)

Flip EPG NanoBiT	pcDNA 3.1(+)	MVFTLEDFVGDWEQTAAYNLDQVLEQGGVSSLLQNLAVSVTPIQRI VRSGENALKIDIHVIIPYEGLSADQMAQIEEVFKVVYPVDDHHFKVIL PYGTLVIDGVTPNMLNYFGRPYEGIAVFDGKKITVTGTLWNGNKIID ERLITPDGSMLFRVTINGGGGSGGAAGHGVAVVCAAAGLSDRVRRT QDGPGHGAITLSSLRAALGVEAQEAEDARETGGGGSVTGWRLCERI LA
dEPG NanoBiT	pcDNA 3.1(+)	MVFTLEDFVGDWEQTAAYNLDQVLEQGGVSSLLQNLAVSVTPIQRI VRSGENALKIDIHVIIPYEGLSADQMAQIEEVFKVVYPVDDHHFKVIL PYGTLVIDGVTPNMLNYFGRPYEGIAVFDGKKITVTGTLWNGNKIID ERLITPDGSMLFRVTINGGGGSLTCNTCSVSLIGICLNPATATCSTNTS VCTTGRASFTGVLGFLGFNSQGCTEGAQCNGTVSGSILGASYTVTQT CCSTNNCNPVTSGASLTCNTCSVSLIGICLNPATATCSTNTSVCTTGR ASFTGVLGFLGFNSQGCTEGAQCNGTVSGSILGASYTVTQTCCSTNN CNPVTSGASGGGGSVTGWRLCERILA
EPG split NanoBiT FF86	pcDNA 3.1(+)	MVFTLEDFVGDWEQTAAYNLDQVLEQGGVSSLLQNLAVSVTPIQRI VRSGENALKIDIHVIIPYEGLSADQMAQIEEVFKVVYPVDDHHFKVIL PYGTLVIDGVTPNMLNYFGRPYEGIAVFDGKKITVTGTLWNGNKIID ERLITPDGSMLFRVTINGGGGSLTCNTCSVSLIGICLNPATATCSTNTS VCTTGRASFTGVLGFLGFNSQGCTEGAQCNGTVSGSILGASYTVTQT CCSTNNCNPVTSGASGGGGSVSGWRLFKKIS
EPG split NanoBiT FR86	pcDNA 3.1(+)	MVFTLEDFVGDWEQTAAYNLDQVLEQGGVSSLLQNLAVSVTPIQRI VRSGENALKIDIHVIIPYEGLSADQMAQIEEVFKVVYPVDDHHFKVIL PYGTLVIDGVTPNMLNYFGRPYEGIAVFDGKKITVTGTLWNGNKIID ERLITPDGSMLFRVTINGGGGSLTCNTCSVSLIGICLNPATATCSTNTS VCTTGRASFTGVLGFLGFNSQGCTEGAQCNGTVSGSILGASYTVTQT CCSTNNCNPVTSGASPAPAPVSGWRLFKKIS
EPG split NanoBiT RF86	pcDNA 3.1(+)	MVFTLEDFVGDWEQTAAYNLDQVLEQGGVSSLLQNLAVSVTPIQRI VRSGENALKIDIHVIIPYEGLSADQMAQIEEVFKVVYPVDDHHFKVIL PYGTLVIDGVTPNMLNYFGRPYEGIAVFDGKKITVTGTLWNGNKIID ERLITPDGSMLFRVTINPAPAPLTCNTCSVSLIGICLNPATATCSTNTS VCTTGRASFTGVLGFLGFNSQGCTEGAQCNGTVSGSILGASYTVTQT CCSTNNCNPVTSGASGGGGSVSGWRLFKKIS
EPG split NanoBiT mRF86	pcDNA 3.1(+)	MVFTLEDFVGDWEQTAAYNLDQVLEQGGVSSLLQNLAVSVTPIQRI VRSGENALKIDIHVIIPYEGLSADQMAQIEEVFKVVYPVDDHHFKVIL PYGTLVIDGVTPNMLNYFGRPYEGIAVFDGKKITVTGTLWNGNKIID ERLITPDGSMLFRVTINPAPAPLTCNTCSVSLIGICLNPATATCSTNTS VCTTGRASFTGVLGFLGFNSQGCTEGAQCNGTVSGSILGASYTVTQT CYSTNNCNPVTSGASGGGGSVSGWRLFKKIS
EPG split NanoBiT RR86	pcDNA 3.1(+)	MVFTLEDFVGDWEQTAAYNLDQVLEQGGVSSLLQNLAVSVTPIQRI VRSGENALKIDIHVIIPYEGLSADQMAQIEEVFKVVYPVDDHHFKVIL PYGTLVIDGVTPNMLNYFGRPYEGIAVFDGKKITVTGTLWNGNKIID

Table 1 (cont'd)

		ERLITPDGSMLFRVTINPAPAPLTCNTCSVSLIGICLNPATATCSTNTS VCTTGRASFTGVLGFLGFNSQGCTEGAQCNGTVSGSILGASYTVTQT CCSTNNCNPVTSGASPAPAPVSGWRLFKKIS
NanoLuc	pcDNA 3.1(+)	MVFTLEDFVGDWRQTAGYNLDQVLEQGGVSSLFQNLGVSVTPIQRI VLSGENGLKIDIHVIIPYEGLSGDQMGQIEKIFKVVYPVDDHHFKVILH YGTLVIDGVTPNMIDYFGRPYEGIAVFDGKKITVTGTLWNGNKIIDER LINPDGSLLFRVTINGVTGWRLCERILA
EPG APEX2	pcDNA 3.1(+)	MGKSYPTVSADYQDAVEKAKKRLGGFIAEKRCAPLMLRLAFHSAGT FDKRTKTGGPFGTIRYPAELAHSANSGLDIAVRLLEPLKAEFPILSYADF YQLAGVVAVEVTGGPKVPFHPGREDKPELPPEGRLPDPTKGSDHLR DVFGKAMGLTDQDIVALSGGHTLGAAHKERSGFEGPWTSNPLVFD NSYFTELLSGEKEKGSGSTSKCVLLGFAAVIGFFAIAESLTCNTCSVSLI GICLNPATATCSTNTSVCTTGRASFTGVLGFLGFNSQGCTEGAQCNG TVSGSILGASYTVTQTCCSTNNCNPVTSGASYVQISVSAALSAALLAC VWGQSVYGSKGSGSTSGSGGLLQLPSDKALLSDPVFRPLVDKYAAD EDAFFADYAEAHQKLSELGFADA
EPG NoSS APEX2	pcDNA 3.1(+)	MGKSYPTVSADYQDAVEKAKKRLGGFIAEKRCAPLMLRLAFHSAGT FDKRTKTGGPFGTIRYPAELAHSANSGLDIAVRLLEPLKAEFPILSYADF YQLAGVVAVEVTGGPKVPFHPGREDKPELPPEGRLPDPTKGSDHLR DVFGKAMGLTDQDIVALSGGHTLGAAHKERSGFEGPWTSNPLVFD NSYFTELLSGEKEKGSGSTSGSGSTSGSGTGLTCNTCSVSLIGICLNPA TATCSTNTSVCTTGRASFTGVLGFLGFNSQGCTEGAQCNGTVSGSIL GASYTVTQTCCSTNNCNPVTSGASYVQISVSAALSAALLACVWGQS VYGSKGSGSTSGSGGLLQLPSDKALLSDPVFRPLVDKYAADEDAFFA DYAEAHQKLSELGFADA
EPG NoTM APEX2	pcDNA 3.1(+)	MGKSYPTVSADYQDAVEKAKKRLGGFIAEKRCAPLMLRLAFHSAGT FDKRTKTGGPFGTIRYPAELAHSANSGLDIAVRLLEPLKAEFPILSYADF YQLAGVVAVEVTGGPKVPFHPGREDKPELPPEGRLPDPTKGSDHLR DVFGKAMGLTDQDIVALSGGHTLGAAHKERSGFEGPWTSNPLVFD NSYFTELLSGEKEKGSGSTSGSGSTSGSGTGKCVLLGFAAVIGFFAIAE SLTCNTCSVSLIGICLNPATATCSTNTSVCTTGRASFTGVLGFLGFNSQ GCTEGAQCNGTVSGSILGASGSKGSGSTSGSGGLLQLPSDKALLSDP VFRPLVDKYAADEDAFFADYAEAHQKLSELGFADA
dEPG APEX2	pcDNA 3.1(+)	MGKSYPTVSADYQDAVEKAKKRLGGFIAEKRCAPLMLRLAFHSAGT FDKRTKTGGPFGTIRYPAELAHSANSGLDIAVRLLEPLKAEFPILSYADF YQLAGVVAVEVTGGPKVPFHPGREDKPELPPEGRLPDPTKGSDHLR DVFGKAMGLTDQDIVALSGGHTLGAAHKERSGFEGPWTSNPLVFD NSYFTELLSGEKEKGSGSTSKCVLLGFAAVIGFFAIAESLTCNTCSVSLI GICLNPATATCSTNTSVCTTGRASFTGVLGFLGFNSQGCTEGAQCNG TVSGSILGASYTVTQTCCSTNNCNPVTSGASYVQISVSAALSAALLAC VWGQSVYKCVLLGFAAVIGFFAIAESLTCNTCSVSLIGICLNPATATCS

Table 1 (cont'd)

		TNTSVCTTGRASFTGVLGFLGFNSQGCTEGAQCNGTVSGSILGASYT VTQTCCSTNNCNPVTSGASYVQISVSAALSAALLACVWGQSVYGSK GSGSTSGSGGLLQLPSDKALLSDPVFRPLVDKYAADEDAFFADYAEA HQKLSELGFADA
dEPG NoSSTM APEX2	pcDNA 3.1(+)	MGKSYPTVSADYQDAVEKAKKRLGGFIAEKRCAPLMLRLAFHSAGT FDKRTKTGGPFGTIRYPAELAHSANSGLDIAVRLLEPLKAEFPILSYADF YQLAGVVAVEVTGGPKVPFHPGREDKPELPPEGRLPDPTKGSDHLR DVFGKAMGLTDQDIVALSGGHTLGAAHKERSGFEGPWTSNPLVFD NSYFTELLSGEKEKGSGSTSGSGSTSGSGTGLTCNTCSVSLIGICLNPA TATCSTNTSVCTTGRASFTGVLGFLGFNSQGCTEGAQCNGTVSGSIL GASYTVTQTCCSTNNCNPVTSGASLTCNTCSVSLIGICLNPATATCST NTSVCTTGRASFTGVLGFLGFNSQGCTEGAQCNGTVSGSILGASYTV TQTCCSTNNCNPVTSGASGSGSTSGSGGLLQLPSDKALLSDPVFRPL VDKYAADEDAFFADYAEAHQKLSELGFADA
HSV1-tk	pcDNA 3.1(+)	MASYPCHQHASAFDQAARSRGHSNRRTALRPRRQQEATEVRLEQK MPTLLRVYIDGPHGMGKTTTTQLLVALGSRDDIVYVPEPMTYWQVL GASETIANIYTTQHRLDQGEISAGDAAVVMTSAQITMGMPYAVTDA VLAPHIGGEAGSSHAPPPALTLIFDRHPIAALLCYPAARYLMGSMTP QAVLAFVALIPPTLPGTNIVLGALPEDRHIDRLAKRQRPGERLDLAML AAIRRVYGLLANTVRYLQGGGSWREDWGQLSGTAVPPQGAEPQS NAGPRPHIGDTLFTLFRAPELLAPNGDLYNVFAWALDVLAKRLRPM HVFILDYDQSPAGCRDALLQLTSGMVQTHVTTPGSIPTICDLARTFAR EMGEAN
EPG HSV1-tk	pcDNA 3.1(+)	MALTPQGAEPQSNAGPRPHIGETLFTLFRAPELLAPNGDLYNVFAW ALDVLAKRLRPMHVFILDYDQSPAGCRDALLQLTSGMVQTHVTTPG SIPTICDLARTFAREMGEAHGGGGSGGGGSGGGGSKCVLLGFAAVI GFFAIAESLTCNTCSVSLIGICLNPATATCSTNTSVCTTGRASFTGVLGF LGFNSQGCTEGAQCNGTVSGSILGASYTVTQTCCSTNNCNPVTSGA SYVQISVSAALSAALLACVWGQSVYGGGGSGGGGSGGGGSASYPC HQHASAFDQAARSRGHSNRRTALRPRRQQEATEVRPEQKMPTLLR VYIDGPHGMGKTTTTQLLVALGSRDDIVYVPEPMTYWRVLGASETI ANIYTTQHRLDQGEISAGDAAVVMTSAQITMGMPYAVTDAVLAPH IGGEAGSSHAPPPALTIFLDRHPIAFMLCYPAARYLMGSMTPQAVLA FVALIPPTLPGTNIVLGALPEDRHIDRLAKRQRPGERLDLAMLAAIRR VYGLLANTVRYLQCGGSWREDWGQLSGT
EPG split HSV1-tk FF	pcDNA 3.1(+)	MALTPQGAEPQSNAGPRPHIGETLFTLFRAPELLAPNGDLYNVFAW ALDVLAKRLRPMHVFILDYDQSPAGCRDALLQLTSGMVQTHVTTPG SIPTICDLARTFAREMGEAHGGGGSKCVLLGFAAVIGFFAIAESLTCN TCSVSLIGICLNPATATCSTNTSVCTTGRASFTGVLGFLGFNSQGCTE GAQCNGTVSGSILGASYTVTQTCCSTNNCNPVTSGASYVQISVSAAL SAALLACVWGQSVYGGGGSASYPCHQHASAFDQAARSRGHSNRRT ALRPRRQQEATEVRPEQKMPTLLRVYIDGPHGMGKTTTTQLLVALG

Table 1 (cont'd)

		SRDDIVYVPEPMTYWRVLGASETIANIYTTQHRLDQGEISAGDAAVV MTSAQITMGMPYAVTDAVLAPHIGGEAGSSHAPPPALTIFLDRHPIA FMLCYPAARYLMGSMTPQAVLAFVALIPPTLPGTNIVLGALPEDRHI DRLAKRQRPGERLDLAMLAAIRRVYGLLANTVRYLQCGGSWREDW GQLSGT
EPG split HSV1-tk FR	pcDNA 3.1(+)	MALTPQGAEPQSNAGPRPHIGETLFTLFRAPELLAPNGDLYNVFAW ALDVLAKRLRPMHVFILDYDQSPAGCRDALLQLTSGMVQTHVTTPG SIPTICDLARTFAREMGEAHGGGGSKCVLLGFAAVIGFFAIAESLTCN TCSVSLIGICLNPATATCSTNTSVCTTGRASFTGVLGFLGFNSQGCTE GAQCNGTVSGSILGASYTVTQTCCSTNNCNPVTSGASYVQISVSAAL SAALLACVWGQSVYPAPAPASYPCHQHASAFDQAARSRGHSNRRT ALRPRRQQEATEVRPEQKMPTLLRVYIDGPHGMGKTTTTQLLVALG SRDDIVYVPEPMTYWRVLGASETIANIYTTQHRLDQGEISAGDAAVV MTSAQITMGMPYAVTDAVLAPHIGGEAGSSHAPPPALTIFLDRHPIA FMLCYPAARYLMGSMTPQAVLAFVALIPPTLPGTNIVLGALPEDRHI DRLAKRQRPGERLDLAMLAAIRRVYGLLANTVRYLQCGGSWREDW GQLSGT
EPG split HSV1-tk RF	pcDNA 3.1(+)	MALTPQGAEPQSNAGPRPHIGETLFTLFRAPELLAPNGDLYNVFAW ALDVLAKRLRPMHVFILDYDQSPAGCRDALLQLTSGMVQTHVTTPG SIPTICDLARTFAREMGEAHPAPAPKCVLLGFAAVIGFFAIAESLTCNT CSVSLIGICLNPATATCSTNTSVCTTGRASFTGVLGFLGFNSQGCTEG AQCNGTVSGSILGASYTVTQTCCSTNNCNPVTSGASYVQISVSAALS AALLACVWGQSVYGGGGSASYPCHQHASAFDQAARSRGHSNRRT ALRPRRQQEATEVRPEQKMPTLLRVYIDGPHGMGKTTTTQLLVALG SRDDIVYVPEPMTYWRVLGASETIANIYTTQHRLDQGEISAGDAAVV MTSAQITMGMPYAVTDAVLAPHIGGEAGSSHAPPPALTIFLDRHPIA FMLCYPAARYLMGSMTPQAVLAFVALIPPTLPGTNIVLGALPEDRHI DRLAKRQRPGERLDLAMLAAIRRVYGLLANTVRYLQCGGSWREDW GQLSGT
EPG split HSV1-tk RR	pcDNA 3.1(+)	MALTPQGAEPQSNAGPRPHIGETLFTLFRAPELLAPNGDLYNVFAW ALDVLAKRLRPMHVFILDYDQSPAGCRDALLQLTSGMVQTHVTTPG SIPTICDLARTFAREMGEAHPAPAPKCVLLGFAAVIGFFAIAESLTCNT CSVSLIGICLNPATATCSTNTSVCTTGRASFTGVLGFLGFNSQGCTEG AQCNGTVSGSILGASYTVTQTCCSTNNCNPVTSGASYVQISVSAALS AALLACVWGQSVYPAPAPASYPCHQHASAFDQAARSRGHSNRRTA LRPRRQQEATEVRPEQKMPTLLRVYIDGPHGMGKTTTTQLLVALGS RDDIVYVPEPMTYWRVLGASETIANIYTTQHRLDQGEISAGDAAVV MTSAQITMGMPYAVTDAVLAPHIGGEAGSSHAPPPALTIFLDRHPIA FMLCYPAARYLMGSMTPQAVLAFVALIPPTLPGTNIVLGALPEDRHI DRLAKRQRPGERLDLAMLAAIRRVYGLLANTVRYLQCGGSWREDW GQLSGT

Table 1 (cont'd)

EPG split HSV1-tk sFF	pcDNA 3.1(+)	MALTPQGAEPQSNAGPRPHIGETLFTLFRAPELLAPNGDLYNVFAW ALDVLAKRLRPMHVFILDYDQSPAGCRDALLQLTSGMVQTHVTTPG SIPTICDLARTFAREMGEAHGGGGSLTCNTCSVSLIGICLNPATATCST NTSVCTTGRASFTGVLGFLGFNSQGCTEGAQCNGTVSGSILGASYTV TQTCCSTNNCNPVTSGASGGGGSASYPCHQHASAFDQAARSRGHS NRRTALRPRRQQEATEVRPEQKMPTLLRVYIDGPHGMGKTTTTQLL VALGSRDDIVYVPEPMTYWRVLGASETIANIYTTQHRLDQGEISAGD AAVVMTSAQITMGMPYAVTDAVLAPHIGGEAGSSHAPPPALTIFLD RHPIAFMLCYPAARYLMGSMTPQAVLAFVALIPPTLPGTNIVLGALP EDRHI
EPG split HSV1-tk sRF	pcDNA 3.1(+)	MALTPQGAEPQSNAGPRPHIGETLFTLFRAPELLAPNGDLYNVFAW ALDVLAKRLRPMHVFILDYDQSPAGCRDALLQLTSGMVQTHVTTPG SIPTICDLARTFAREMGEAHPAPAPLTCNTCSVSLIGICLNPATATCST NTSVCTTGRASFTGVLGFLGFNSQGCTEGAQCNGTVSGSILGASYTV TQTCCSTNNCNPVTSGASGGGGSASYPCHQHASAFDQAARSRGHS NRRTALRPRRQQEATEVRPEQKMPTLLRVYIDGPHGMGKTTTTQLL VALGSRDDIVYVPEPMTYWRVLGASETIANIYTTQHRLDQGEISAGD AAVVMTSAQITMGMPYAVTDAVLAPHIGGEAGSSHAPPPALTIFLD RHPIAFMLCYPAARYLMGSMTPQAVLAFVALIPPTLPGTNIVLGALP EDRHI
EPG split HSV1-tk sRR	pcDNA 3.1(+)	MALTPQGAEPQSNAGPRPHIGETLFTLFRAPELLAPNGDLYNVFAW ALDVLAKRLRPMHVFILDYDQSPAGCRDALLQLTSGMVQTHVTTPG SIPTICDLARTFAREMGEAHPAPAPLTCNTCSVSLIGICLNPATATCST NTSVCTTGRASFTGVLGFLGFNSQGCTEGAQCNGTVSGSILGASYTV TQTCCSTNNCNPVTSGASPAPAPASYPCHQHASAFDQAARSRGHS NRRTALRPRRQQEATEVRPEQKMPTLLRVYIDGPHGMGKTTTTQLL VALGSRDDIVYVPEPMTYWRVLGASETIANIYTTQHRLDQGEISAGD AAVVMTSAQITMGMPYAVTDAVLAPHIGGEAGSSHAPPPALTIFLD RHPIAFMLCYPAARYLMGSMTPQAVLAFVALIPPTLPGTNIVLGALP EDRHI
EPG split Beta Lactamase	pLacIQ	MSIQHFRVALIPFFAAFCLPVFAHPETLVKVKDAEDQLGARVGYIELD LNSGKILESFRPEERFPMMSTFKVLLCGAVLSRVDAGQEQLGRRIHYS QNDLVEYSPVTEKHLTDGMTVRELCSAAITMSDNTAANLLLTTIGGP KELTAFLHNMGDHVTRLDRWEPELNEAIPNDERDTTTPAAMATTLR KGGGGSGGGGSKCVLLGFAAVIGFFAIAESLTCNTCSVSLIGICLNPAT ATCSTNTSVCTTGRASFTGVLGFLGFNSQGCTEGAQCNGTVSGSILG ASYTVTQTCCSTNNCNPVTSGASYVQISVSAALSAALLACVWGQSVY GGGGSGGGGSTGELLTLASRQQLIDWMEADKVAGPLLRSALPAGW FIADKSGAGERGSRGIIAALGPDGKPSRIVVIYTTGSQATMDERNRQI AEIGASLIKHW

Table 2: Cell Lines

Cell Line	Cell Type	Source
One Shot™ TOP10	Chemically Competent *E. coli*	Invitrogen
One Shot™ BL21(DE3)	Chemically Competent *E. coli*	Invitrogen
NEB 5-alpha	Chemically Competent *E. coli*	New England Biolabs
HEK 293FT	Human Embryonic Kidney	Invitrogen
4T1 Luc2	Mouse Breast Cancer	ATCC

A1: Enzymatic Synthesis of 5-MDHT

One field of study in synthetic biology is to take complicated chemical synthesis procedures and attempt to simplify them through engineering enzymes to complete the synthesis more efficiently and safer in comparison to the chemical means. One such chemical synthesis is for the creation of the 5-methyl dihydroxythymidine (5-MDHT), an established CEST MRI contrast agent[79, 80]. The chemical synthesis starts with thymidine and involves a four-step synthesis to the final product of 5-MDHT as shown in Figure 38A. To simplify this, we proposed using a two-step enzymatic approach to create the 5-MDHT (Figure 38B). The two proposed enzymes were dihydropyrimidine dehydrogenase (DPD) to reduce the double bond on thymidine and an S-adenosyl–methionine dependent methyltransferase to add a methyl group to the carbon at the 5 position of the reduced base.

A

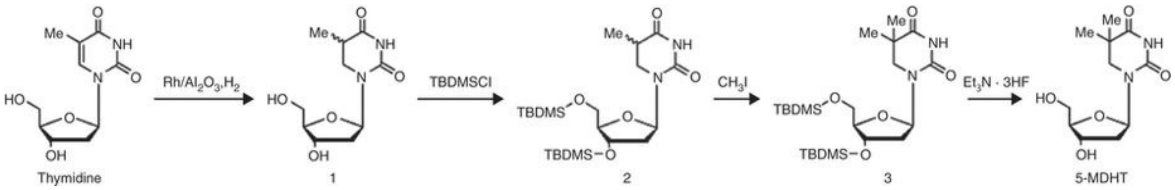

B

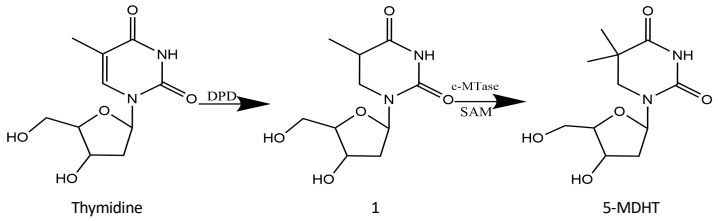

Figure 38: Chemical and proposed enzymatic synthesis methods of 5-MDHT. A) Chemical Synthesis involving a four-step approach to make 5-MDHT. B) Enzymatic approach using a two-step method using dihydropyrimidine dehydrogenase (DPD) and an S-adenosyl–methionine dependent methyltransferase to create 5-MDHT.

The DPD enzyme was chosen because one of its natural products is thymine and it preforms the same reaction at the position we were trying to reduce on the thymidine. We first wanted to check we could express the DPD in *E. coli* and then purify the enzyme before we performed any characterization to examine the activity of DPD with thymine and thymidine. As shown from the western blot in Figure 39, we were able to induce the expression of the DPD enzyme and then purify the protein. The blot shows three distinct bands in lanes 1,3, and 4. The band in lane 1 is the positive control of standard Green Fluorescent Protein (stGFP) at 35 kDa. The bands in lanes 4 and 5 show the DPD protein at 110 kDa. In lane 3 we see the bacterial lysate of the DPD and the purified product from cobalt resin in lane 4. We believe excess bands in lane 4 were due to not saturating the column during the purification process. This data showed the ability to express and purify the DPD enzyme to be tested in the biosynthesis of 5-MDHT.

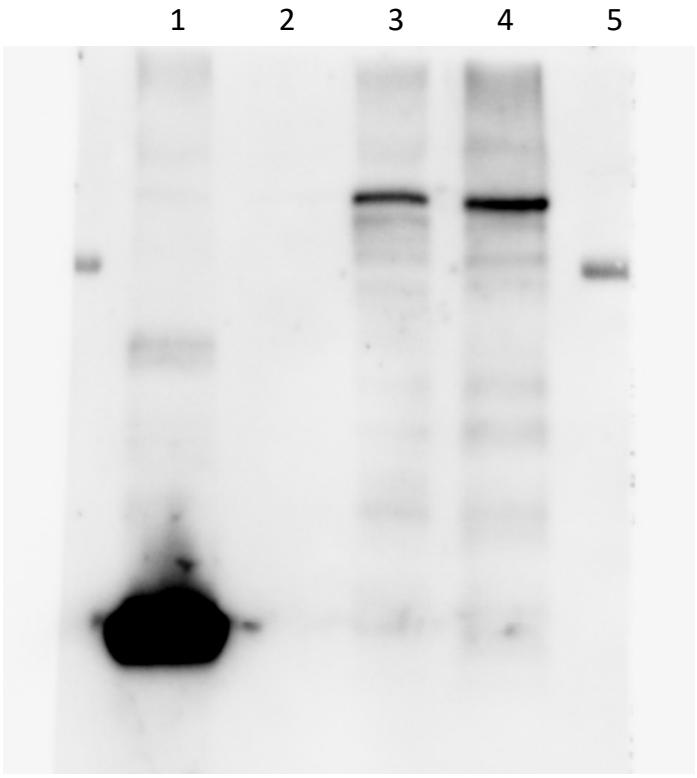

Figure 39: Western blot results showing expression purification of DPD using Anti-6x His antibody. Lane 1: Induced stGFP extract. Lane 2: DPD in LB broth without induction. Lane 3: DPD extract in Magic Media. Lane 4: Purified DPD from extract (lane 3). Lane 5: Molecular weight marker.

Once we were able to express the enzyme, we wanted to characterize it with both thymine and thymidine. The first goal was to determine the substrate to read for the reaction progression. The first option was to use NADPH since it is necessary for DPD to perform the reduction. This substrate is also an ideal substrate as it absorbs at 340nm but after donating its electrons to reduce the double bond converts to NADP+ and no longer has absorbance at 340nm. A standard curve was performed with NADPH up 2mg/ml and it shows a strong linear relationship (Figure 40A). The other option is to use thymidine which has absorbance at 280nm. A standard curve of was performed with thymidine up to 1.25mg/ml (Figure 40B). We also wanted to see if

this thymidine reading would be affected by conversion of thymidine to 5,6 Dihydrothymidine. To test this a mixture of the thymidine 5,6 Dihydrothymidine were measure at 280nm (Figure 40C). Although it appears the 5,6 Dihydrothymidine did not have an effect the readings of the thymidine, we decided to use the NADPH 340nm reading to measure the enzyme activity as it allowed for larger scale experiments with the equipment available to measure at 340nm compared to 280nm.

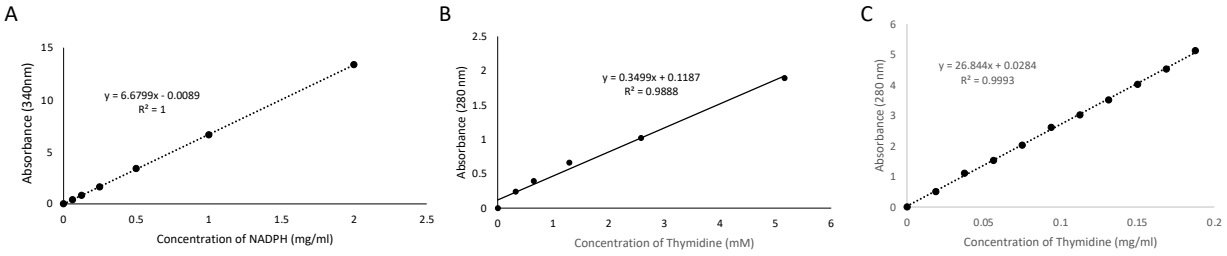

Figure 40: Standard curves for substrate absorbance for DPD enzyme reaction. A) NADPH absorbance at 340nm from serial dilution concentrations up to 2mg/ml, or 2.68mM with a linear regression fit of R2 =0.99. B) Thymidine absorbance at 280nm from serial dilutions with concentrations up to 1.25mg/ml, or 5mM with linear regression fit of R2 =0.988. C) Serial dilutions of Thymidine and 5,6-Dihydrothymidine absorbance at a wavelength of 280 nm. This produced a linear relationship between concentration of Thymidine and absorbance up to a thymidine and dihydrothymidine concentration of at least 0.1875 mg/ml. The linear regression fit is R2 = 0.99.

To characterize the DPD enzyme we ran a kinetic enzyme using its natural substrate of thymine. The three reactions in the experiment were the cellular extract from cultures grown in an induction media (Magic Media, Thermo Fisher), cell extract from cultures grown in LB broth and a control group with no cell extract. Reactions were measured for 200 min at 340nm with the results shown in Figure 41A. As predicted the induced DPD samples consumed a larger amount of NADPH than the non-induced samples. The average difference in NADPH consumption was 30% and was statistically significant, with a p-value of p=0.001. (Figure 41B).

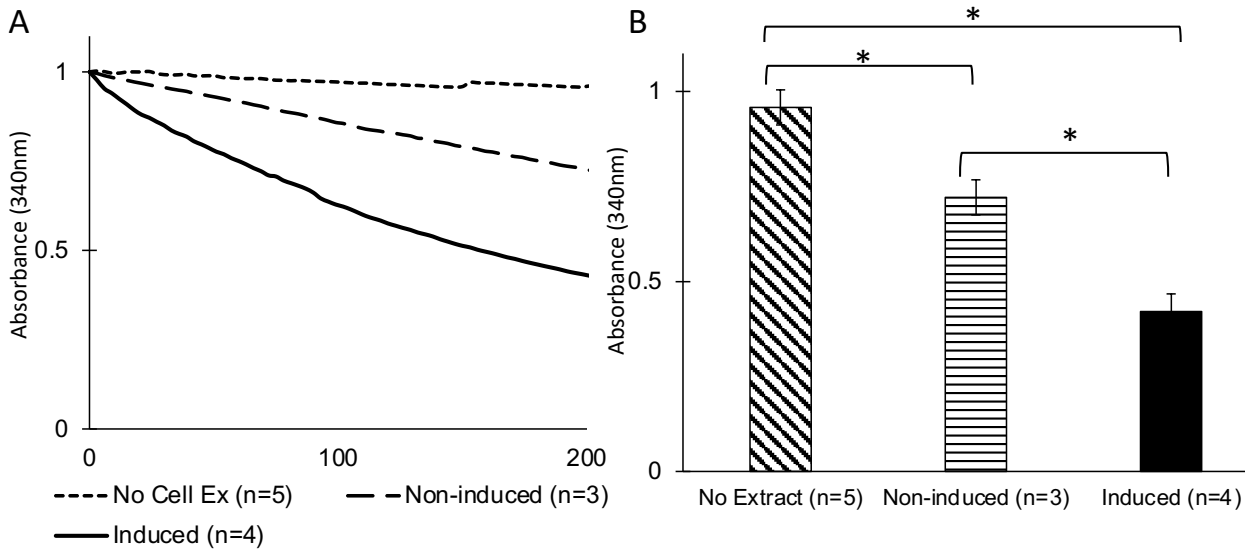

Figure 41: Enzyme assays comparing enzymatic activity of Induced and Non-induced Dihydropyrimidine Dehydrogenase. (A) Absorbance was measured at a wavelength of 340 nm, every 3 minutes for 3.3 hours for No Cell Extract (control), Cell Extract from induced *E. coli*, and Cell Extract from non-induced *E. coli* (B) Means and standard deviation of end point absorbance for each sample. The induced DPD samples consumed a larger amount of NADPH than the non-induced samples. The average difference in NADPH consumption was 30%. Statistical analysis was performed using an unpaired t-test. The (*) denotes a p-value <0.05.

We further wanted to characterize the DPD against another enzyme, the Heavy Metal Binding Protein (HMBP), as a control to see the effect of the cellular lysates. In these figures (4A and 5B) you can see that both samples consumed NADPH. Figure 42A shows the progression of the reaction and Figure 42B shows the final end point absorbance of each sample. The DPD expressing samples consumed a larger amount of NADPH than the Heavy Metal Binding Protein samples. The average difference in NADPH consumption was 12.5%, with a p-value of p=0.04.

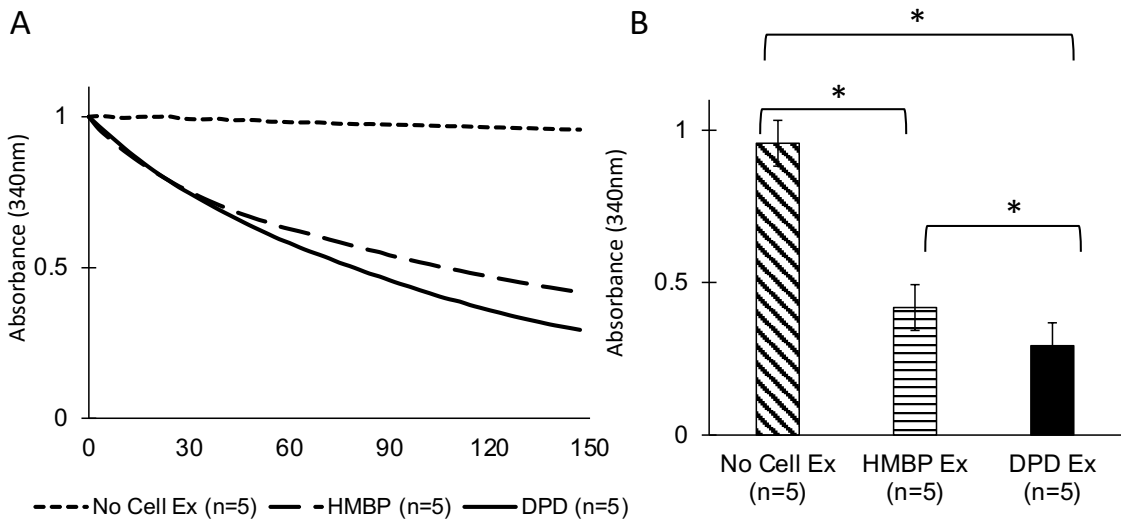

Figure 42: Enzyme assays comparing activity of Dihydropyrimidine Dehydrogenase and Heavy Metal Binding Protein. (A) Mean absorbance was measured every 3 minutes 2.5 hours for No Cell Extract (control), Cell Extract from E. coli expressing Heavy Metal Binding Protein (HMBP) or Dihydropyrimidine Dehydrogenase (DPD.) (B) Means and standard deviation of final end point absorbance for each sample. The DPD samples consumed a larger amount of NADPH than the HMBP samples. Statistical analysis was performed using an unpaired t-test. The (*) denotes a p-value <0.05.

Mutations were proposed to engineer DPD to bind thymidine more efficiently. Random mutagenesis using an error prone polymerase was chosen to perform the action on the binding region of DPD to thymine. After the initial screening of the mutagenesis, six colonies were selected for screening. Of the six potential mutants 3 were mutated successfully (Figure 43A). When the reaction was run on these three mutants, there was no difference between the mutated groups, wild-type DPD, and the no enzyme control group (Figure 43B).

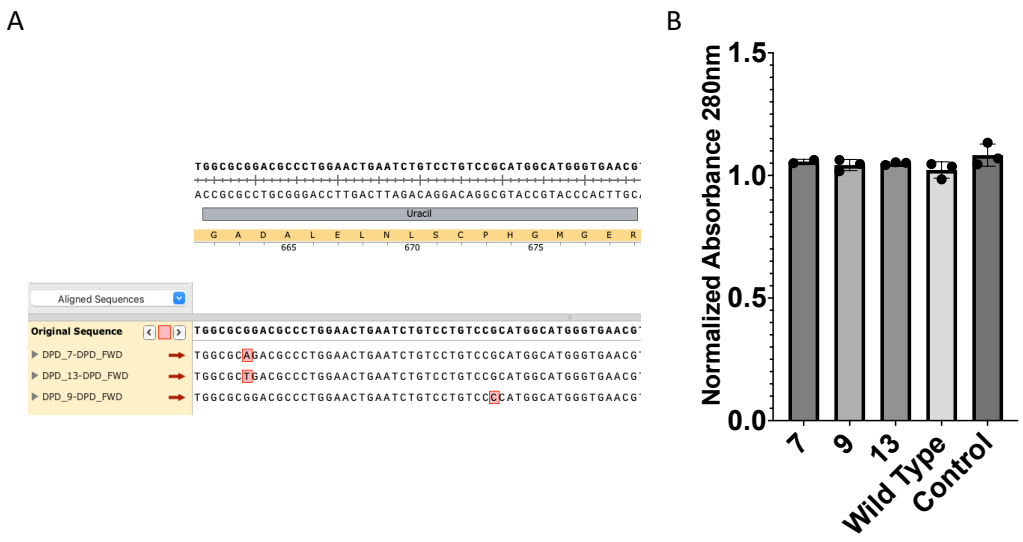

Figure 43: Analysis of DPD mutants. (A) Sequence alignments of the three successful mutants of DPD. (B) Endpoint absorbance of DPD mutants, wild-type DPD and no enzyme control after 3 hours of incubation. The resulting endpoint shows no difference in any of the groups.

After the initial round of mutagenesis, we decided the mutational method would have to be changed. Since thymine, the natural product of DPD, is roughly half the size of thymidine (126.1 g/mol to 242.3 g/mol) the binding pocket of DPD would have to be greatly opened to allow efficient binding, but also allow it to maintain enzymatic properties. Focusing solely on the binding motif of thymine would not be sufficient in engineering the DPD to convert thymindine to dihydrothymidine.

At this point, the project was halted as there the structural biology expertise needed was not available at this time. The future direction of this project would incorporate stability calculations with programs such as FoldX [81] or Rosetta[82] to better optimize the mutations to allow for thymidine binding. The second option would be to attempt to skip the first step of the enzymatic synthesis and try to convert thymidine to 5-MDHT with a methyl transferase. This would simplify the synthesis and allow for optimization of one enzyme rather than two.

A2: Methods for Enzymatic Synthesis of 5-MDHT

A2.1: Expression and purification of DPD enzyme

The DPD gene was cloned into the expression vector pET28a(+) vector. This was transformed into BL21 (DE3) cells (Thermo Scientific). To induced expression of DPD we used MagicMedia™ *E. coli* Expression Medium (Invitrogen). If culture volume was less than 100mL colony was picked directly from plate and used to inoculate culture. For cultures 100mL or greater, an overnight starter culture grown in LB broth was used to inoculate culture. The inoculated culture of MagicMedia™ was grown overnight at 30C or 37C in a shaking incubator. Overnight cultures were spun down by centrifugation into a pellet.

Pellets were resuspended in PBST (Phosphate-buffered saline with 0.1% Tween 20). Lysis was performed using a probe sonicator with 10 second on and 20 second off cycle while on ice. After sonication lysate was spun down in 4C centrifuge and supernatant was collected. Purification was performed using HisPur™ Cobalt Purification Kit (Thermo Scientific). To check the expression and purification of the protein, samples were run on a SDS-PAGE gel. The gels used from the Stain-Free gels (Bio-Rad) that can be directed imaged on a Gel-doc system from Bio-Rad. After gels were imaged, they were transferred to a PVDF membrane and then a western blot was performed using an Anti-6x His Tag primary antibody (Thermo Scientific) and a HRP conjugated anti-mouse IgG secondary antibody (Cell Signaling) each according to manufactures protocol.

A2.2: DPD Enzymatic Activity

To measure enzymatic activity of DPD the following reaction was prepared in TRIS buffer (pH 7.5). This consisted of 1mM dithiothreitol, 200μM NADPH, 32μM each of FAD, FMN, and FeS04, and to start the reaction 200μM thymine or thymidine for a total reaction volume of

200μL. The use of FAD, FMN and FeS04 were only used when using purified protein and not used when cell lysate was used. Measurements were performed in UV permeable 96 well plates and reads were taken every 3-5 minutes at 340nm for 3-24 hours depending on the assay/experiment.

A2.3: Mutagenesis of DPD Enzyme

Mutagenesis of the DPD enzyme was performed using the Genemorph II Random mutagenesis kit (Agilent). The mutagenesis protocol was performed using 100ng of starting DNA and 30 cycles of PCR with the Mutazyme II polymerase. Sanger sequencing was used to analyze the sequences and Snapgene was used to align to sequences to the wild-type.

PUBLICATIONS, CONFERENCE PRESENTATIONS, AND PATENTS

PUBLICATIONS

1. Lee, HD, **Grady, CJ**, Krell, K, Strebeck, C, Good, NM, Martinez-Gomez, NC, & Gilad, AA (2023). A Novel Protein for the Bioremediation of Gadolinium Waste. *bioRxiv*. doi:10.1101/2023.01.05.522788

2. Ricker, B, Mitra, S, Castellanos, A, **Grady, CJ**, Pelled, G, & Gilad, AA (2022). Proposed three-phenylalanine motif involved in magnetoreception signaling of an Actinopterygii protein expressed in mammalian cells. *bioRxiv*. doi:10.1101/2022.12.08.519643

3. **Grady, CJ**, Schossau, J, Ashbaugh, R, Pelled, G, & Gilad, AA (2022). A putative design for electromagnetic activation of split proteins for molecular and cellular manipulation. *bioRxiv*. doi:10.1101/2022.11.30.518522

4. Petersen, ED. Lapan, AP, Castellanos Franco, EA, Fillion, AJ, Crespo, EL, Lambert, GG, **Grady, CJ**, Torreblanca Zanca, A, Orcutt, R, Hochgeschwender, U, Shaner, NC, & Gilad, AA (2021). Bioluminescent Genetically Encoded Glutamate Indicator for Molecular Imaging of Neuronal Activity. *bioRxiv* doi:10.1101/2021.06.16.448690

PEER REVIEWED CONFERENCE PAPERS

1. Ackles, AL, Ferguson, AJ, **Grady, C**, & Ofria, C (2020). Rank epistasis: A new model for analyzing epistatic interactions in the absence of quantifiable fitness interactions. *Artificial Life Conference Proceedings*(32), 160-162. doi:10.1162/isal_a_00325

2. Ruvio, T, **Grady, C**, Bricco, A, & Gilad, AA. (2020). *AI assisted encryption into DNA sequence of a functional protein*. Paper presented at the Proceedings of the 7th ACM International Conference on Nanoscale Computing and Communication, Virtual Event, USA. https://doi.org/10.1145/3411295.3411316

CONFERENCE PRESENTATIONS

1. 2022-**Talk,** World Molecular Imaging Congress, “Expanding and Evolving Magnetogenetic Tools Toward in vivo Imaging Applications”

2. 2022-**Poster,** Engineering Graduate Research Symposium, “GEMInI-Genetically Encoded Magnetically Induced Indicators”

3. 2021-**Talk,** World Molecular Imaging Congress, “Utilizing Magnetogenetics to Control Optical Imaging Reporters”

4. 2021-**Poster**, Engineering Graduate Research Symposium, “Utilizing Magnetogenetics to Control Enzyme Function”

5. 2020-**Talk,** BEACON Congress, “Magnetobiomaniupulation: A Novel Synthetic Biology Approach to Control Enzymes”

6. 2019-**Poster,** Engineering Graduate Research Symposium “Biosynthesis of an MRI Contrast Agent”

7. 2018-**Poster,** BEACON Congress, “Evolution of a Biosynthetic Pathway of an MRI Contrast Agent”

PATENT

1. Pending PCT International Patent application for “Lanmodulin-Based Protein.” Lee, **Grady** and Gilad